AFFDL-TR-77-46

12

CALCULATIONS OF SOME UNSTEADY TRANSONIC FLOWS ABOUT THE NACA 64A006 AND 64A010 AIRFOILS

GENERAL DYNAMICS CONVAIR DIVISION
KEARNY MESA PLANT
5001 KEARNY VILLA ROAD
SAN DIEGO, CALIFORNIA 92138

JULY 1977

TECHNICAL REPORT AFFDL-TR-77-46
FINAL REPORT FOR PERIOD NOVEMBER 1975 – APRIL 1977

Approved for public release; distribution unlimited

Prepared for
AIR FORCE FLIGHT DYNAMICS LABORATORY
Air Force Wright Aeronautical Laboratories
Air Force Systems Command
Wright-Patterson Air Force Base, Ohio 45433

NOTICE

When Government drawings, specifications, or other data are used for any purpose other than in connection with a definitely related Government procurement operation, the United States Government thereby incurs no responsibility nor any obligation whatsoever; and the fact that the Government may have formulated, furnished, or in any way supplied the said drawings, specifications, or other data, is not to be regarded by implication or otherwise as in any manner licensing the holder or any other person or corporation, or conveying any rights or permission to manufacture, use, or sell any patented invention that may in any way be related thereto.

This report has been reviewed by the Information Office (OI) and is releasable to the National Technical Information Service (NTIS). At NTIS, it will be available to the general public, including foreign nations.

This technical report has been reviewed and is approved for publication.

James J Olsen

JAMES J. ØLSEN, Technical Manager
Optimization Group
Analysis and Optimization Branch

Richard D. Krobusek

RICHARD D. KROBUSEK, Maj, USAF
Chief, Analysis and Optimization Branch
Structural Mechanics Division

FOR THE COMMANDER

Howard L Farmer

HOWARD L. FARMER, Colonel, USAF
Chief, Structural Mechanics Division

Copies of this report should not be returned unless return is required by security considerations, contractual obligations, or notice on a specific document.

AIR FORCE/56780/17 October 1977 — 100

Unclassified

SECURITY CLASSIFICATION OF THIS PAGE (When Data Entered)

REPORT DOCUMENTATION PAGE	READ INSTRUCTIONS BEFORE COMPLETING FORM
1. REPORT NUMBER: AFFDL-TR-77-46	2. GOVT ACCESSION NO. / 3. RECIPIENT'S CATALOG NUMBER
4. TITLE (and Subtitle): Calculations of Some Unsteady Transonic Flows About the NACA 64A006 and 64A010 Airfoils	5. TYPE OF REPORT & PERIOD COVERED: Final Report, for period Nov 75 — Apr 77
	6. PERFORMING ORG. REPORT NUMBER
7. AUTHOR(s): Dr. R. J. Magnus	8. CONTRACT OR GRANT NUMBER(s): F33615-76-C-3018
9. PERFORMING ORGANIZATION NAME AND ADDRESS: General Dynamics Convair Division, P. O. Box 80847, San Diego, California 92138	10. PROGRAM ELEMENT, PROJECT, TASK AREA & WORK UNIT NUMBERS: 61102F, 2307 0505
11. CONTROLLING OFFICE NAME AND ADDRESS: Air Force Flight Dynamics Laboratory, FBR, Air Force Wright Aeronautical Laboratories, Air Force Systems Command, Wright-Patterson Air Force Base, Ohio 45433	12. REPORT DATE: July 1977
	13. NUMBER OF PAGES: 88 + ix
14. MONITORING AGENCY NAME & ADDRESS (if different from Controlling Office)	15. SECURITY CLASS. (of this report): Unclassified
	15a. DECLASSIFICATION/DOWNGRADING SCHEDULE

16. DISTRIBUTION STATEMENT (of this Report)

Approved for public release; distribution unlimited.

DDC RECEIVED NOV 3 1977 B

17. DISTRIBUTION STATEMENT (of the abstract entered in Block 20, if different from Report)

18. SUPPLEMENTARY NOTES

19. KEY WORDS (Continue on reverse side if necessary and identify by block number)

Transonic Airfoil Flow
Unsteady Flow
Finite Difference

20. ABSTRACT (Continue on reverse side if necessary and identify by block number)

Unsteady transonic flows over airfoils were calculated using a program based on the unsteady Euler equations. The approximate numerical solutions were obtained using an explicit (Lax-Wendroff) difference scheme.

Calculations were made for the 64A006 airfoil at zero angle-of-attack in flows with Mach number 0.822, 0.854 and 0.875. Three unsteady flows caused by a quarter-chord flap oscillating with an amplitude on the order of one degree at specific reduced

→ next page

DD FORM 1 JAN 73 1473 EDITION OF 1 NOV 65 IS OBSOLETE

Unclassified

SECURITY CLASSIFICATION OF THIS PAGE (When Data Entered)

147 650

frequencies ($k = \omega C/U_\infty$) near 0.4 were analyzed. The results were compared with other available calculations and the experimental data of Tijdeman.

Responses for an airfoil in a ventilated-wall wind tunnel rather than in a free-stream were also calculated. Exploratory study of the changes to be expected with a weakened shock (an attempt to simulate a main effect of the interaction of the shock with the airfoil boundary layer) was done for one case at Mach number 0.875.

Oscillatory flows over the 64A010 airfoil at zero angle-of-attack in a Mach 0.80 stream were also calculated. Plunging motion at reduced frequency 0.4 and pitching motions at reduced frequencies 0.4 and 0.5 were calculated.

FOREWORD

This report was prepared by the Convair Division of General Dynamics, San Diego, California, for the Analysis and Optimization Branch of the Air Force Flight Dynamics Laboratory (AFFDL), Wright-Patterson Air Force Base, Ohio. The research was conducted under Contract F33615-76-C-3018, "Time Dependent Finite-Difference Solutions for Transonic Flow." Dr. James J. Olsen, FBR, of AFFDL was the Air Force task engineer.

At Convair, Dr. H. Yoshihara was the principal investigator during the period from November 1975 through October 1976. The preparation of computer programs and the calculations were carried out by Dr. R. J. Magnus.

This report was submitted in April 1977 to cover research performed from November 1975 through April 1977.

The support of this research by Harvard Lomax, Charles Coe, and Sanford Davis of the NASA Ames Research Center and the furnishing of calculations and data for comparisons by William Ballhaus, Peter Goorjian, Joseph Steger, and Louis Stivers of NASA Ames are gratefully acknowledged.

TABLE OF CONTENTS

LIST OF FIGURES

LIST OF FIGURES (continued)

LIST OF FIGURES (Continued)

LIST OF FIGURES (Concluded)

LIST OF TABLES

SECTION I

INTRODUCTION

Except for some quite restrictive special problems, analysis of unsteady flows over airfoils in the transonic range was regarded with some uneasiness for a number of years. Tolerance for the use of numerical solutions on such problems has grown, and many efforts to provide useful transonic computation procedures have been carried out. Because an adequate assessment of the probability of encountering transonic aeroelastic instabilities may require checking many modes over a range of flight conditions, high value is placed upon keeping the aerodynamic calculation methods simple. Thus, assessments of the perturbation methods by comparison of solutions done by such methods with calculations done by methods containing fewer restrictive assumptions are of interest.

The work being reported here generated numerical solutions to a few problems on unsteady transonic flows over the NACA 64A006 and the NACA 64A010 airfoils. These examples include the 64A006 with oscillating quarter-chord flap at Mach numbers 0.822, 0.854, and 0.875 and the 64A010 in pitching and plunging motions at Mach number 0.80. Exploratory calculations of the effect on the oscillating flap results of wind tunnel walls were also carried out.

The program to generate these solutions is based upon the unsteady Euler equations in conservation form and the finite-difference procedure uses an explicit shock-capturing scheme. The choice of equations, and the numerical method preclude the method being applied to many transonic airfoil problems and the results cannot show flow details of a scale smaller than a few mesh

widths. Further, one should keep in mind that these are exploratory calculations using mesh sizes, means for assuring stability and means for handling boundary conditions which seemed appropriate for the ends desired. Changing the computational details would no doubt affect the results; however, little has been done to assess the effects of changing the details.

SECTION II

METHOD OF COMPUTATION

The unsteady Euler equations in conservation form are solved approximately with an explicit shock-capturing scheme. The program uses features quite similar to those described in earlier works.[1,2]

1. EQUATIONS

The computer program is designed to obtain numerical approximations to solutions for the unsteady Euler equations in conservation form:

$$\partial(\rho)/\partial t = -\partial(\rho u)/\partial x - \partial(\rho v)/\partial y \tag{1}$$

$$\partial(\rho u)/\partial t = -\partial(\rho u^2 + p)/\partial x - \partial(\rho uv)/\partial y \tag{2}$$

$$\partial(\rho v)/\partial t = -\partial(\rho uv)/\partial x - \partial(\rho v^2 + p)/\partial y \tag{3}$$

$$\partial(E)/\partial t = -\partial[u(E + p)]/\partial x - \partial[v(E + p)]/\partial y \tag{4}$$

Here, the usual meanings for fluid mechanics problems apply:

$$\begin{aligned} \rho &= \text{fluid density} \\ p &= \text{pressure} \\ u, v &= \text{Cartesian fluid velocity components} \\ x, y &= \text{Cartesian coordinates} \\ t &= \text{time} \\ \gamma &= \text{adiabatic index} \\ E &= p/(\gamma - 1) + (\rho/2)(u^2 + v^2) \\ &= \text{total energy per unit volume} \end{aligned} \tag{5}$$

[1] Magnus, R. and Yoshihara, H., "Inviscid Transonic Flow over Airfoils" AIAA Journal, Vol. 8, No. 12, pp. 2157-2162, December 1970

[2] Magnus, R. and Yoshihara, H., "Unsteady Transonic Flows over an Airfoil" AIAA Journal, Vol. 13, No. 12, pp. 1622-1628, December 1975

The coupled system, Equations 1 through 4, has the form:

$$\partial W/\partial t = -\partial F/\partial x - \partial G/\partial y \qquad (6)$$

where W, F and G are four-element vectors whose elements may be discerned by inspection.

In the computer program the system represented by Equation 6 is solved approximately by setting up arrays of about 5500 points in the x-y plane at which the 4 components of the dependent variable W are defined; the elements of F and G are non-linear functions of the elements of W. The partial derivatives on the right hand side are approximated by finite-differences between values of F and G at suitably adjoining mesh nodes near the point being worked on and the values of W are integrated, approximately, in time using discrete time steps. In the existing computer program, airfoil boundary conditions are maintained at (on the order of) 100 of the mesh nodes distributed along a contour which would coincide with the airfoil if the airfoil were in its mean position.

2. GRID ARRANGEMENT

The geometric field is covered with a number of grids having a total of about 5500 nodes. The grids of the outer part of the field are rectangular with uniform spacing in the chordwise direction and non-uniform lateral spacing (y-stretched spacing outboard of $|y| = 0.32$ chord). Within a rectangle circumscribed about the airfoil ($-0.26 \leq x \leq 1.34$ chords and $-0.32 \leq y \leq 0.32$ chords) two grids with uniform $\Delta x = 0.04$ chords and nonuniform y - spacing with $\Delta y \leq 0.04$ chords are used. These two grids have y - squashing and y - overlap so that there are nodes of these systems distributed along the upper and lower airfoil surfaces except on the blunt part of the nose. The two systems of distorted lines become horizontal and coincident a short distance behind the trailing edge and ahead of the nose. A portion of the lenticular gap containing and conforming to the non-blunt part of the airfoil is covered over at the nose by a local sheared

elliptic system conforming to the blunt part of the airfoil nose. To provide added detail of shocks, bands of $\Delta x = 0.01$ mesh are established where needed to override the 0.04 chord quasi-squares immediately surrounding the airfoil. The shock-resolving mesh bands are 0.20 chord wide and are shifted fore and aft in 0.08 chord steps if the shock moves out of the central 8 spaces of the band.

The central block of rectangular mesh outboard of the 0.04 chord quasi-squares surrounding the airfoil has $\Delta x = 0.08$ chord spacing as do two blocks of mesh ahead of and behind the airfoil. Further upstream and downstream there are blocks with $\Delta x = 0.16$ and $\Delta x = 0.32$ chords; the field is thus extended to about 10 chords ahead of and behind the airfoil.

The spacing in each coarser rectangular mesh is a power of two larger than the spacing in each finer mesh, and lines of the coarser meshes form the perimeter lines and some of the interior lines of the finer meshes. This conformation of grids makes the data exchanges between the various systems simple and also simplifies the synchronization of the calculations that progress at different rates in the various grids.

Waves propagating in one grid may be partially reflected when passing into another grid of different coarseness because of inevitable differences in the dispersive and diffusive truncation errors for the two systems.

3. DIFFERENCE SCHEME

An explicit two-step, finite-difference scheme of the Lax-Wendroff type was used. The scheme is the one described by Thommen[3] and has been adapted for the present work by dropping the true viscous terms and substituting a diffusion. The diffusive damping was used in the region of the shock.

[3] Thommen, Hans U., "Numerical Integration of the Navier-Stokes Equations" Journal of Applied Mathematics and Physics, (ZAMP) Vol. 17, Fasc. 3, pp. 369-384, May 1966

In calculating steady flows, the diffusive damping was adjusted according to shock strength to suppress the ragged overshoots at shocks which are a characteristic of Lax-Wendroff difference schemes. On unsteady problems, a single (compromise) damping factor was usually used and there was some tendency for weak shocks to become indistinct because of unnecessarily large damping.

4. SYNCHRONIZATION

With an explicit differencing scheme, the calculation is stable only if the time step is limited. Based upon typical expected flow conditions and a knowledge of the characteristics of the scheme, Δt was set at $0.35\ \Delta x$; here, a time unit is defined as C/a^*_∞ where C is the airfoil chord and a^*_∞ is the critical speed in the free stream.

In advancing the solution in a finer mesh region imbedded in a (say, twice greater mesh-size) coarser region, two time steps are made in the finer region for each one in the coarser. Thereafter, the two solutions are adjusted by an exchange of data. The solution in the finer mesh is assigned to replace the coarser mesh solution at corresponding points in the interior of the finer mesh, and the solution in the coarser mesh is interpolated onto the perimeter of the finer mesh region. Similar principles are used in exchanging data between the Cartesian and the sheared regions.

5. BOUNDARY CONDITIONS

The problems treated here all deal with rigid body motion of the profile or flap. The mesh system is independent of time (except for the fine-mesh patches around shocks) and the airfoil boundary conditions are satisfied at those mesh nodes which lie along the time-averaged position of the airfoil surface.

When tangency boundary conditions are to be satisfied at the airfoil surface the advanced values of the dependent variables at the airfoil nodes are found by a sequential process: a) A one-sided difference procedure (obtaining data only from the exterior of the airfoil) is used to obtain tentative values for the density, energy and velocity components. b) The flow velocity component along the surface normal (whose direction may be a function of time) is adjusted to match the mechanical velocity of the surface in that direction. The adjustment alters the normal velocity, density, and energy in the manner that they would be altered by a plane isentropic wave propagating outward from the surface.

Similar wave principles are used to match pressures and flow directions along the upper and lower sides of the line extending aft of the trailing edge. The geometric trailing edge lies between mesh nodes and no further specific steps are in the program to enforce the Kutta condition.

If the boundary condition to be enforced were to be the assignment of a particular pressure, the wave emitted (substituting for step (b) in the sequential process described above) would be chosen to cause the desired pressure and the "final" velocity normal to the surface would be a consequence of the wave. Suitable modifications to this wave process thus allowed enforcement of free-jet boundary conditions and idealized conditions at ventilated wind tunnel walls.

At the perimeter of the computation field the flow variables have been held fixed at some pre-selected values during the solution of each unsteady flow problem. When steady flow problems of lifting airfoils were solved, the circulation on the perimeter would be adjusted periodically to match the lift (obtained by integrating airfoil pressures).

The effects of some of the approximations in satisfying airfoil and field-perimeter boundary conditions were studied in another recent work[4] and found to be non-negligible for the problems studied. The mesh system used in the present program (with y-stretching) probably lessens the errors from the inaccuracy of the field perimeter boundary conditions. The errors due to satisfying unsteady airfoil boundary conditions at fixed nodes rather than at nodes on the translating airfoil surface necessitates a warning to the reader that the "solutions" generated in the present work might be applicable only for vanishingly small oscillation amplitudes.

6. COMPUTATIONAL NOTES

Geometric information on each problem was digested, mesh setup operations were carried out and interpolation instructions for exchanges of data between meshes were written by a preparatory program. The time-integrations to solve the unsteady problems were carried out by a main program which required about 150K (octal) words of storage on a CDC system. The programs are coded in FORTRAN extended language with some measures to take advantage of the particular capabilities of the CDC 7600 central processor. An FTN (OPT = 2) compilation was made and, generally, the problem would be run in stages of no more than about 10 minutes computing for each stage. This would permit inspection of progress before electing to continue. A typical problem, the Mach 0.875 flow over the 64A006 airfoil with flap oscillating at reduced frequency 0.468, might be followed for 3 1/2 oscillation cycles before a (loosely stated) repeatable oscillatory response was obtained; this would require about 2400 seconds of central processor time.

[4] Magnus, R. J., "Computational Research on Inviscid, Unsteady, Transonic Flow Over Airfoils" Convair Rpt. CASD/LVP 77-010, January 1977

A few exploratory calculations were made using special vector-algebra routines (coded for the CDC-7600 by the NASA-Ames Computer Fluid Dynamics group) in the principal centered-finite-difference scheme of the program. There was little increase in computational speed, probably because the computational field was broken into small blocks of mesh having no more than 410 nodes in each block and, in fact, the vectors operated upon by the special subroutines never had more than 41 elements. This is too small a number for the routines to be efficient.

Some improvement in program speed was accomplished by coarsening the mesh used around the blunt part of the nose. Because the mesh around the nose is smaller than anywhere else in the field, the explicit difference scheme must make many time steps in the nose region for each time step in the 0.04 chord mesh along the airfoil.

The program had been constructed specifically to calculate flows over the 64A006 with oscillating flap. The program was modified repeatedly to permit calculations over pitching and plunging airfoils, assignment of pressures on parts of the airfoil surface, inclusion of wind tunnel walls, etc. No formal documentation on the program has been prepared.

SECTION III

CALCULATED EXAMPLES

Calculations were made on two airfoils for a small number of operating conditions. Because of the expense of running the computer program, attention has been concentrated on examples which would display transonic phenomena of interest because of related experimental studies or to furnish examples for comparison with calculations done by other methods.

1. THE NACA 64A006 WITH C/4 FLAP

The only readily available modern experimental data on oscillatory transonic flow over airfoils is in the work of Tijdeman.[5-10] The NACA 64A006 airfoil with a quarter-chord oscillating flap was used in these experiments and this configuration was the subject for most of the calculations in the current research.

[5] Tijdeman, H. and Bergh, H., "Analysis of Pressure Distributions Measured on a Wing With Oscillating Control Surface in Two-Dimensional High Subsonic and Transonic Flow" Rpt. NLR-TR F.253, March 1967

[6] Tijdeman, H. and Schippers, P., "Results of Pressure Measurements on an Airfoil with Oscillating Flap in Two-Dimensional High Subsonic and Transonic Flow (Zero Incidence and Zero Mean Flap Position), Rpt. NLR TR 73078U, July 1973

[7] Tijdeman, H. and Schippers, P., "Results of Pressure Measurements on a Lifting Airfoil with Oscillating Flap in Two-Dimensional High Subsonic and Transonic Flow" Rpt. NLR TR 73018L, November 1974

[8] Tijdeman, H., "On the Motion of Shock Waves on an Airfoil With Oscillating Flap in Two-Dimensional Transonic Flow" Rpt. NLR TR 75038U, March 1975

[9] Tijdeman, H., "High Subsonic and Transonic Effects in Unsteady Aerodynamics" Rpt. NLR TR 75079U, May 1975

[10] Tijdeman, H., "On the Unsteady Aerodynamic Characteristics of Oscillating Airfoils in Two-Dimensional Transonic Flow" Rpt. NLR MP 76003U, March 1976

1.1 STEADY FLOW WITH NO FLAP DEFLECTION

Figure 1a shows the pressure distribution calculated for the flow over a NACA 64A006 airfoil at zero angle of attack at three Mach numbers. Tijdeman's experimental pressure distributions[6,7] are reproduced in Figure 1b for comparison.

It may be seen that there are appreciable differences between the calculated and experimental results. At any specified Mach number the calculated flows are more supercritical than the experimental and the calculated pressures on the aft part of the airfoil are more positive than the experimental values. These discrepancies may be attributed to computational inaccuracies and the influences of wind tunnel wall interference and the viscous effects which are present in the experiments but not accounted for in the calculations.

Inasmuch as the magnitude and the lag of unsteady pressure excursions (behind the flap motion) on the forward parts of airfoils with oscillating flaps depend on the streamwise lengths and the heights of the supersonic regions (see Tijdeman[5,8,9,10]) one should not expect to find good agreement between inviscid unsteady calculations of flow over an airfoil in a free stream and the unsteady wind tunnel experiments at any specified Mach number when the basic steady flows over the airfoil differ significantly.

1.2 STEADY FLOW WITH DEFLECTED FLAP

Pressure distributions calculated at Mach numbers 0.822, 0.854, and 0.875 for the 64A006 with quarter-chord flap deflected by 1.5, 1.0 and 1.0 degrees respectively are compared to the experimental results of Tijdeman in Figures 2a through 2c which present the normalized pressure excursions (calculated as $(p_{lower} - p_{upper})/\delta$ flap) at a number of points along the airfoil chord. In each case the calculated pressure excursions exceed the measured

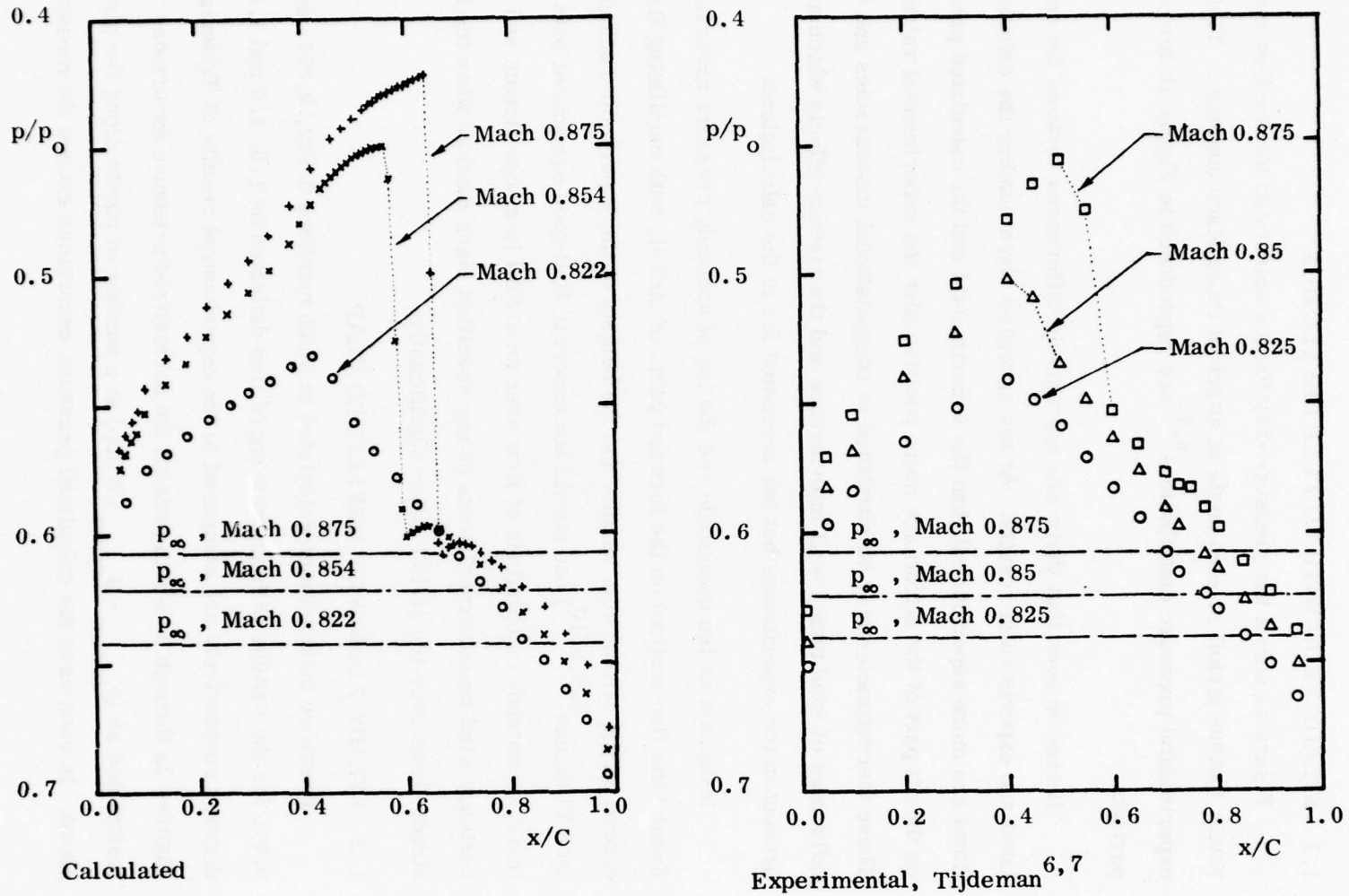

Figures 1a & b. Pressure Distributions on NACA 64A006 at Zero Angle-Of-Attack

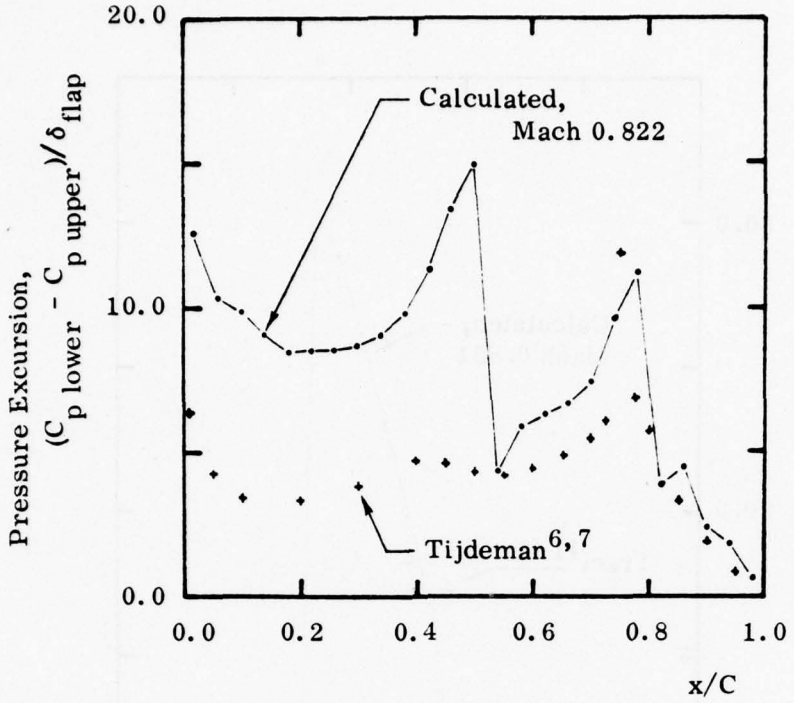

Mach 0.825

Figure 2a. Pressure Excursions due to Flap Deflection in Steady Flow. NACA 64A006 at Zero Angle-Of-Attack (continued)

values by a large factor over the forward portion of the airfoil. Traci[11] has also calculated this flow at Mach 0.85 and 0.875, and except for some parts of the airfoil ahead of the shock, the present calculations are in relatively poor agreement with Traci's results. Normalizing the data by dividing by the magnitude of the flap deflection unfortunately does not lead to a uniform presentation of the loading on the part of the airfoil traversed by the displaced shock. The pressure jump across the shock is determined by the upstream

[11]Traci, R. M., Albano, E. D. and Farr, J. L. Jr., "Small Disturbance Transonic Flows About Oscillating Airfoils and Planar Wings" Rpt. AFFDL-TR-75-100, August 1975

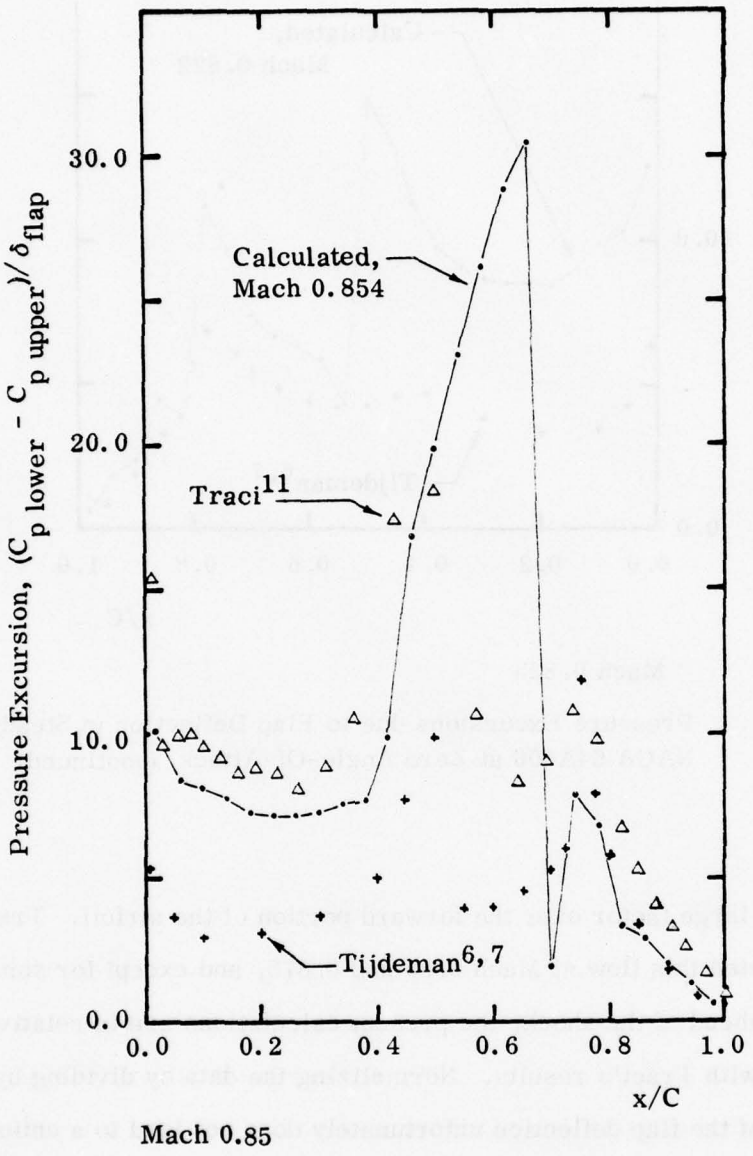

Figure 2b. (Continued)

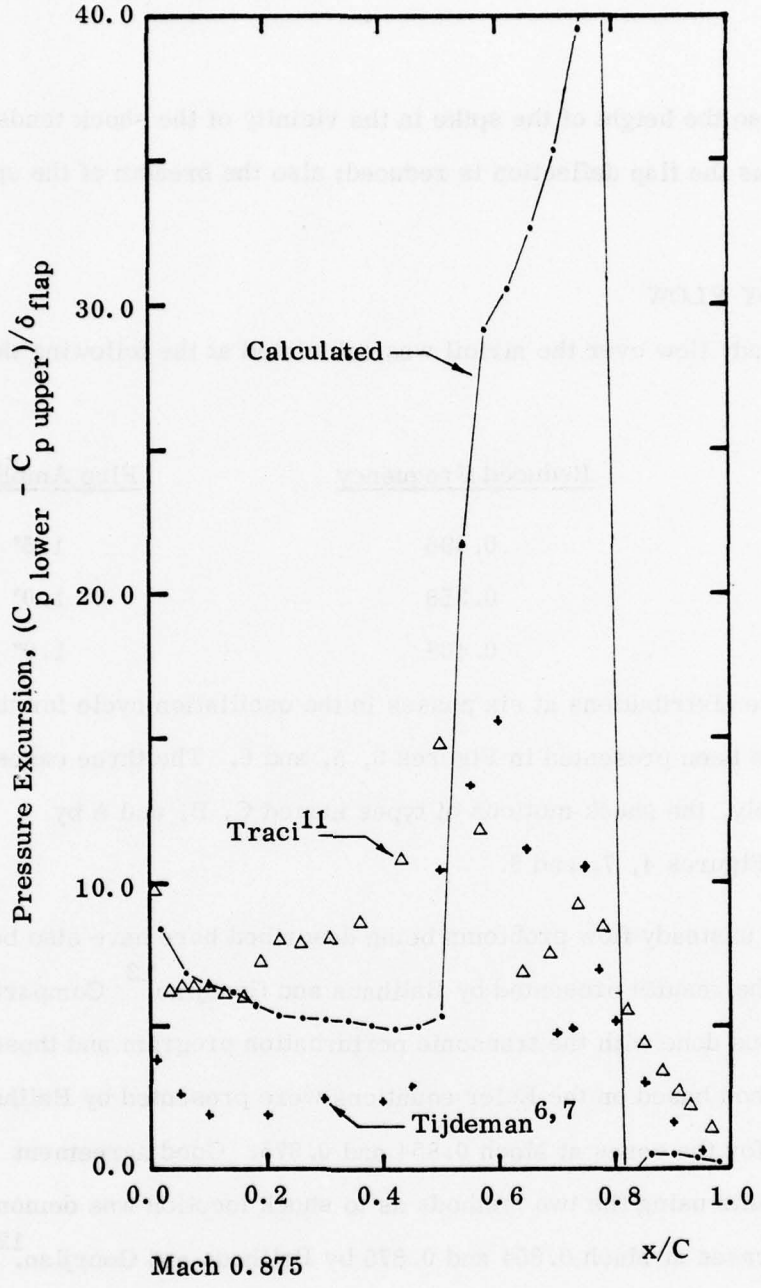

Figure 2c. Pressure Excursions due to Flap Deflection in Steady Flow. NACA 64A006 at Zero Angle-Of-Attack (Concluded)

flow conditions so the height of the spike in the vicinity of the shock tends toward infinity as the flap deflection is reduced; also the breadth of the spike decreases.

1.3 UNSTEADY FLOW

The unsteady flow over the airfoil was calculated at the following three conditions:

Mach Number	Reduced Frequency	Flap Amplitude
0.822	0.496	1.5°
0.854	0.358	1.0°
0.875	0.468	1.0°

Typical pressure distributions at six phases in the oscillation cycle for these three cases have been presented in Figures 3, 5, and 6. The three cases display, respectively, the shock motions of types named C, B, and A by Tijdeman;[8] see Figures 4, 7, and 8.

The three unsteady flow problems being described here have also been calculated and the results presented by Ballhaus and Goorjian.[12] Comparisons of the calculations done with the transonic perturbation program and those done here by the method based on the Euler equations were presented by Ballhaus and Goorjian[12] for the cases at Mach 0.854 and 0.875. Good agreement between the results using the two methods as to shock location was demonstrated for the cases at Mach 0.854 and 0.875 by Ballhaus and Goorjian.[12]

[12] Ballhaus, W. F. and Goorjian, P. M., "Implicit Finite-Difference Computations of Unsteady Transonic Flows About Airfoils, Including the Treatment of Irregular Shock-Wave Motions" AIAA Paper 77-205, Los Angeles, California, January 1977

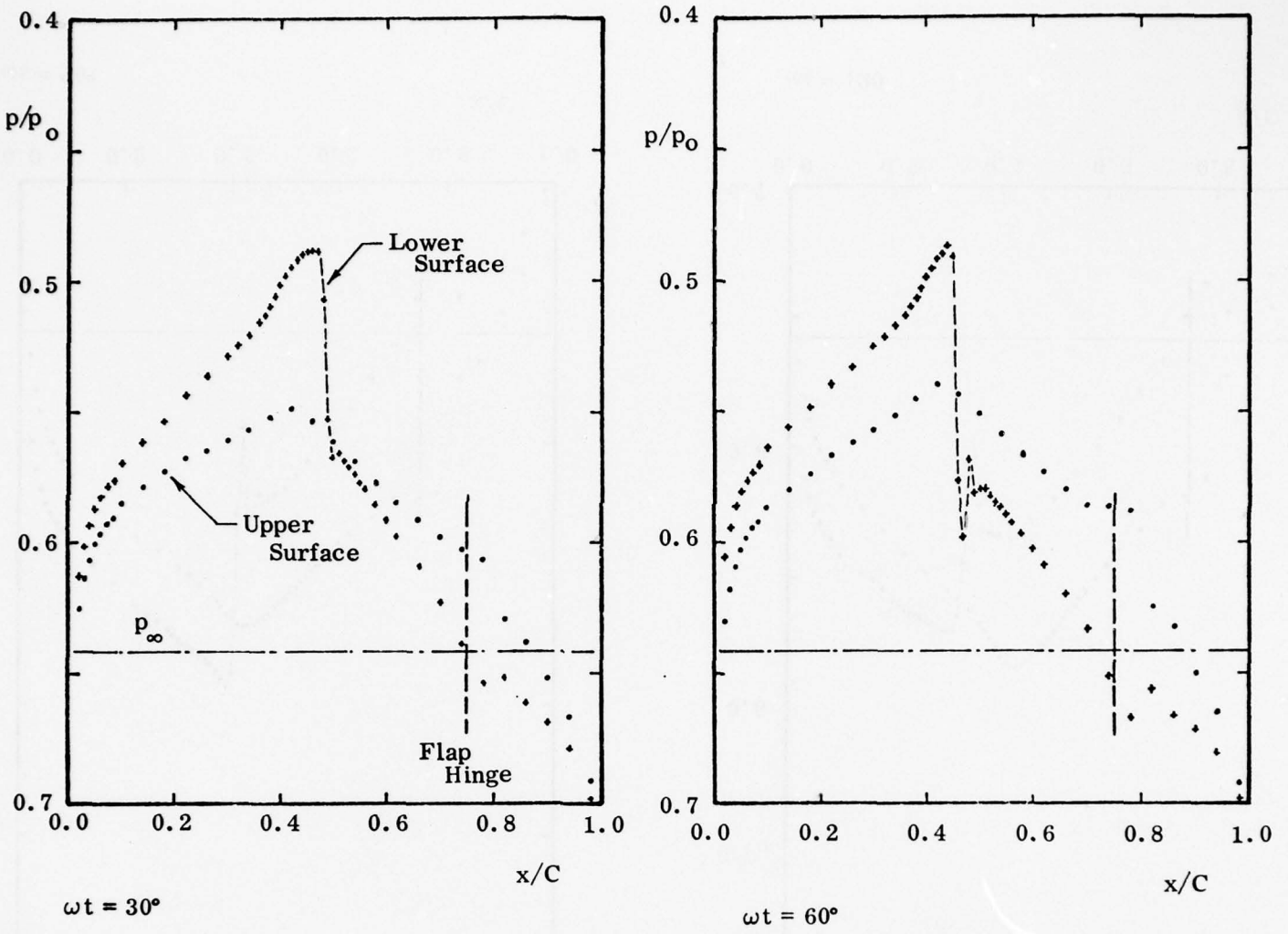

Figures 3a & b. Instantaneous Pressure Distributions on NACA 64A006 with Quarter-Chord Oscillating Flap Mach 0.822, Zero Angle-Of-Attack, Flap $\delta = 0 \pm 1.5°$, $k = 0.496$ (Continued)

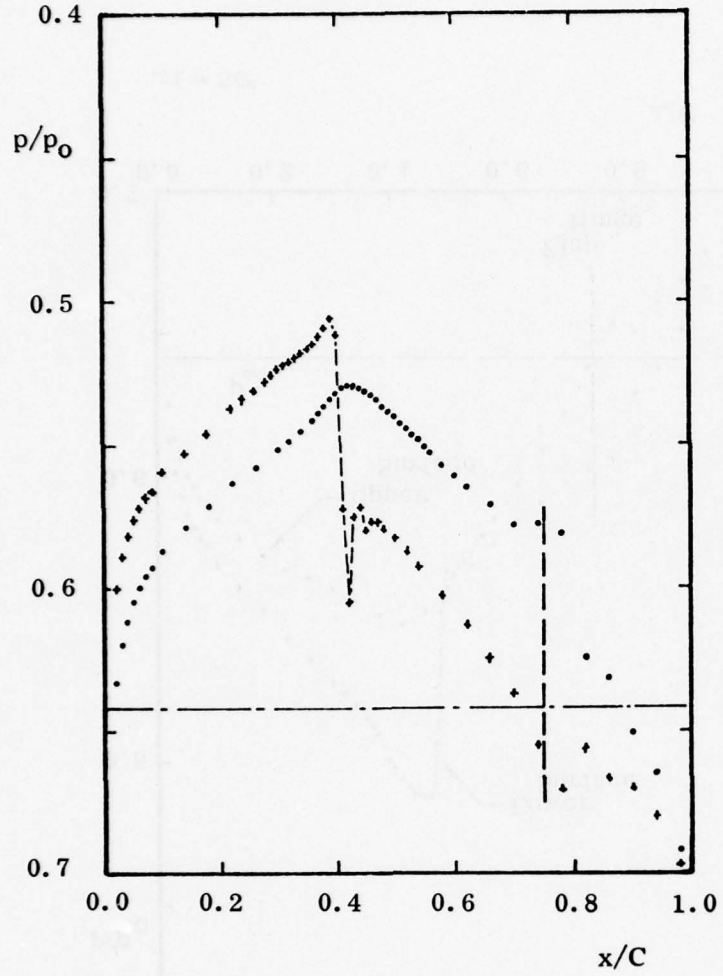

ωt = 90°

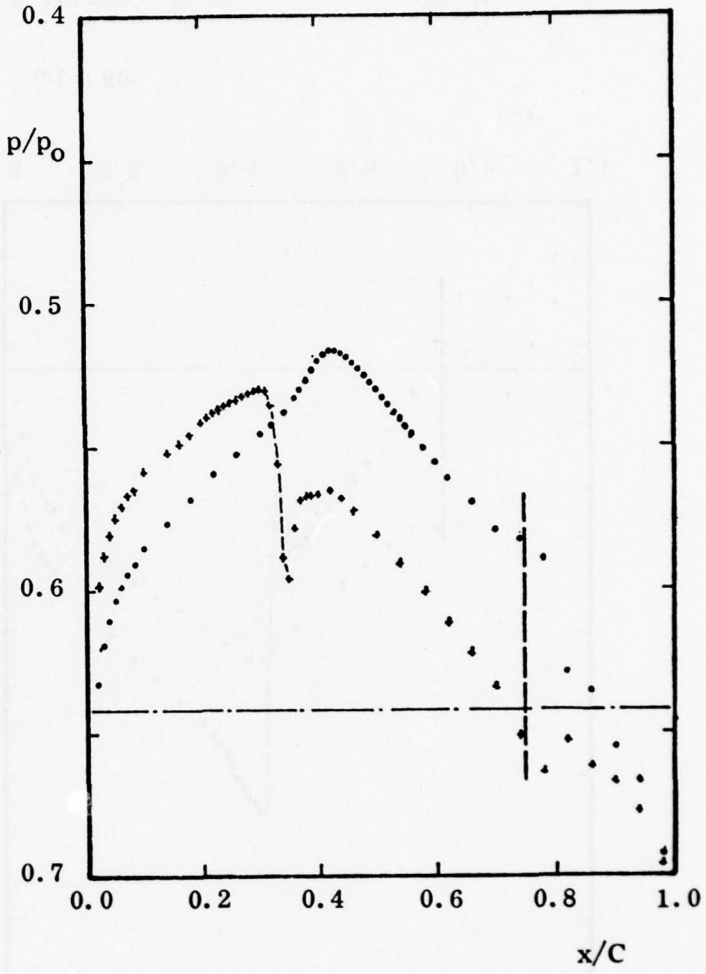

ωt = 120°

Figures 3c & d. (Continued)

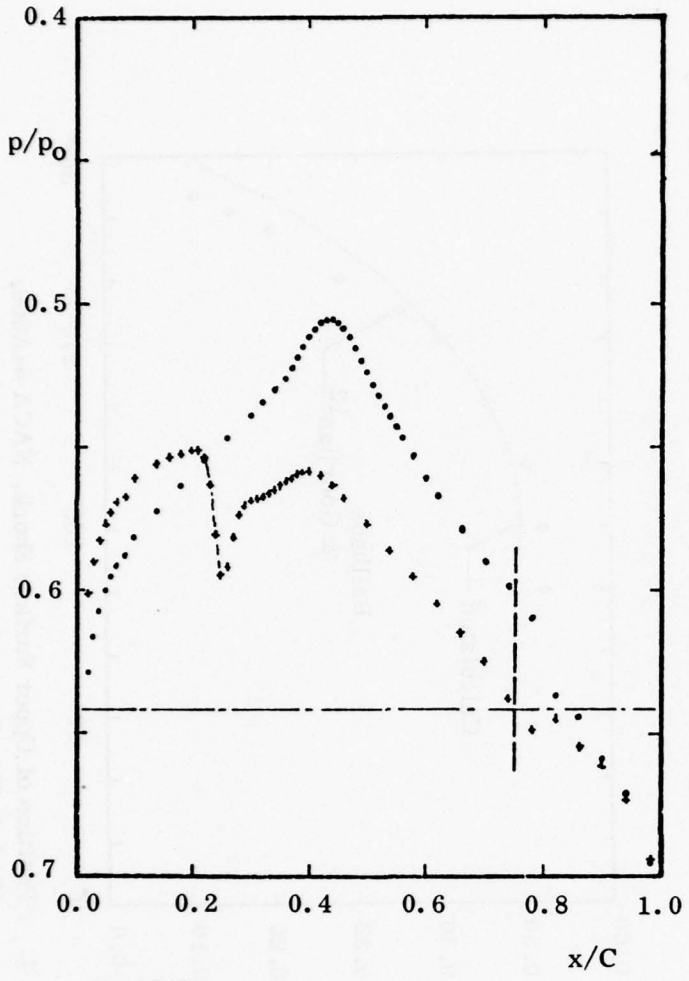

$\omega t = 150°$

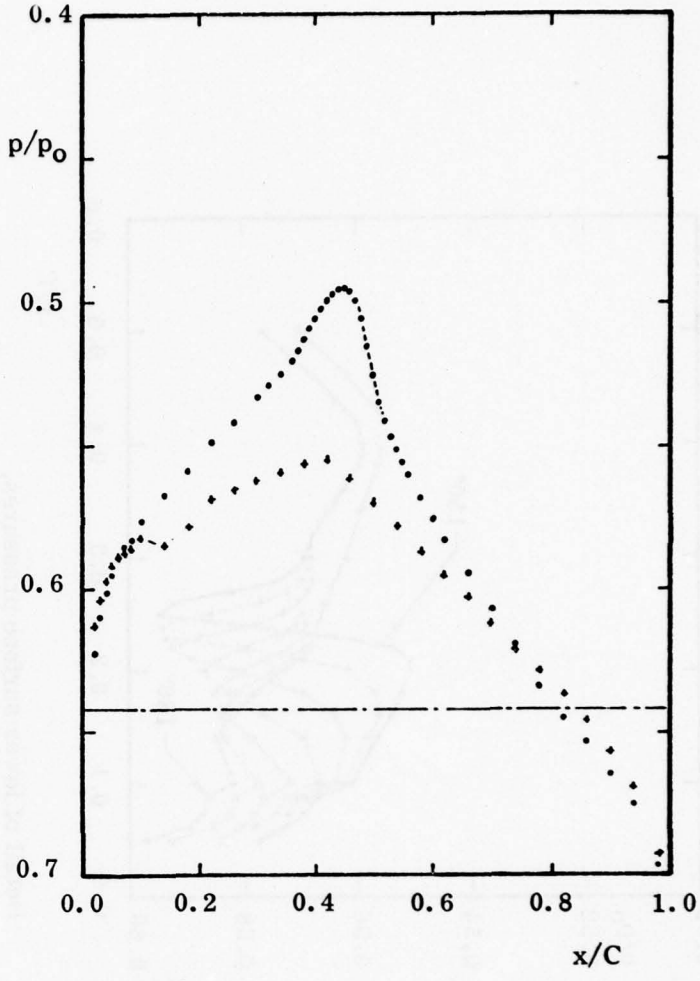

$\omega t = 180°$

Figures 3e & f. (Continued)

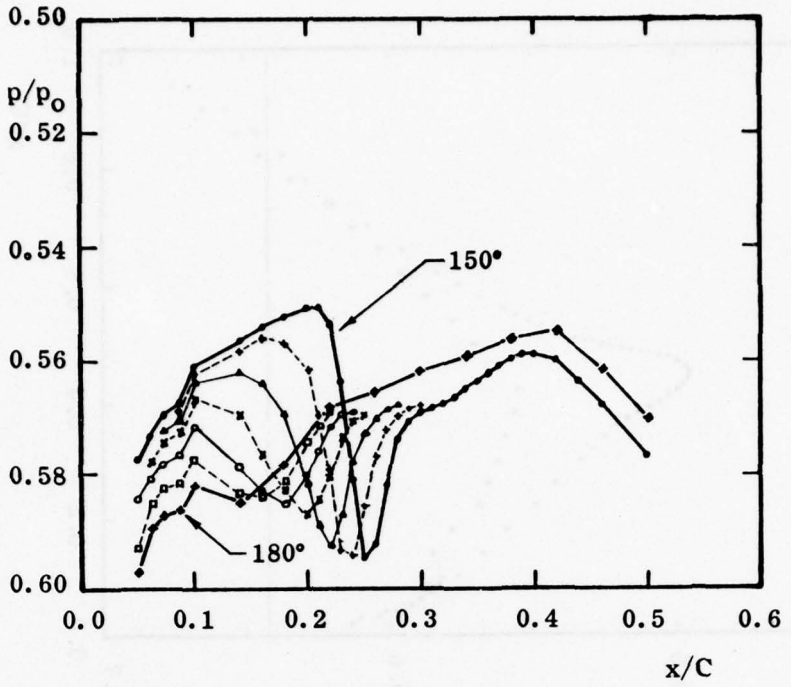

Detail of lower surface pressures,
$\omega t = 150°$ to $180°$

Figure 3g. Instantaneous Pressure Distributions on NACA 64A006 with Quarter-Chord Oscillating Flap. Mach 0.822, Zero Angle-Of-Attack, Flap $\delta = 0 \pm 1.5°$, $k = 0.496$ (Concluded)

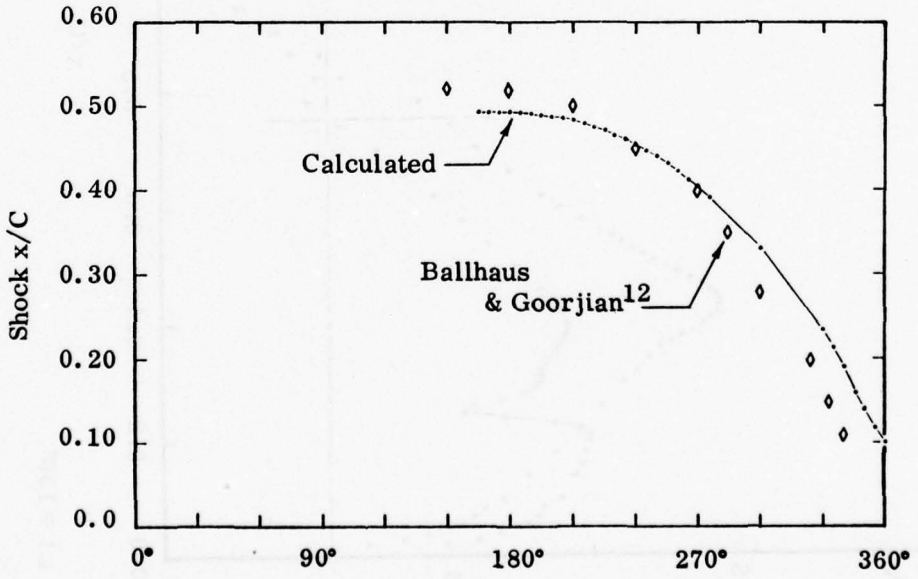

Figure 4. Position of Upper Surface Shock, NACA 64A006, Mach 0.822, $k = 0.496$

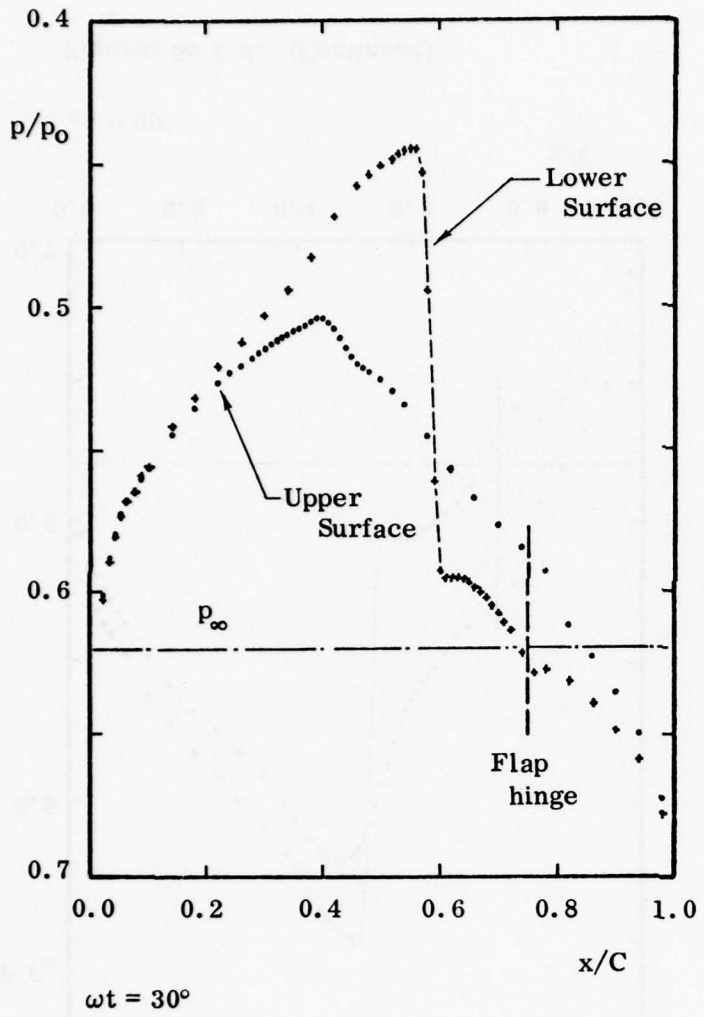

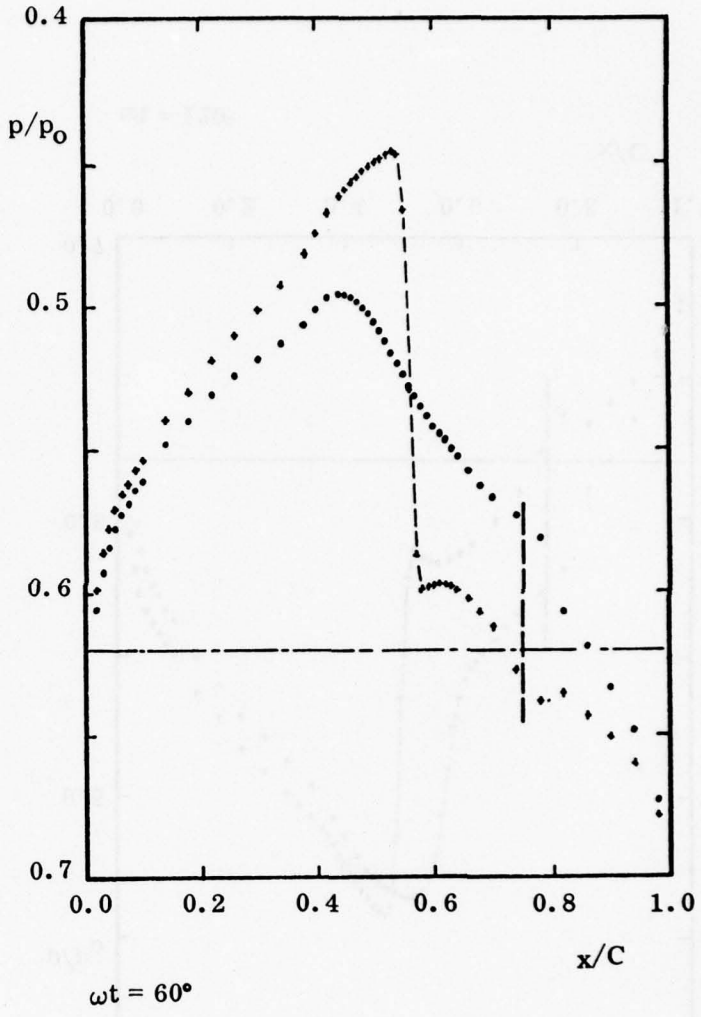

Figures 5a & b. Instantaneous Pressure Distributions on NACA 64A006 with Quarter-Chord Oscillating Flap Mach 0.854, Zero Angle-Of-Attack, Flap $\delta = 0 \pm 1.0°$, k = 0.358 (Continued)

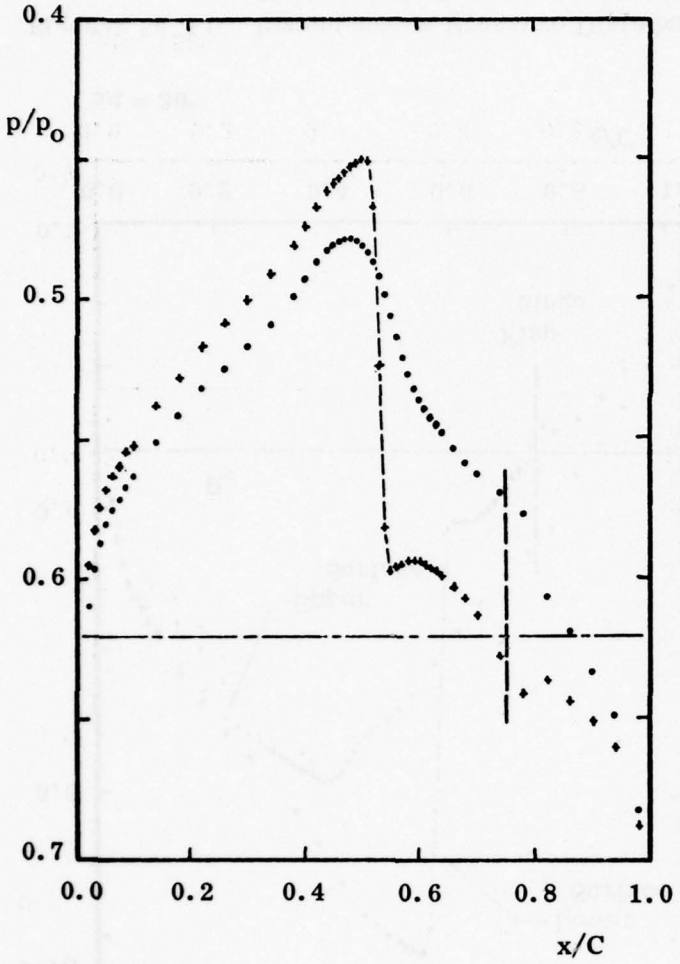

ωt = 90°

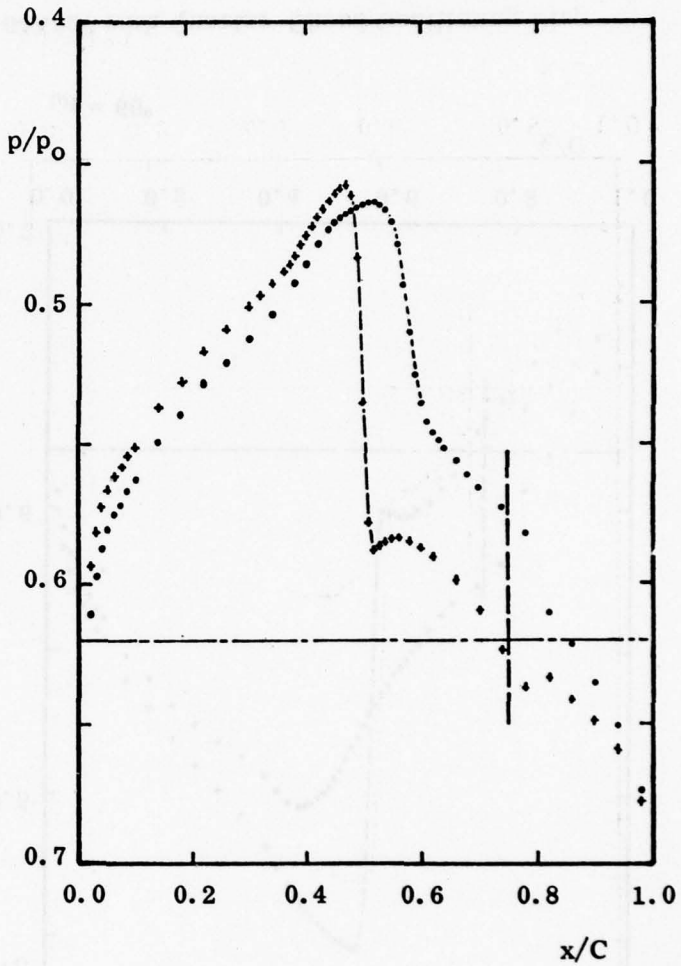

ωt = 120°

Figures 5c & d. (Continued)

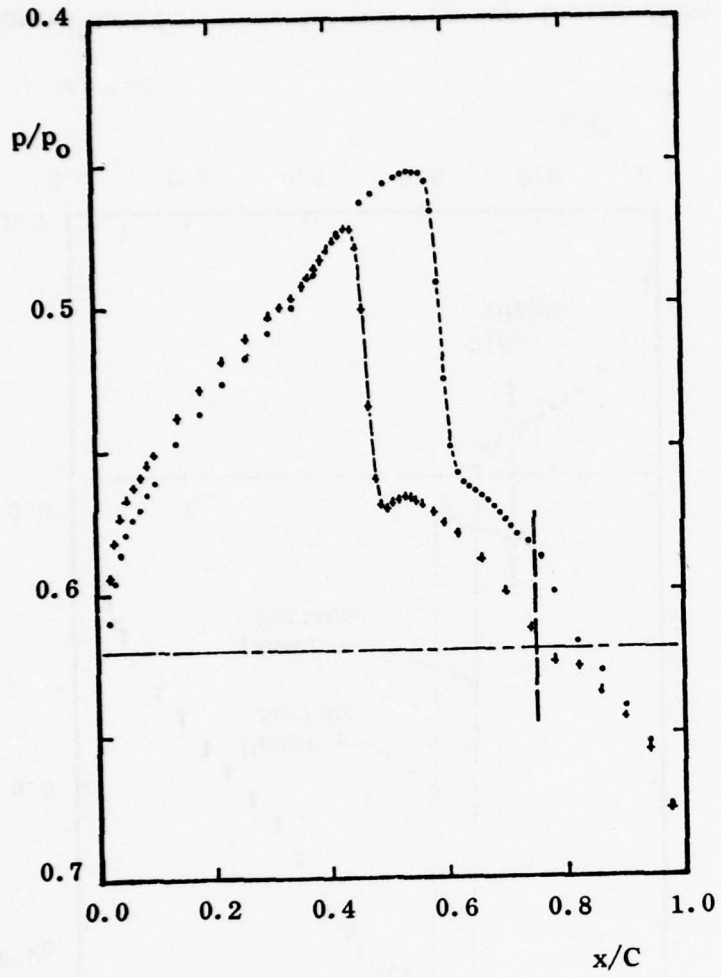

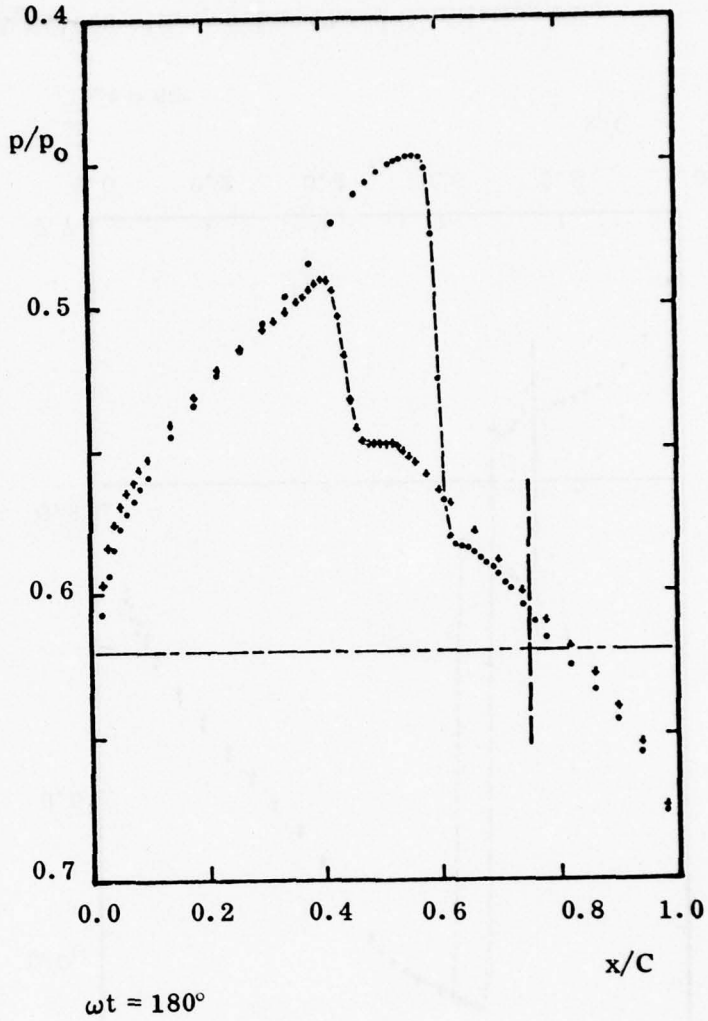

Figures 5e & f. Instantaneous Pressure Distributions on NACA 64A006 with Quarter-Chord Oscillating Flap Mach 0.854, Zero Angle-Of-Attack, Flap $\delta = 0 \pm 1°$, $k = 0.358$ (Concluded)

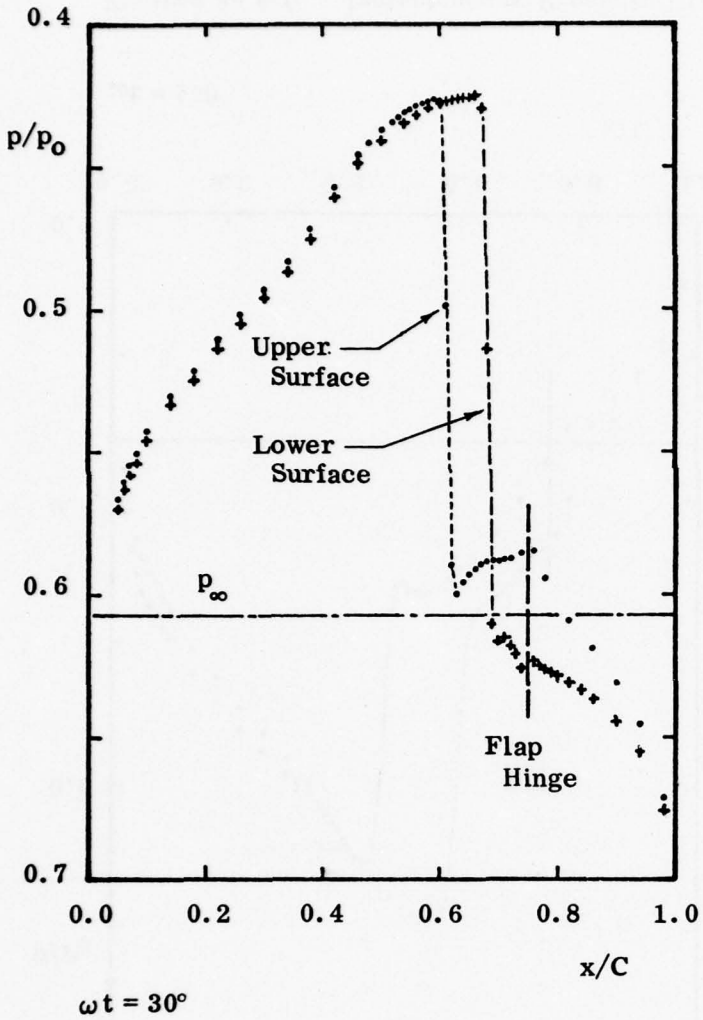

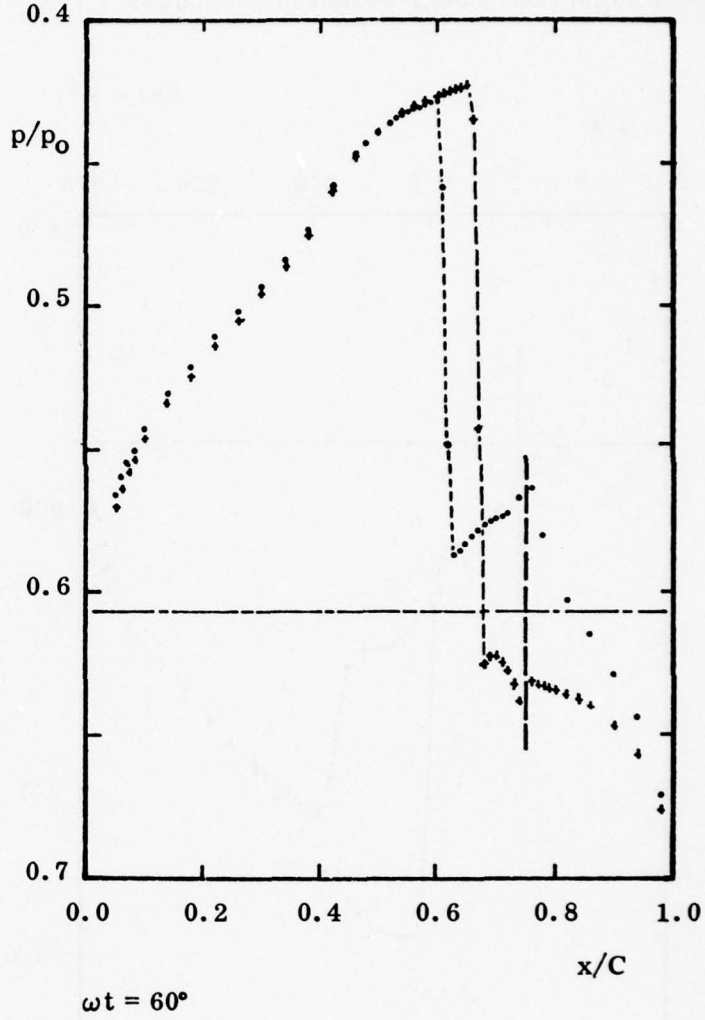

Figures 6a & b. Instantaneous Pressure Distributions on NACA 64A006 with Quarter-Chord Oscillating Flap Mach 0.875, Zero Angle-Of-Attack, Flap $\delta = 0 \pm 1.0°$, $k = 0.468$ (Continued)

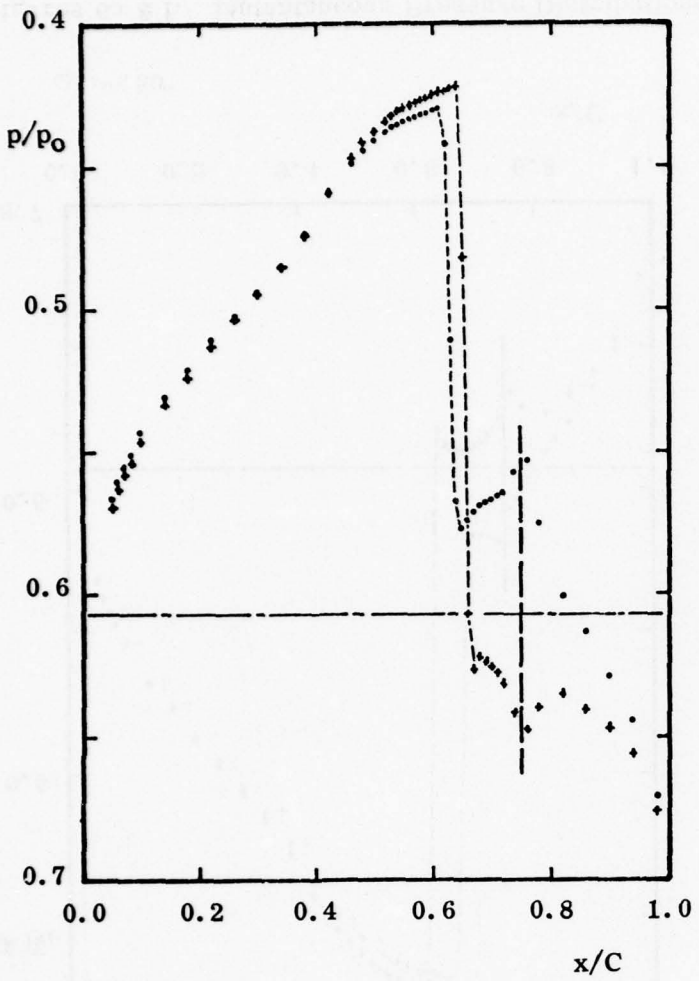

$\omega t = 90°$

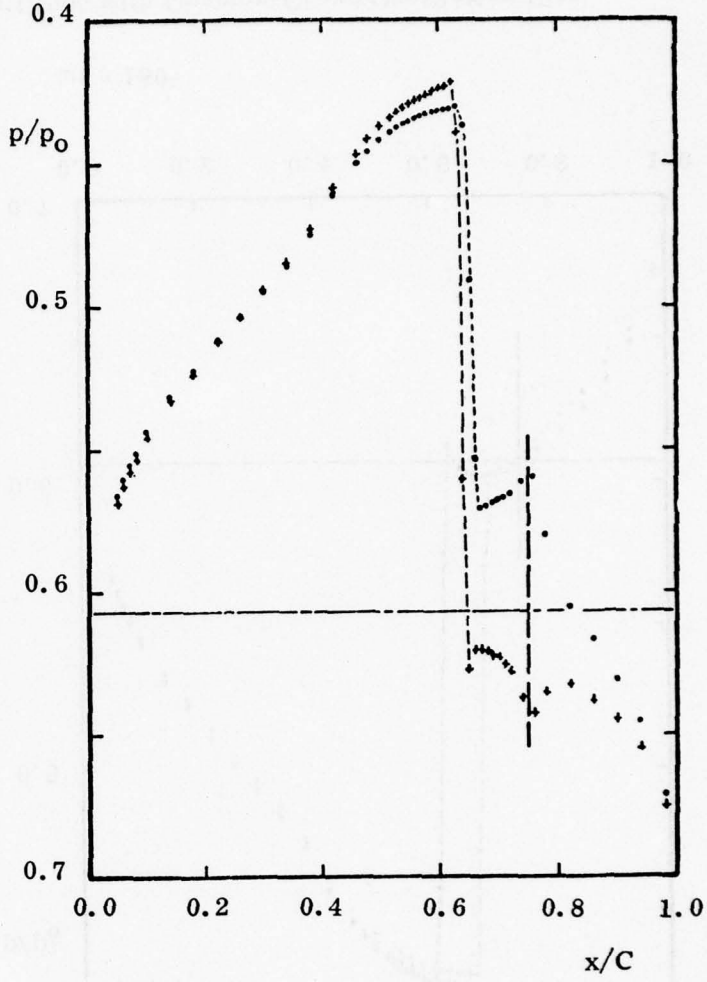

$\omega t = 120°$

Figures 6c & d. (Continued)

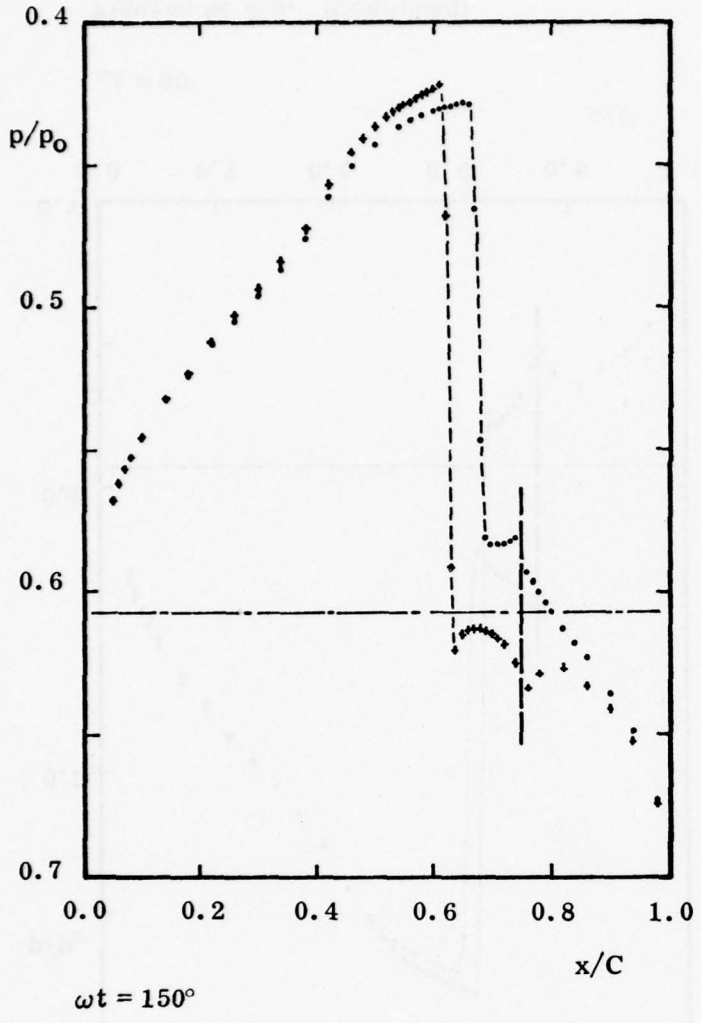

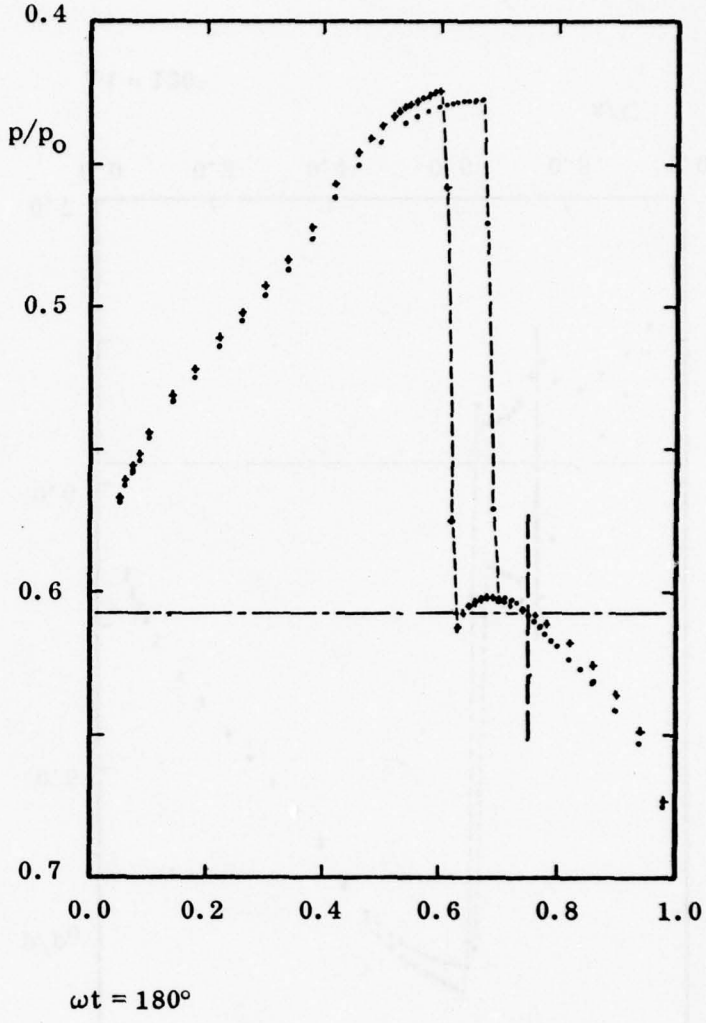

Figures 6e & f. Instantaneous Pressure Distributions on NACA 64A006 with Quarter-Chord Oscillating Flap Mach 0.875, Zero Angle-Of-Attack, Flap $\delta = 0 \pm 1.0°$, $k = 0.468$ (Concluded)

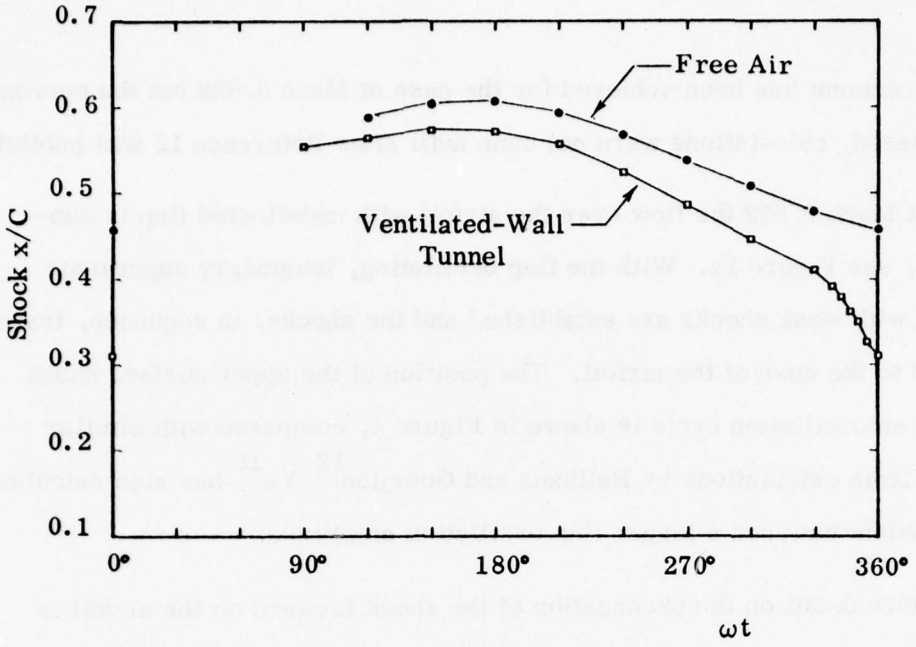

Figure 7. Position of Upper Surface Shock, NACA 64A006, Mach 0.854, k = 0.358

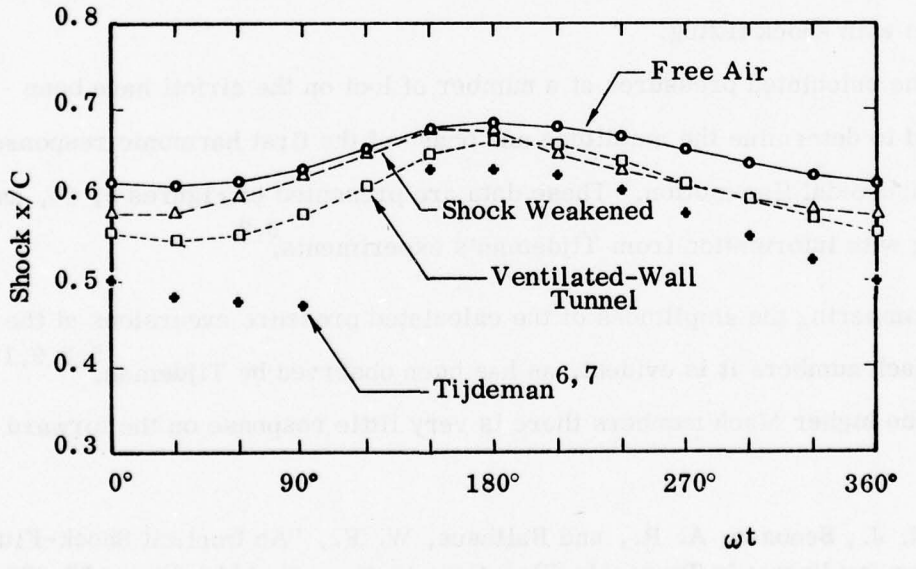

Figure 8. Position of Upper Surface Shock, NACA 64A006, Mach 0.875, k = 0.468

Fair agreement has been achieved for the case at Mach 0.822 but the current, Euler-based, calculations were not done until after Reference 12 was published.

At Mach 0.822 the flow over the airfoil with undeflected flap is subcritical, see Figure 1a. With the flap oscillating, temporary supersonic regions with weak shocks are established and the shocks, in sequence, travel forward to the nose of the airfoil. The position of the upper surface shock through an oscillation cycle is shown in Figure 4, compared with similar results from calculations by Ballhaus and Goorjian.[12] Yu[15] has also calculated this problem but used a larger flap oscillation amplitude.

More detail on the propagation of the shock forward on the airfoil is furnished in the pressure distributions shown in Figure 3g. Limitations on the forward movement of the refined "shock" mesh imposed by logic in the current program prevented the presentation of the shock profile in a 0.01 chord mesh if the shock ran forward of 0.20 chord. Better detail of the shock motion on this kind of problem has been obtained by Yu[15] using a transonic perturbation program with shock fitting.

The calculated pressures at a number of loci on the airfoil have been analyzed to determine the amplitude and phase of the first harmonic responses to the sinusoidal flap motion. These data are presented in Figures 9, 10, and 11 along with information from Tijdeman's experiments.[6,7]

Comparing the amplitudes of the calculated pressure excursions at the three Mach numbers it is evident, as has been observed by Tijdeman,[5,8,9,10] that at the higher Mach numbers there is very little response on the forward

[15] Yu, N. J., Seebass, A. R., and Ballhaus, W. F., "An Implicit Shock-Fitting Scheme for Unsteady Transonic Flow Computations," AIAA Paper 77-633, AIAA 3rd Computational Fluid Dynamics Conference, Albuquerque, New Mexico June 27-28, 1977

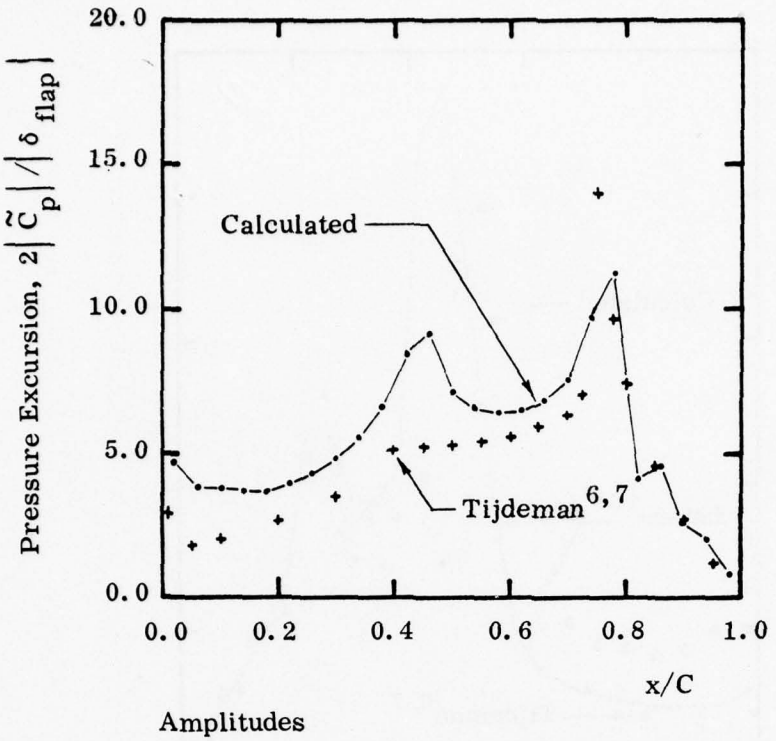

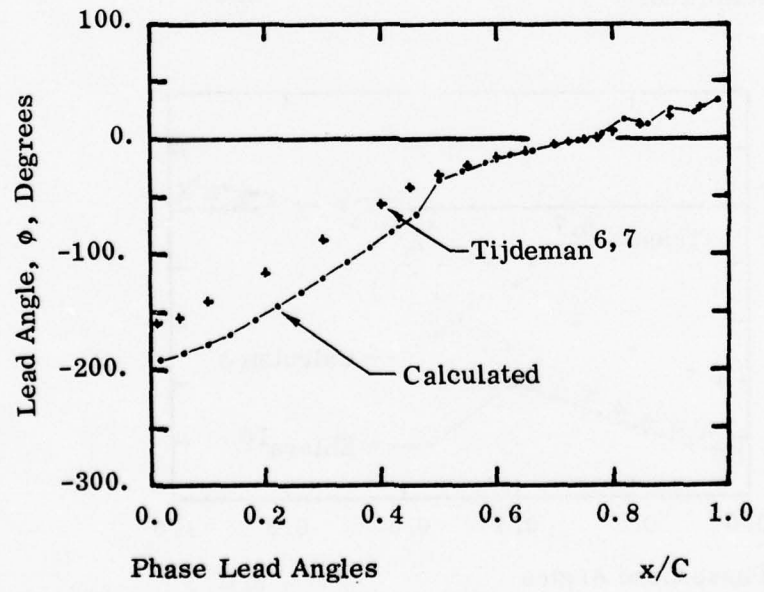

Figures 9a & b. Pressure Excursions Per Radian of Flap Deflection in Unsteady Flow. NACA 64A006 at Zero Angle-Of-Attack. Mach 0.822, k = 0.496

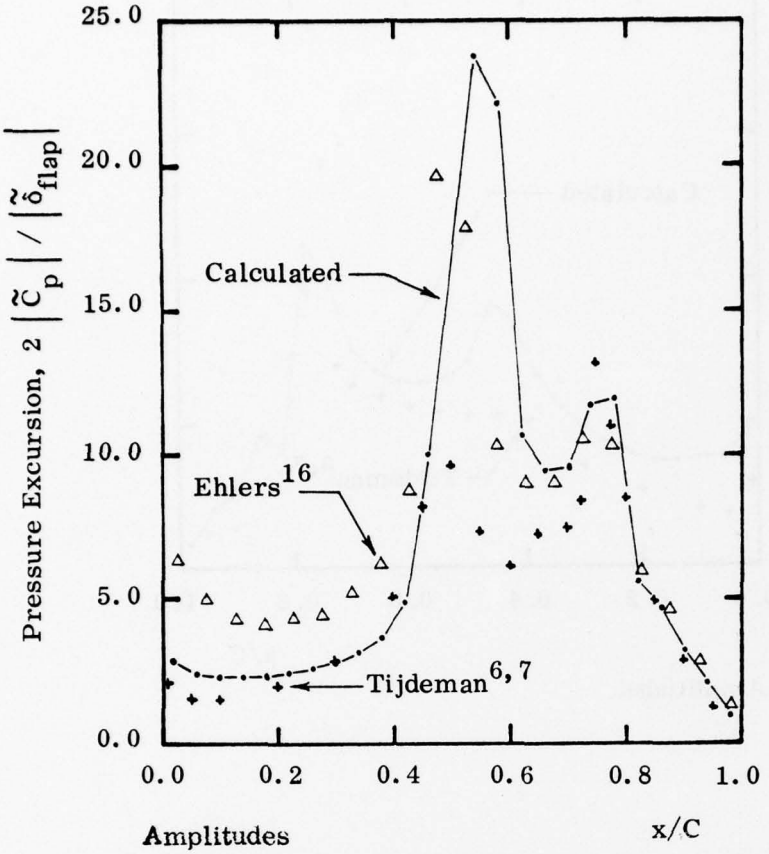

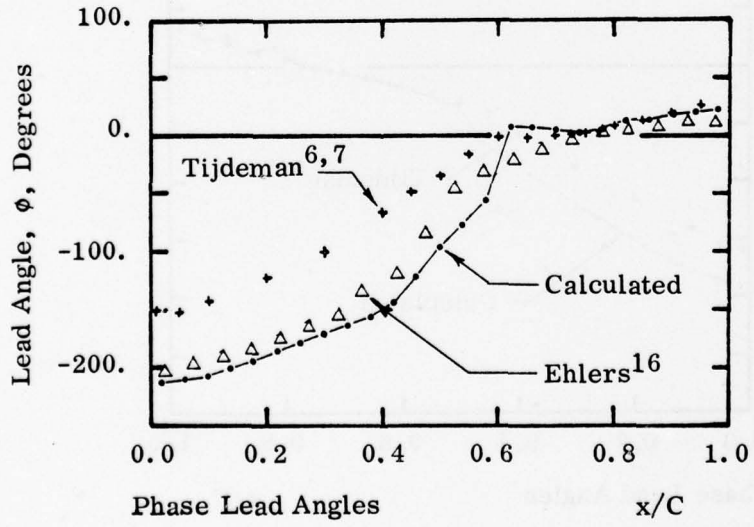

Figures 10a & b. Pressure Excursions Per Radian of Flap Deflection in Unsteady Flow. NACA 64A006 at Zero Angle-Of- Attack, Mach 0.854, k = 0.358

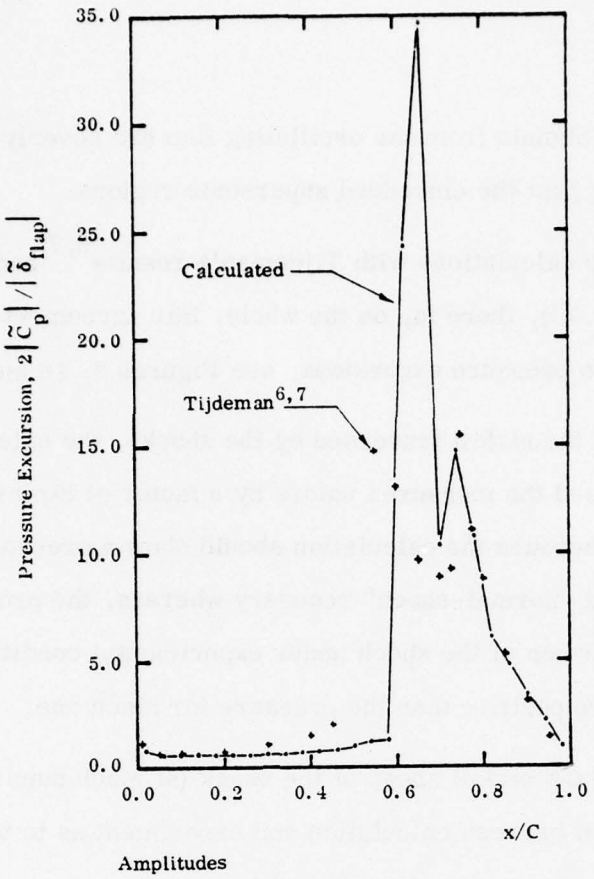

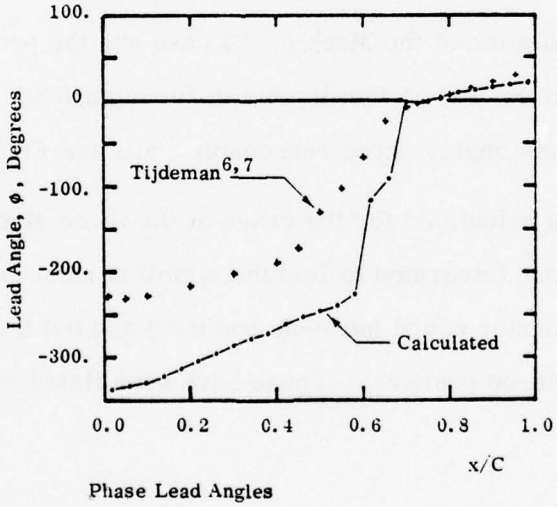

Figures 11a & b. **Pressure Excursions Per Radian of Flap Deflection in Unsteady Flow. NACA 64A006 at Zero Angle-Of-Attack. Mach 0.875, k = 0.468**

part of the airfoil. Signals from the oscillating flap are severly delayed and attenuated in getting past the embedded supersonic regions.

Comparing the calculations with Tijdeman's results[6,7] and looking first at the flap (X/C > 0.75), there is, on the whole, fair agreement in both amplitude and phase of the pressure excursions, see Figures 9, 10 and 11.

On the part of the airfoil traversed by the shocks, the calculated excursions generally exceed the measured values by a factor of two or more. This should be expected because the calculation should show a pressure rise at the shock approximating "normal-shock" recovery whereas, the pressure immediately downstream of the shock under experimental conditions ought to be only slightly more positive than the pressure for Mach one.

On the part of the airfoil ahead of the shock (at Mach numbers 0.854 and 0.875) the agreement between calculation and experiment as to both magnitude and phase of the pressure excursions is rather poor.

Ehlers[16] calculation of the Mach 0.854 case and the present results are in relatively good agreement on the flap but differ significantly in magnitude elsewhere. The phase angles agree reasonably well; see Figure 10.

The pressures calculated for the cases at the three Mach numbers mentioned previously were integrated to find the airfoil normal force, pitching moment about the quarter chord (nose-up positive) and the flap hinge moment (also considered nose-up positive). These have been listed in Table 1 for

[16]Ehlers, F. Edward, "A Finite Difference Method for the Solution of the Transonic Flow Around Harmonically Oscillating Wings" Rpt. NASA CR-2257, July 1974

TABLE 1. NORMALIZED FORCES AND MOMENTS DUE TO FLAP DEFLECTION, NACA 64A006 WITH QUARTER-CHORD FLAP, FIRST HARMONIC VALUES

Forces and Moments are per radian flap deflection

Flap Motion:

$\delta(t) = \sin(\omega t)$

Trailing edge down is positive flap deflection δ.

ω = oscillation rate, radian/time unit

Reduced Frequency

$$k = \frac{\omega C}{U_\infty}$$

C = chord

U_∞ = Free stream velocity

Coefficients:

C_L = Airfoil Lift/q C

C_m = Airfoil nose-up moment about quarter chord/ q C^2

C_n = Flap hinge moment/q C^2, moment forcing trailing edge down is considered positive.

q = Free stream dynamic pressure

Typical Response Function:

$C_L(t) = \left|\tilde{C}_L\right| \sin(\omega t + \phi)$

If ϕ is positive, the peak C_L occurs before the flap gets to its fully-down position, tabulated ϕ in degrees.

Motion Description, Researcher, Mach Number	$\left\|\tilde{C}_L\right\|$	ϕ	$\left\|\tilde{C}_m\right\|$	ϕ	$\left\|\tilde{C}_n\right\|$	ϕ
Quasi-Steady, k = 0.00						
Mach number $\doteq$ 0.825						
Inviscid Calculation, Magnus, Mach 0.822	7.93	-	-1.32	-	-.0794	-
Experiment, Tijdeman,[6,7] Mach 0.825	4.24	-	-1.01	-	-.0600	-

TABLE 1 (continued)

Motion Description, Researcher, Mach Number	$\lvert\tilde{C}_L\rvert$	ϕ	$\lvert\tilde{C}_m\rvert$	ϕ	$\lvert\tilde{C}_n\rvert$	ϕ
Quasi-Steady, k = 0.00 Mach Number ≐ 0.85						
Inviscid Calculation, Magnus, Mach 0.854	10.08	-	-2.20	-	-.0594	-
Inviscid Calculation, Magnus, Mach 0.854, Ventilated Wall	4.82	-	-1.45	-	-.0725	-
Perturbation Calculation, Traci,[11] Mach 0.85	10.6	-	-1.54	-	-.092	-
Perturbation Calculation, Traci[11] Mach 0.85, Porous Wall	7.4	-	-	-	-	-
Experiment, Tijdeman[6,7] Mach 0.85	4.43	-	-1.17	-	-.0563	-
Quasi-Steady, k = 0.000 Mach number ≐ 0.875						
Inviscid Calculation, Magnus Mach 0.875	12.39	-	-4.00	-	-.0700	-
Inviscid Calculation, Magnus, Mach 0.875, Ventilated Wall	5.59	-	-1.98	-	-.0425	-
Perturbation Calculation, Traci,[11] Mach 0.875	7.6	-	-1.7	-	-.088	-
Experiment, Tijdeman,[6,7] Mach 0.875	4.93	-	-1.57	-	-.0525	-

Unsteady, k = 0.496 **Mach Number = 0.822**						
Inviscid Calculation, Magnus, Mach 0.822	2.66	-46.	1.46	170.	0.0825	-164.
Perturbation Calculation, Ballhaus,[13] Mach 0.822, Time-Integration	3.3	-49.	1.7	166.	-	-
Perturbation Calculation, Ballhaus,[13] Mach 0.822, Indicial-Method	3.11	-51.	1.56	167.	-	-
Experiment, Tijdeman,[6,7] Mach 0.822, 120 Hz	3.11	-29.	1.36	176.	0.0775	-166.
Unsteady, k = 0 358 **Mach Number ≐ 0.854**						
Inviscid Calculation, Magnus Mach 0.854	3.10	-50.	1.65	157.	0.0944	-165.
Inviscid Calculation, Magnus Mach 0.854, Ventilated Wall	3.82	-36.	1.61	172.	0.0881	-160.
Perturbation Calculation, Ballhaus,[13] Mach 0.854, Time-Integration	3.3	-55.	1.7	157.	-	-
Perturbation Calculation, Ballhaus,[13] Mach 0.854, Indicial Method	3.08	-56.	1.70	154.	-	-
Perturbation Calculation, Ehlers,[16] Mach 0.858	3.2	-57.	1.9	157.	0.10	-174.
Experiment, Tijdeman,[6,7] Mach 0.858, 90 Hz	3.62	-24.	1.55	176.	0.0844	-167.

TABLE 1 (continued)

Motion Description, Researcher, Mach Number	$\lvert\tilde{C}_L\rvert$	ϕ	$\lvert\tilde{C}_m\rvert$	ϕ	$\lvert\tilde{C}_n\rvert$	ϕ
Unsteady, k = 0.468 Mach Number $\doteq$ 0.875						
Inviscid Calculation, Magnus Mach 0.875	2.44	-42.	1.19	143.	0.0981	-168.
Inviscid Calculation, Magnus, Mach 0.875, Ventilated Wall	3.02	-48.	1.51	148.	0.116	-163.
Calculation, Partial Viscous Simulation, Magnus, Mach 0.875,	2.96	-37.	1.33	146.	0.085	-167.
Perturbation Calculation, Ballhaus,[13] Mach 0.875, Time-Integration	2.3	-48.	1.2	142.	-	-
Perturbation Calculation, Ballhaus,[13] Mach 0.875, Indicial Method	1.69	-31.	1.01	141.	-	-
Experiment, Tijdeman,[6,7] Mach 0.879, 120 Hz	2.36	-40.	1.30	157.	0.0900	-165.

comparison with Tijdeman's experimental data[6,7] and calculations by other investigators.[11,12,13,16]

1.4 PARTIAL SIMULATION OF VISCOUS EFFECTS

It has been common knowledge since the earliest experiments on transonic flow over airfoils that the pressure recovery at the foot of a shock at the downstream border of an imbedded supersonic zone on the airfoil is less than normal-shock recovery. For example, T. Theodorsen (NACA TN 1029, March 1946) suggests that Mach 1.0 is attained at the downstream side of the shock and refers to earlier works by H-S. Tsien and A. Fejer (1944) and by C. L. Dailey (1943).

In the absence of any direct evidence on the pressure just aft of the foot of a shock in unsteady flow, it was assumed that the pressure would be close to the value for Mach 0.98. As a computational device for weakening the shock at the airfoil surface, the tangency boundary condition was relaxed over a limited portion of the surface (about 0.1 chord) downstream of the moving shock. To establish a procedure for the shaping and placing of a lump-like protuberance to be added to the wall aft of the shock, "reasonable" pressure profiles based upon Tijdeman's[6,7] measurements were prescribed over the aft part of the 64A006 airfoil and the computer program was used to calculate the required wall shape modifications for shocks of several strengths. A generalized description of these shapes was then incorporated in the unsteady program.

[13] Ballhaus, W. F. and Goorjian, P. M., "Computation of Unsteady Transonic Flows by the Indicial Method" AIAA Paper 77-447, Dynamics Specialist Conference, San Diego, California, March 24-25, 1977

In calculating an oscillatory flow over the airfoil, the pressure distribution in the vicinity of the shock was monitored at each computational pass to establish the shock location and strength (based principally on shock upstream Mach number and translation speed of the wave) and the placement and shape of the lump were adjusted to cause the desired less-than-normal pressure rise. The computational procedure outlined was extremely difficult to keep stable.

It should easily be recognized that the lump shape would have little connection with, say, the displacement thickness profile for the boundary layer near the shock. The lump shape necessary to force the desired pressure recovery depends upon the equations used, computational scheme and mesh spacing. This can be (and was) easily verified by prescribing similar airfoil pressures and calculating the lump shapes using a program based upon the transonic perturbation potential with non-conservative differencing.

Figure 12 shows the calculated "viscous" pressure distribution for the 64A006 at zero lift in a Mach 0.875 free stream. Representative pressure distributions at 6 phases in the cycle for the case of the flap oscillating ±1.0 degree at reduced frequency k = 0.468 are shown in Figure 13. The shock location through a cycle is shown in Figure 8; compared to the calculated inviscid shock motion, the shock is displaced forward and the response-wave form is substantially altered. The deviation of the wave-form (of shock location through the oscillation cycle) from the shape found experimentally by Tijdeman[8] most likely indicates that the shock-weakening computational procedure does not properly simulate the consequences of the real (shock)-(boundary-layer) interaction on the pressure field aft of the shock and on the wave propagation along the airfoil surface.

The oscillatory force and moment coefficients for this case with partial simulation of viscous effects are also listed in Table 1 and first harmonies of the unsteady pressures are shown subsequently in Figure 21.

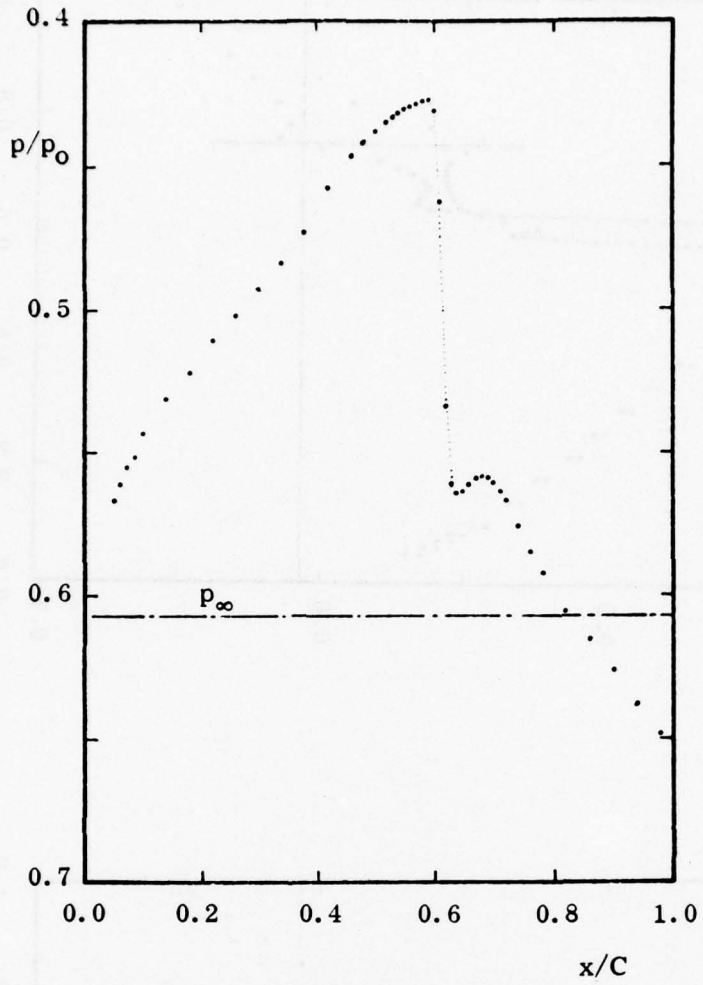

Figure 12. Pressure Distribution on NACA 64A006 at Zero Angle-Of-Attack, Shock Weakened to Simulate Viscous Interaction, Mach 0.875

The programmed procedures for simulating viscous effects did not handle the case of the oscillatory flow over the 64A006 in a Mach 0.854 stream with flap oscillating ±1.0 degree at k = 0.358. With weaker shocks, the lump placement and shaping procedures appeared to be too inexact to maintain the shock-lump locked on the downstream end of the supersonic region. Revisions to the program aimed at correcting this computational instability by use of shock fitting rather than shock capturing were not completed satisfactorily.

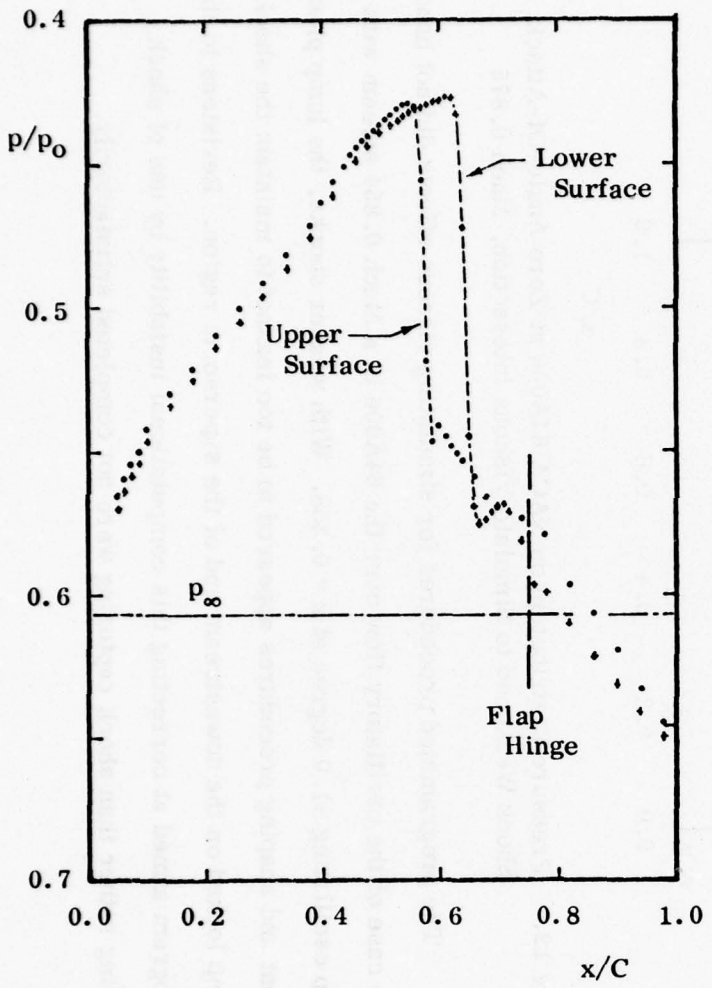

ωt = 30°

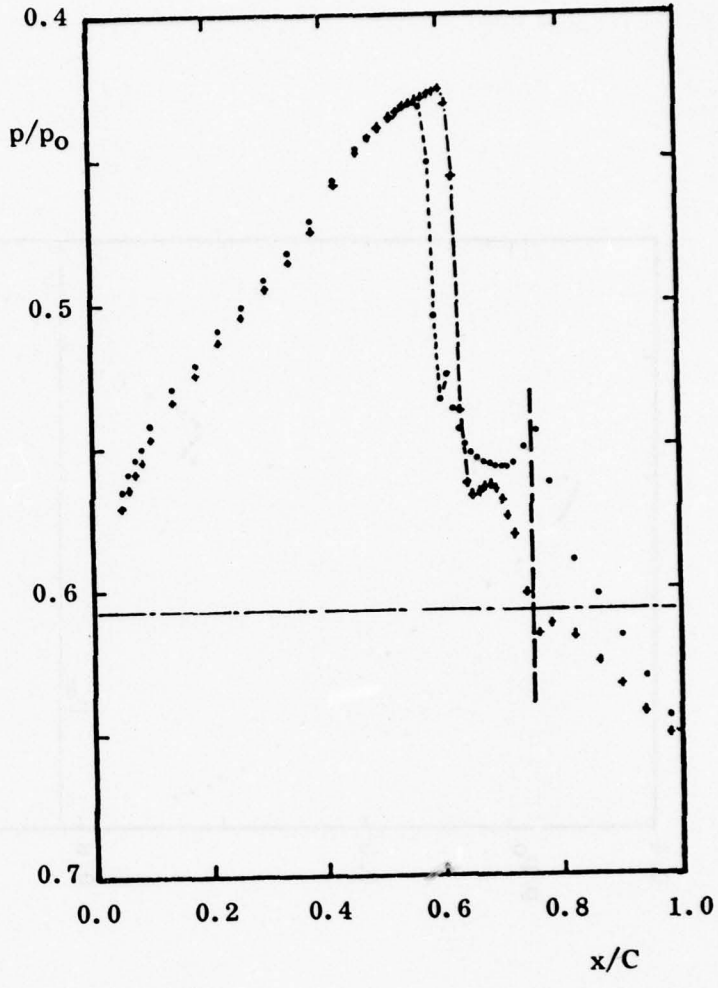

ωt = 60°

Figures 13a & b. Instantaneous Pressure Distributions on NACA 64A006 with Quarter-Chord Oscillating Flap. Shock Weakened to Simulate Viscous Interaction. Mach 0.875, Zero Angle-Of-Attack, Flap $\delta = 0 \pm 1.0°$, $k = 0.468$ (Continued)

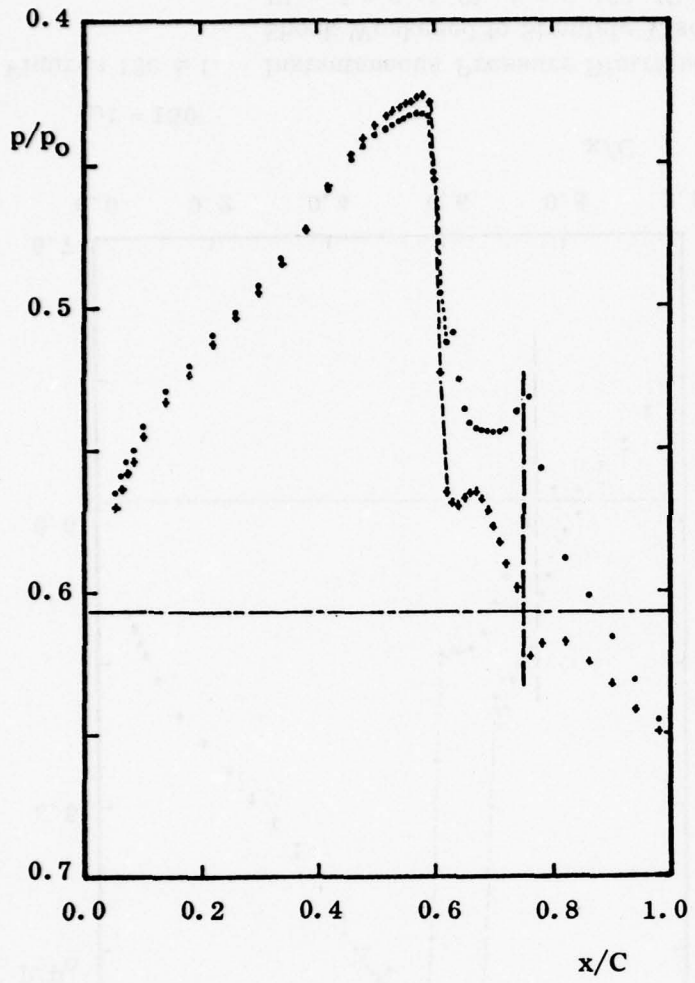

ωt = 90°

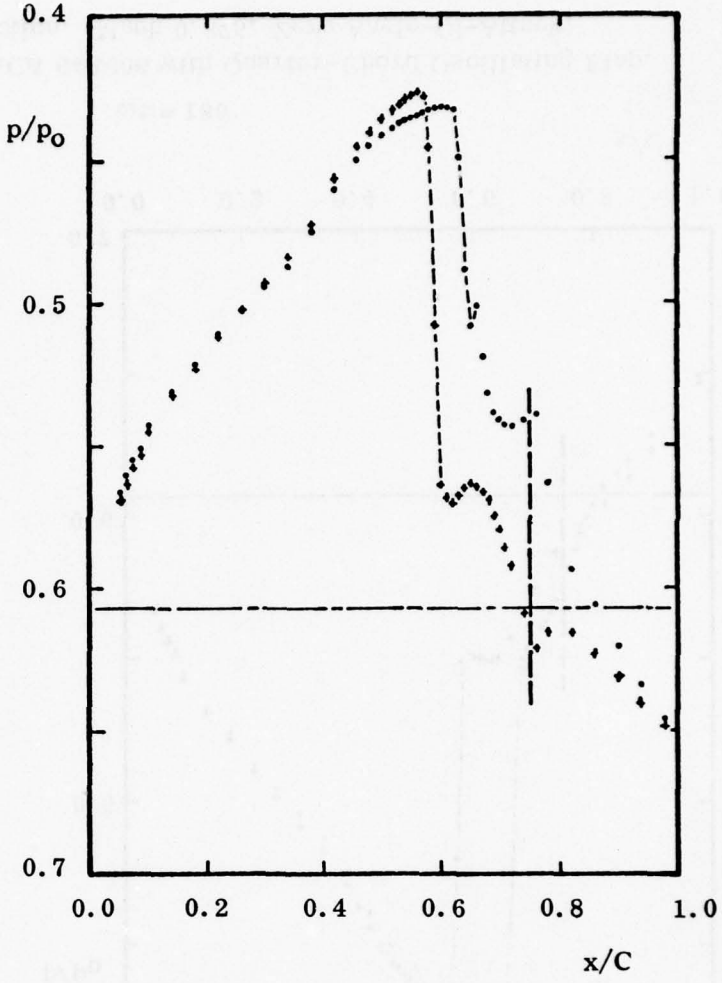

ωt = 120°

Figures 13c & d. (Continued)

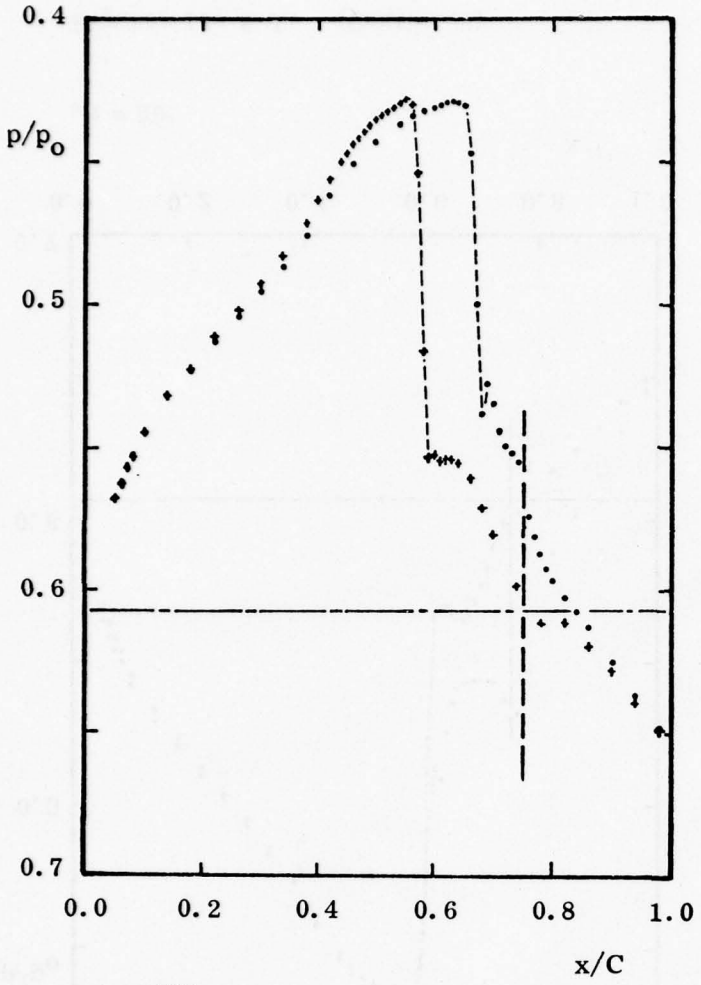

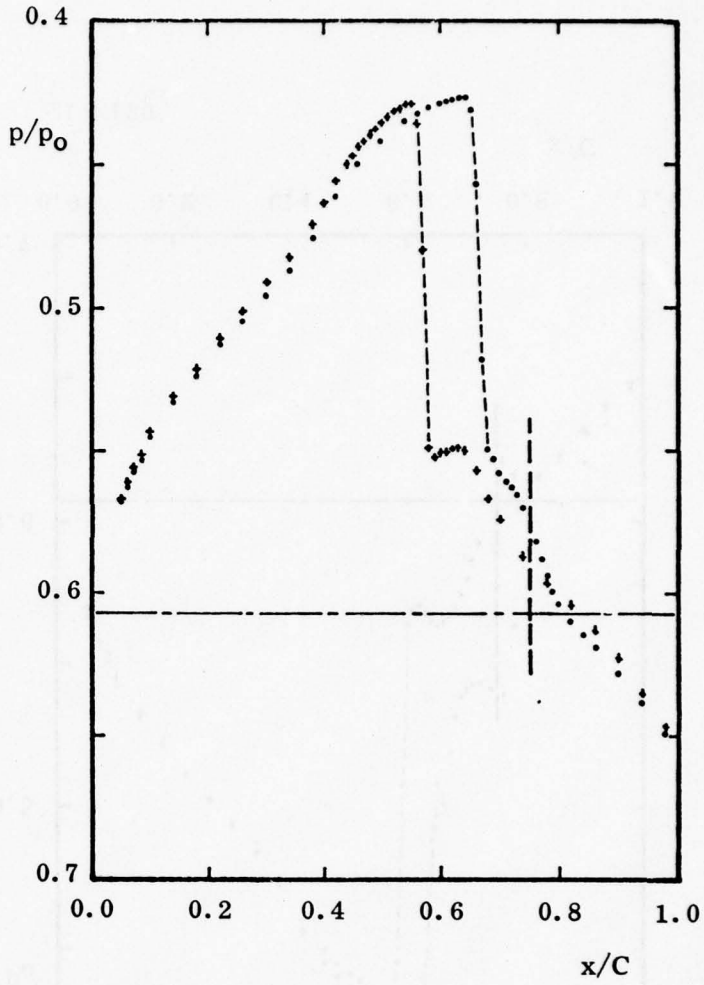

Figures 13e & f. Instantaneous Pressure Distributions on NACA 64A006 with Quarter-Chord Oscillating Flap. Shock Weakened to Simulate Viscous Interaction. Mach 0.875, Zero Angle-Of-Attack, Flap $\delta = 0 \pm 1.0°$, $k = 0.468$ (Concluded)

1.5 SIMULATION OF WIND TUNNEL WALL EFFECTS

The calculations described in Section III 1.1 through 1.4 all had the perimeter of the computation field at least 10 chords from the airfoil to try to simulate free-air conditions. In this section, inviscid calculations of the flow over the 64A006 in a ventilated wall wind tunnel will be described.

Tijdeman's experiments on the unsteady flow over the 64A006[5, 6, 7] airfoil have been conducted in a slotted wall tunnel with a tunnel-height of approximately 3.06 chords. The slots in the floor and ceiling cover about 0.10 of those areas. The walls are solid ahead of the test section; downstream of the test section the physical arrangement makes it appear feasible to apply free-jet boundary conditions.

Only a limited amount of data on the behavior of the pressures near the slotted wall in unsteady tests in this particular tunnel has been made available.[5] Therefore, the computational model of the slotted part of the wall has been based upon information generated in calculations performed to evaluate wall effects on experiments in the slotted wall tunnel at Wright-Patterson Air Force Base.[17] In the aforementioned experiments[17] the airfoil pressures and pressures on the floor and ceiling were measured; finite difference calculations of the transonic flowfields using these data determined the apparent vertical velocity at the tunnel wall. A rough correlation of the wall velocity relations in these experiments has been made:

$$u - 0.73v - 0.17v_x = 0$$

where u and v are perturbations from free stream velocity and the signs are correct for the lower tunnel wall.

[17] Magnus, R., Yoshihara, H., Lee, D., and Rogers, L., "Wall Interference in 2D Ventilated Wind Tunnels at High Subsonic Mach Numbers" Rpt. AFFDL-TR-74-63, June 1974

To avoid drastically rearranging the computer program, the calculations to study the effect of the wind tunnel walls arbitrarily have used solid wall boundary conditions ahead of 2.6 chords forward of the model and free-jet conditions aft of 2.6 chords behind the model, and the slotted wall condition along the intervening part of walls.

Calculations on the NACA 64A006 with quarter-chord flap in a tunnel were carried out at Mach numbers 0.854 and 0.875.

The zero-lift steady pressure distributions are shown in Figures 14 and 15 and agree much closer to the experimental data than do the inviscid free-air calculations, refer back to Figures 1a and 1b. The agreement between calculation and experiment is good at Mach 0.875.

In a calculation of the flow over the 64A006 at Mach 0.85 Traci[11] found that including a porous wall boundary condition made the flow more supercritical than had been calculated for the airfoil in a free stream, that is, the pressures were made more negative on the midsection of the airfoil and the shock was shifted aft. The opposite was found in the present calculations, no doubt, because of a different assumption on the wall characteristics.

With the flap deflected 1.0 degree in steady flow, the pressure excursions on the forward part of the airfoil are greatly reduced from the values noted for the calculations in a free-stream; see Figures 16 and 2. In this respect, the present calculations agree with the trend found by Traci[11] whose results are also shown in Figure 16a.

In Mach 0.854 flow, Figures 17 and 18, including wind tunnel wall effect in the calculations of the flow with the flap oscillating produces relatively good agreement with Tijdeman's experimental data[6,7] in most respects. The calculation still predicts larger pressure excursions on the part of the airfoil traversed by the moving shock than are observed in the experiments; this is inevitable unless the shock is deliberately weakened.

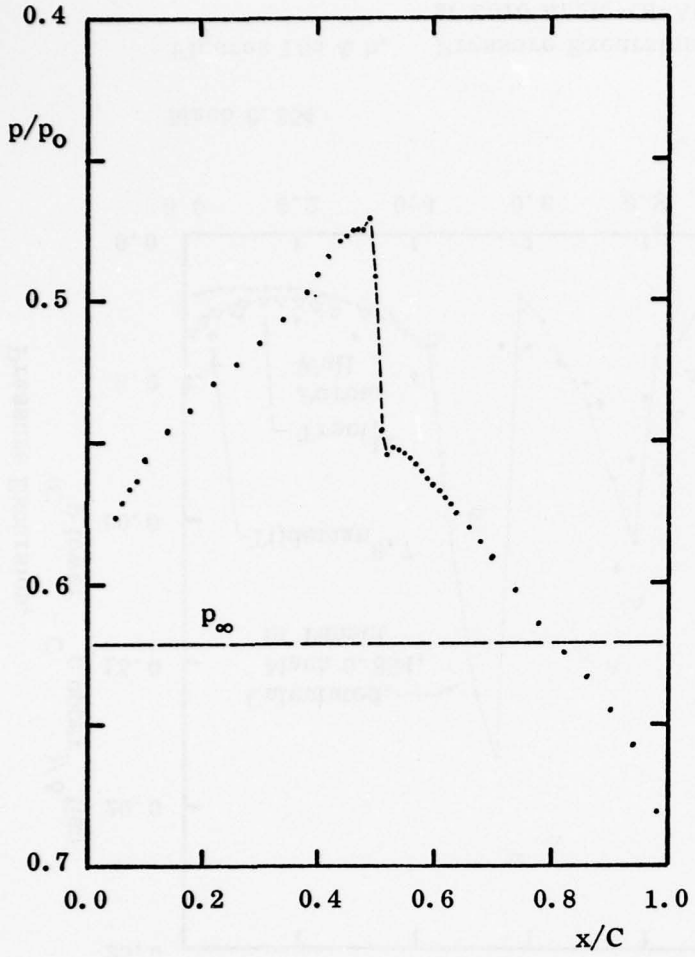

Figure 14. Pressure Distribution on NACA 64A006 at Zero Angle-Of-Attack in Ventilated Wall Tunnel, Mach 0.854

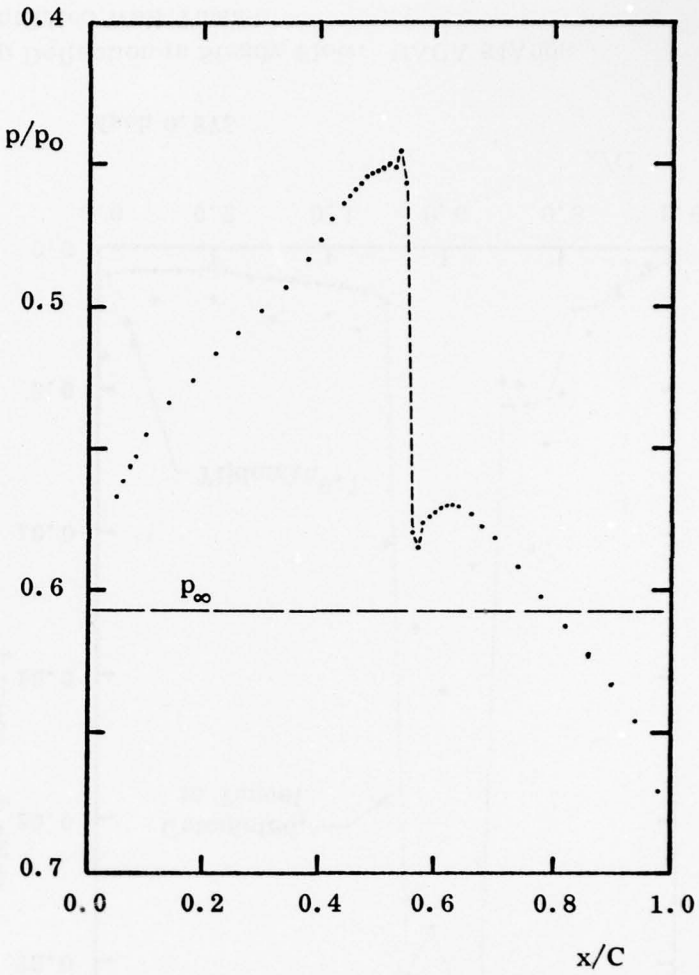

Figure 15. Pressure Distribution on NACA 64A006 at Zero Angle-Of-Attack in Ventilated Wall Tunnel, Mach 0.875

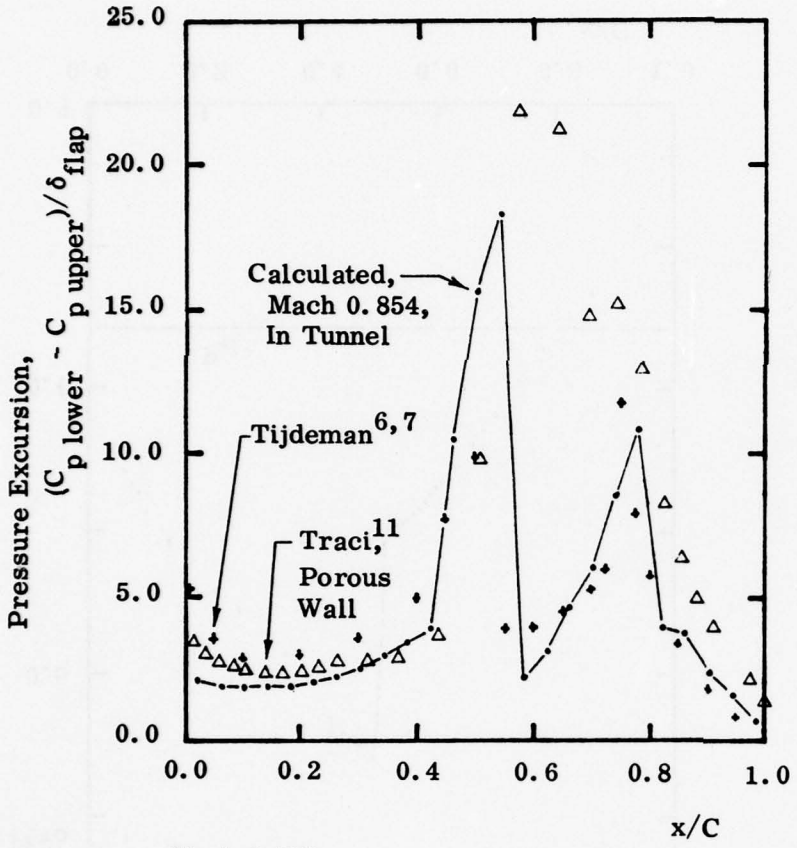

Mach 0.854

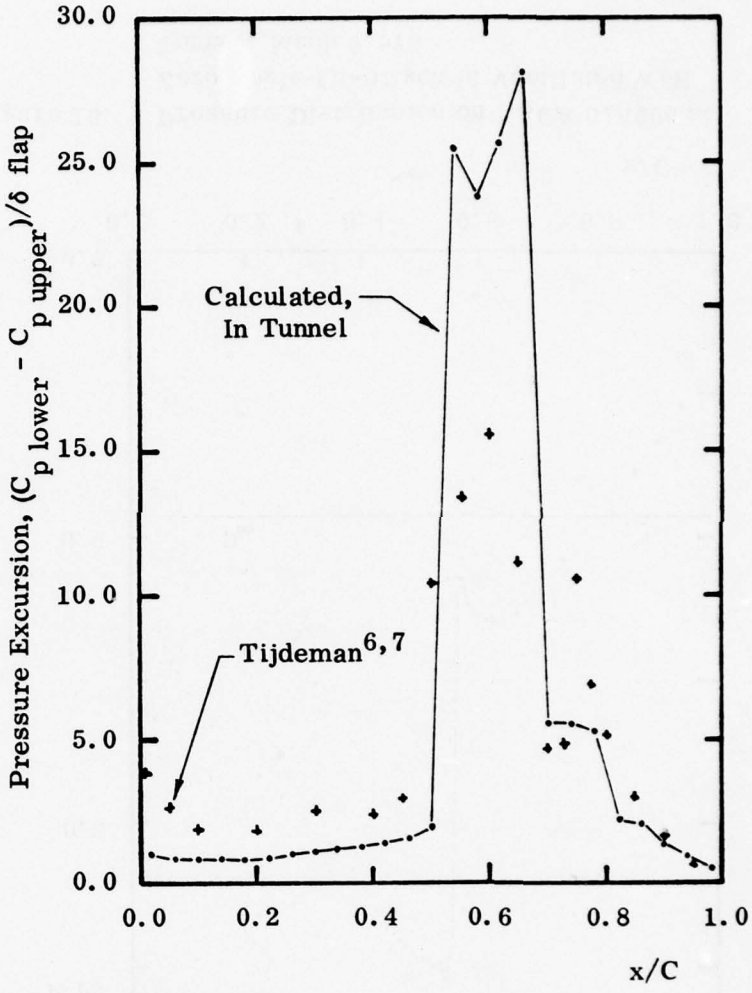

Mach 0.875

Figures 16a & b. Pressure Excursions Due to Flap Deflection in Steady Flow. NACA 64A006 at Zero Angle-Of-Attack in a Ventilated Wall Tunnel

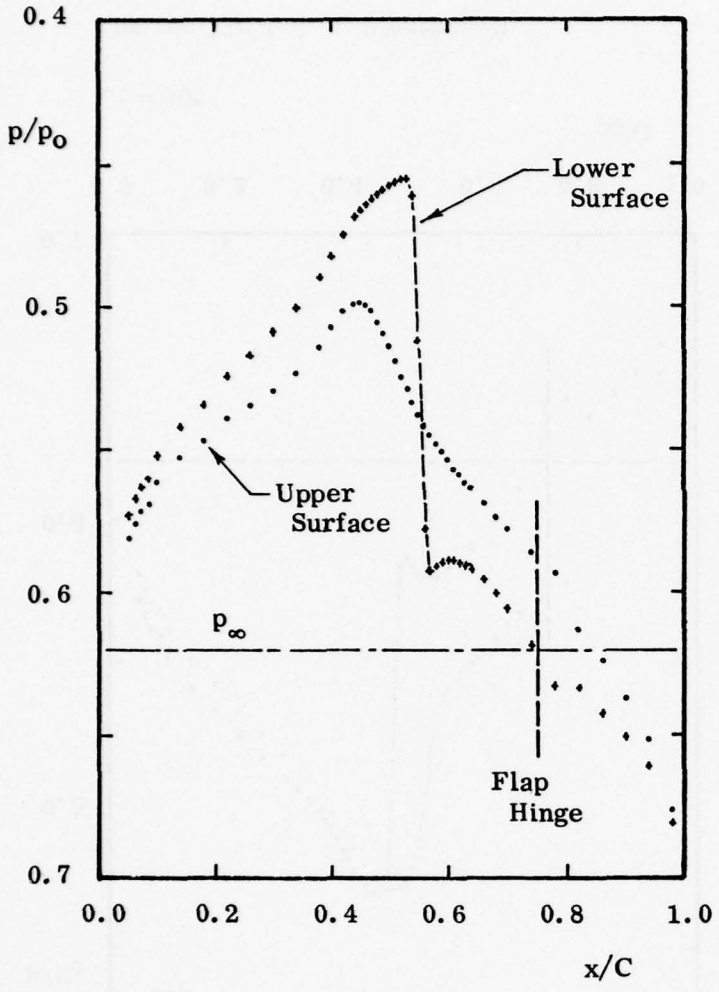

ωt = 30°

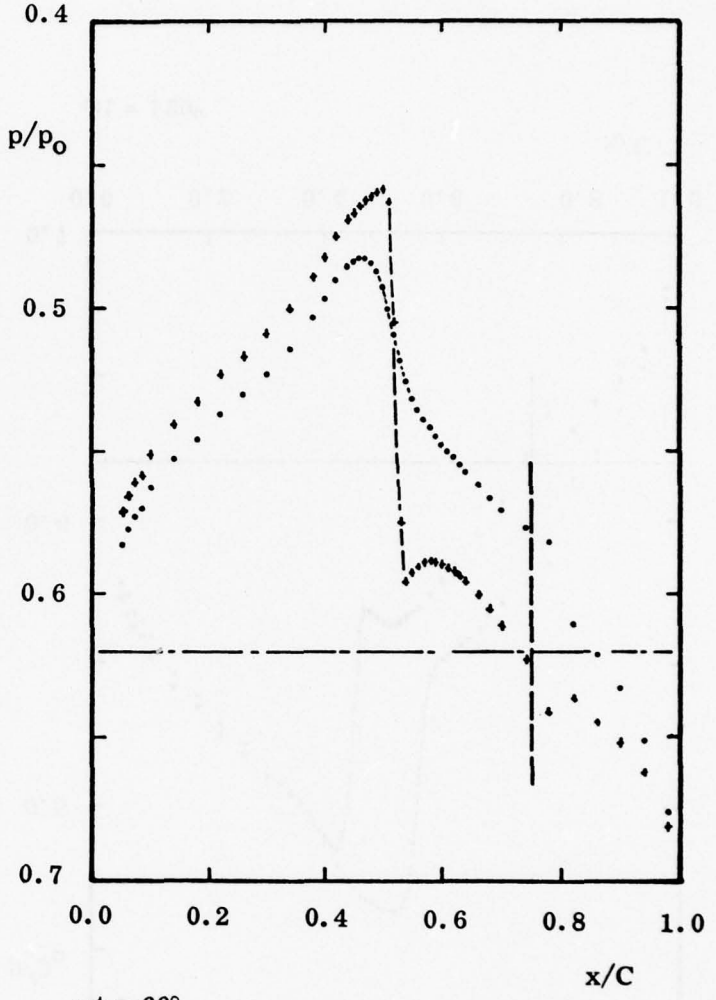

ωt = 60°

Figures 17a & b. Instantaneous Pressure Distributions on NACA64A006 with Quarter-Chord Oscillating Flap. Zero Angle-Of-Attack in Ventilated Wall Tunnel. Mach 0.854, Flap $\delta = 0 \pm 1.0°$, $k = 0.358$ (Continued)

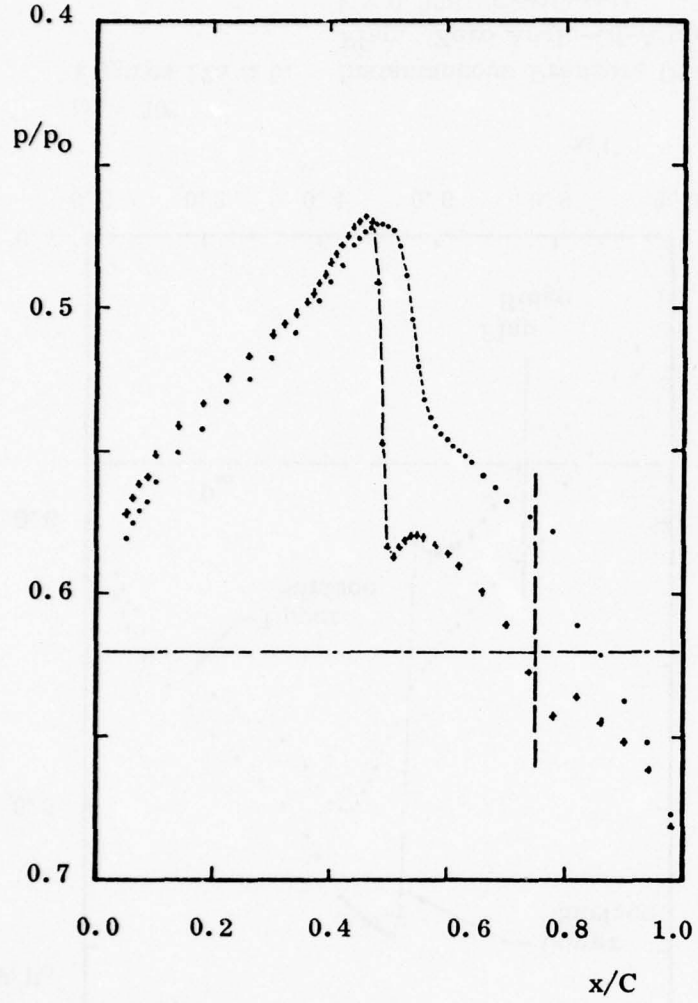

ωt = 90°

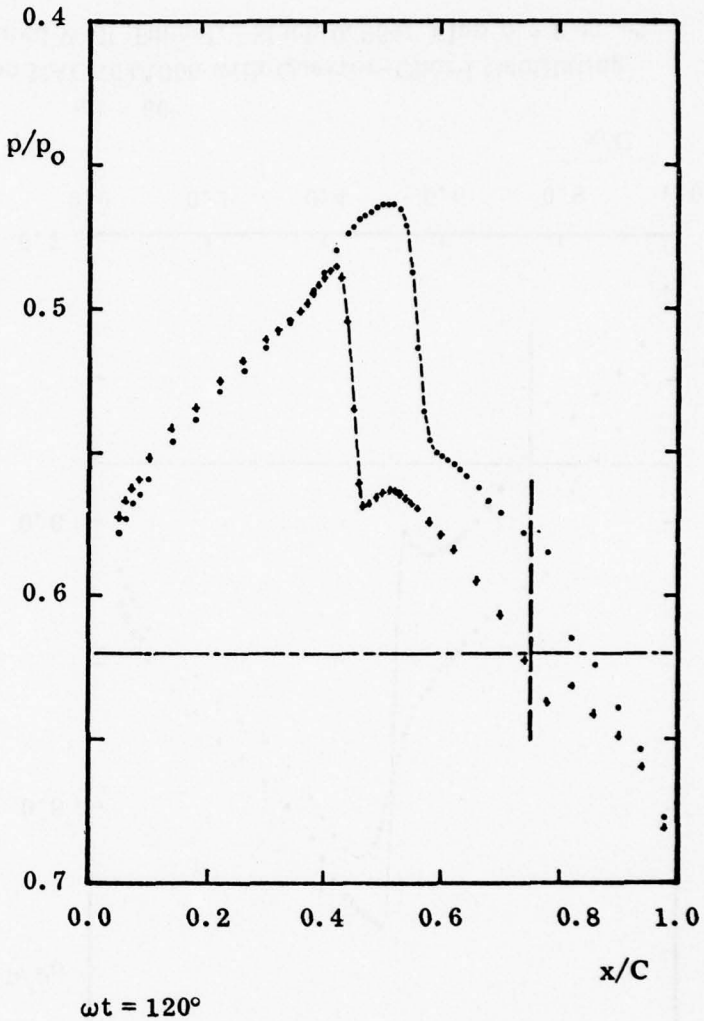

ωt = 120°

Figures 17c & d. (Continued)

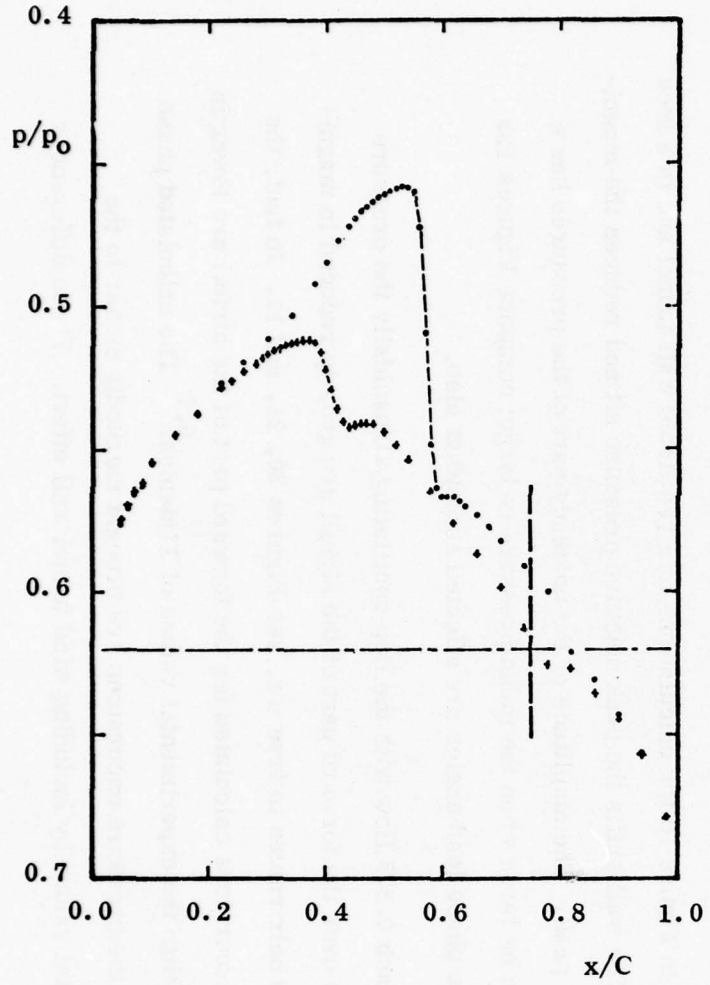

$\omega t = 150°$

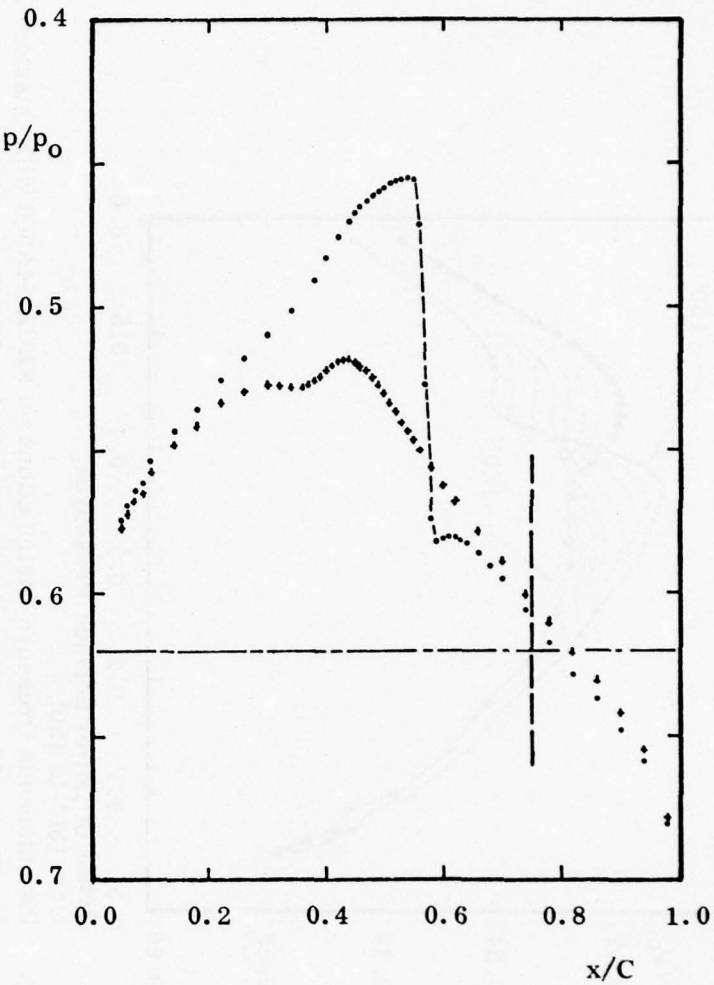

$\omega t = 180°$

Figures 17e & f. (Continued)

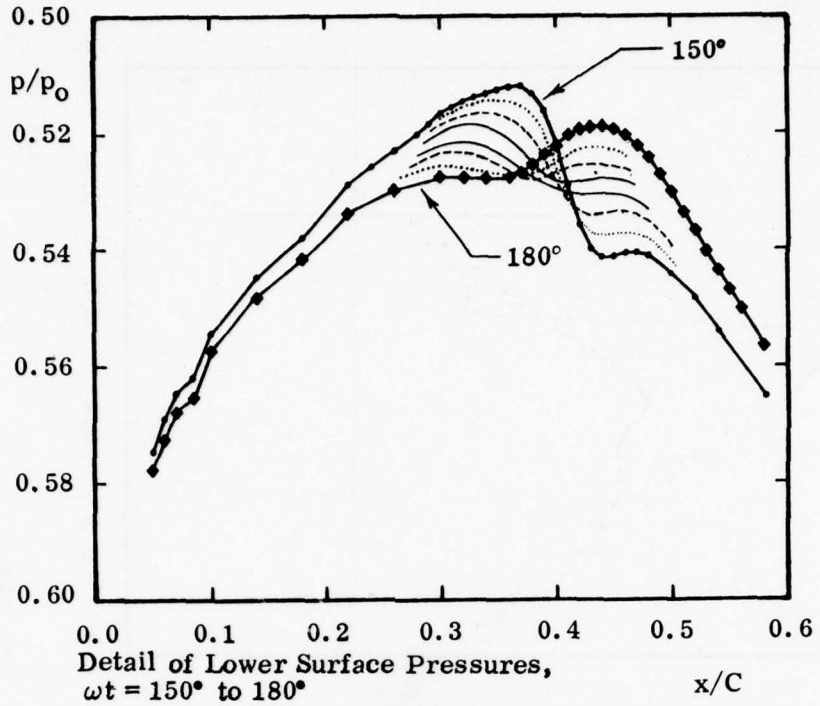

Figure 17g. Instantaneous Pressure Distributions on NACA 64A006 with Quarter-Chord Oscillating Flap. Zero Angle-Of-Attack in Ventilated Wall Tunnel. Mach 0.854, Flap $\delta = 0 \pm 1.0°$, $k = 0.358$ (Concluded)

The distributions of pressure along a line 1.53 chords above the airfoil are shown in Figure 19 for calculations in a ventilated wall tunnel and in a free stream. The wall shifts the peak negative pressure aft and reduces the magnitude of the peak. The amplitude of the unsteady part of the pressures has a tendency to be large when the mean pressure is large; compare Figures 19a and b. The phase lead angles are affected somewhat also.

In Mach 0.875 flow with the flap oscillating sinusoidally the pressure excursions over the forward part of the airfoil are greatly reduced in magnitude from their values in free air, see Figures 20, 21, and 11. In fact, the pressure excursions calculated for the forward part of the airfoil are lower in magnitude than the experimental values of Tijdeman.[6,7] The calculated phase angles for the pressure excursions are brought markedly closer to the experimental values by including wind tunnel wall effect. These differences

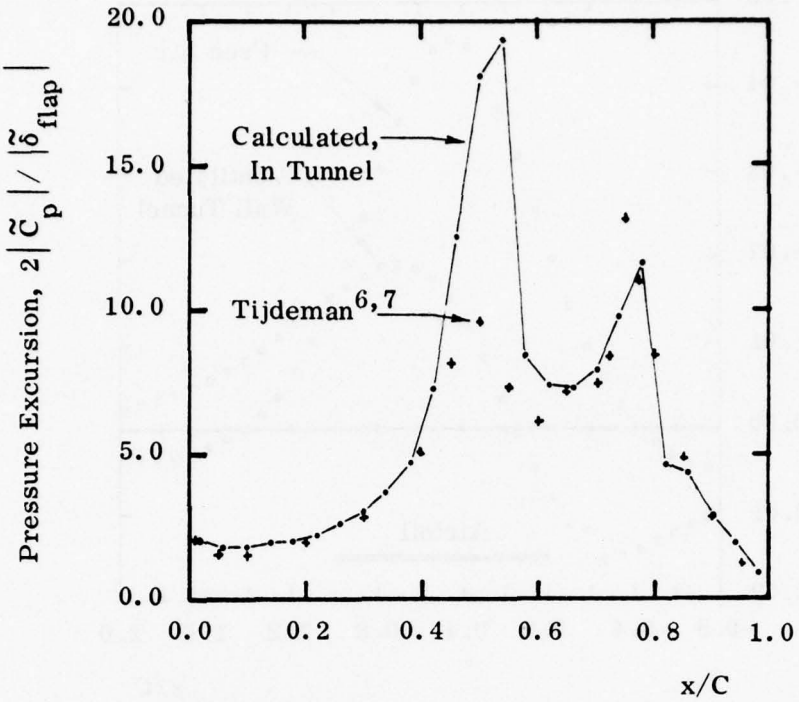

Amplitudes

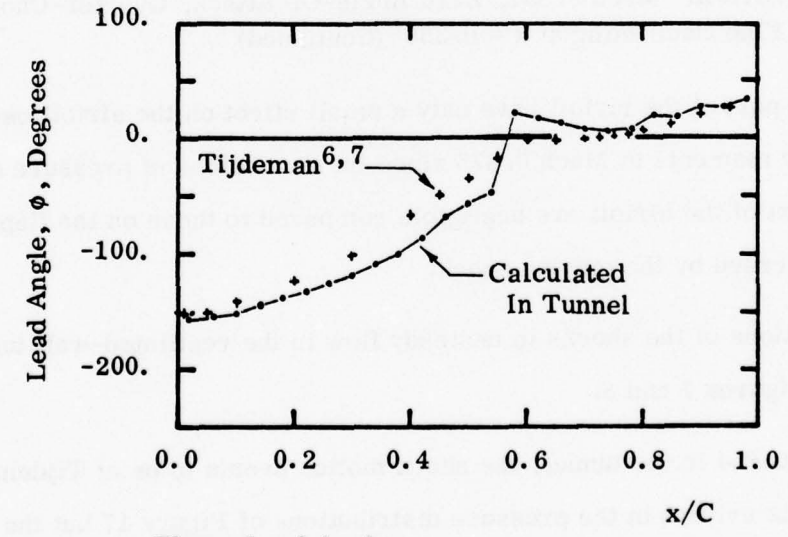

Phase Lead Angles

Figures 18a & b. **Pressure Excursions per Radian of Flap Deflection in Unsteady Flow. NACA 64A006 at Zero Angle-Of-Attack in a Ventilated Wall Tunnel. Mach 0.854, k = 0.358**

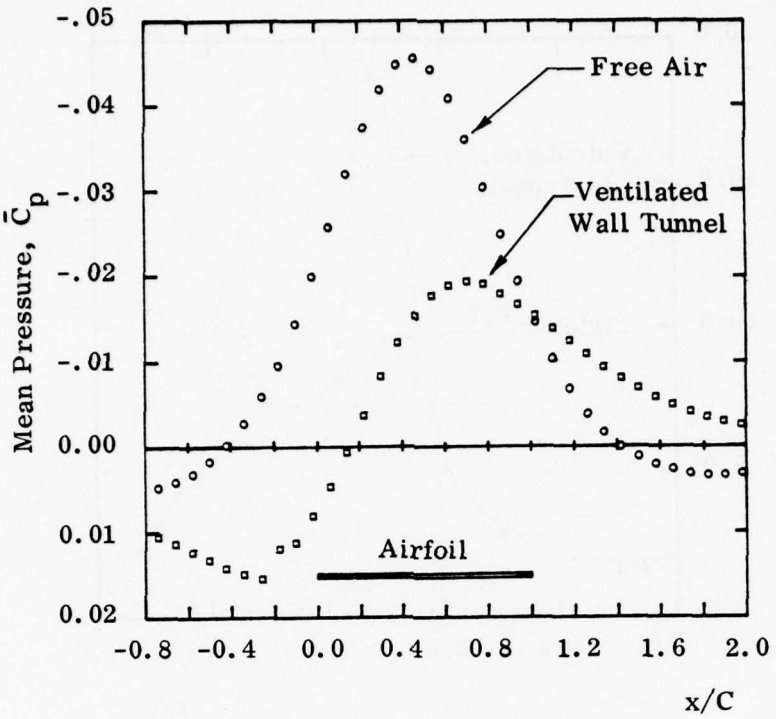

Figure 19a. Pressure Distributions Along a Line 1.53 Chords Above the NACA Airfoil. Mach 0.854, Zero Angle-Of-Attack, Quarter-Chord Flap Oscillating at k = 0.358 (Continued)

on the forward part of the airfoil have only a small effect on the airfoil oscillatory forces and moments at Mach 0.875 since the excursions of pressure on the forward part of the airfoil are negligible compared to those on the flap or in the region traversed by the moving shock.

The positions of the shocks in unsteady flow in the ventilated-wall tunnel are shown in Figures 7 and 8.

At Mach 0.854 in the tunnel, the shock motion seems to be of Tijdeman's[8] Type C. This is evident in the pressure distributions of Figure 17 but the program logic did not insert mesh to provide detail of the pressure rise in this shock as it ran forward in subsonic flow toward the nose. In free air at Mach 0.854 the shock motion seems to be of Type B.

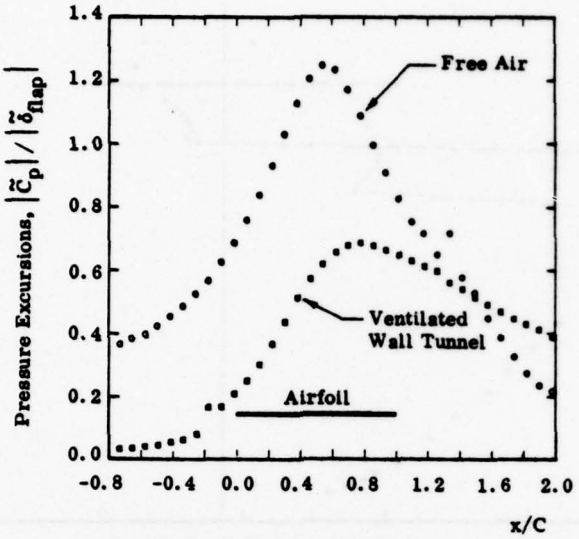

Amplitude of Pressure Oscillations
per Radian Flap Deflection

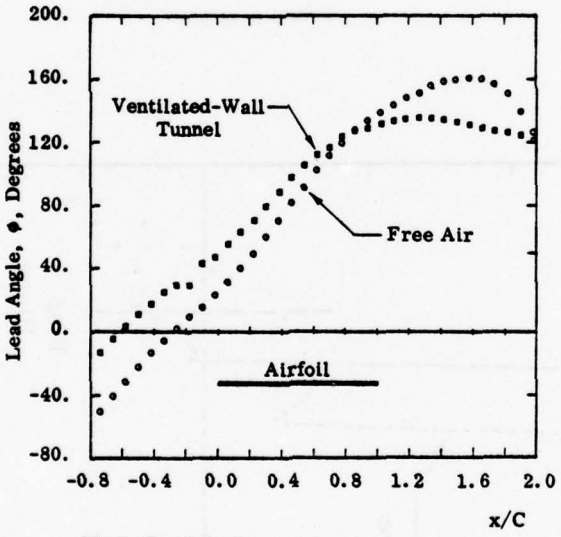

Phase Lead Angle

Figures 19b & c. Pressure Distributions Along a Line 1.53 Chords Above the NACA Airfoil. Mach 0.854, Zero Angle-Of-Attack, Quarter Chord Flap Oscillating at k = 0.358 (Concluded)

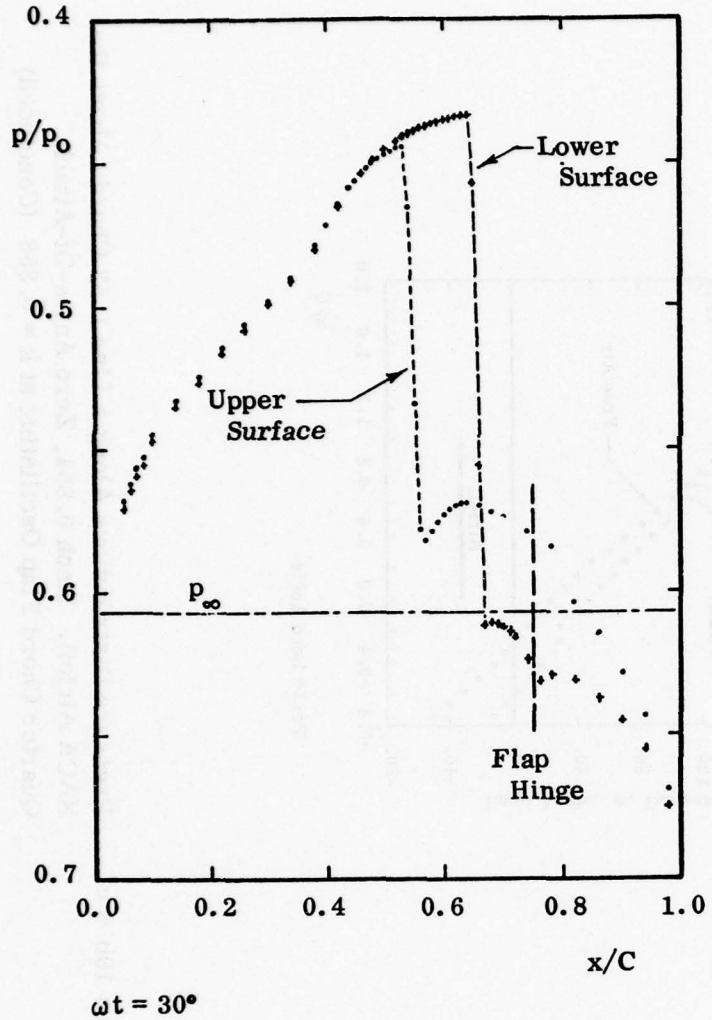

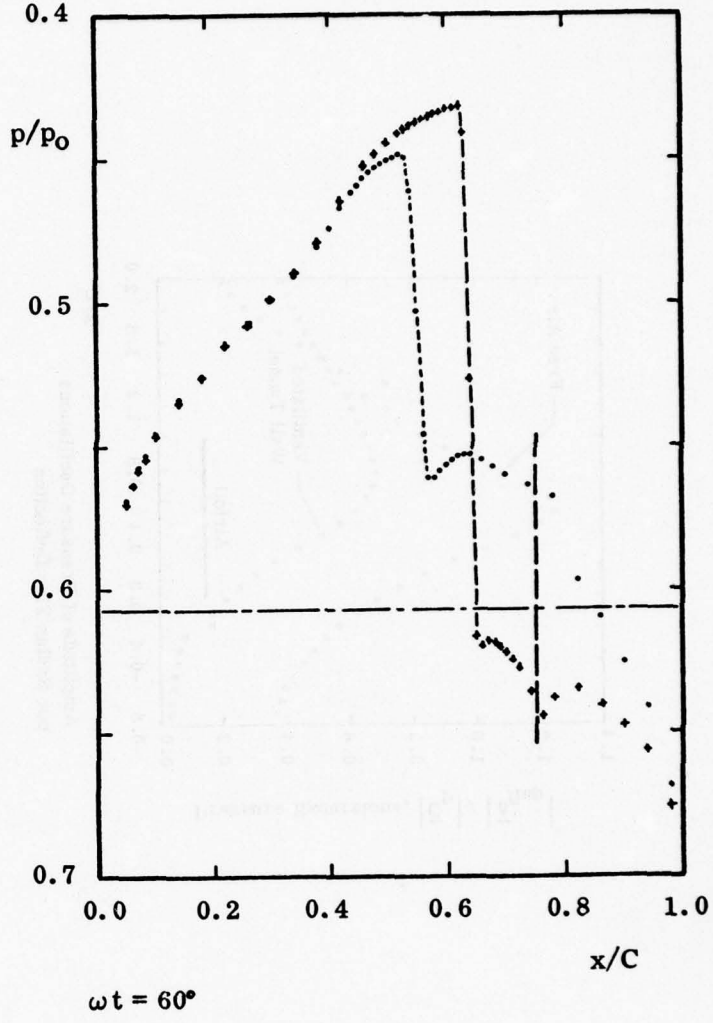

Figures 20a & b. Instantaneous Pressure Distributions on NACA 64A006 with Quarter-Chord Oscillating Flap. Zero Angle-Of-Attack in Ventilated Wall Tunnel. Mach 0.875, Flap $\delta = 0 \pm 1.0°$, $k = 0.468$ (Cont)

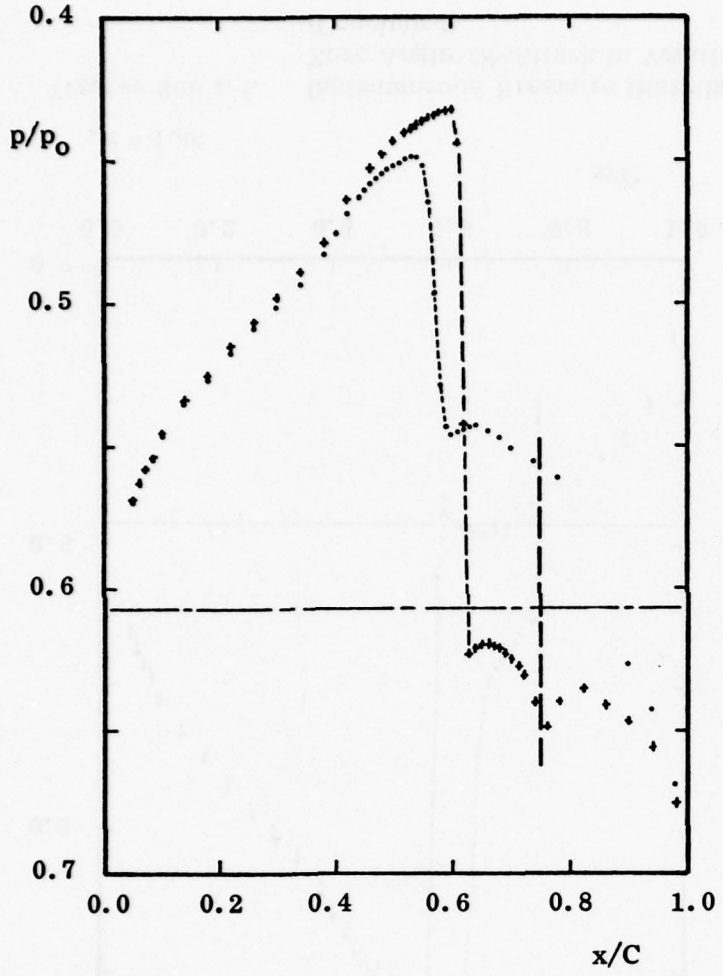

ωt = 90°

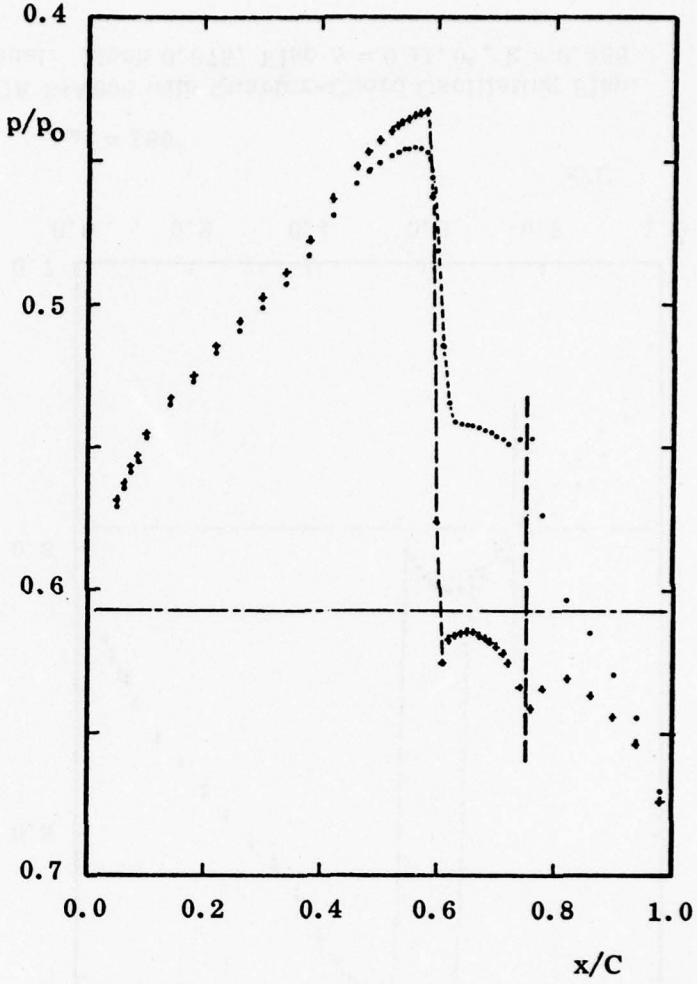

ωt = 120°

Figures 20c & d (Continued)

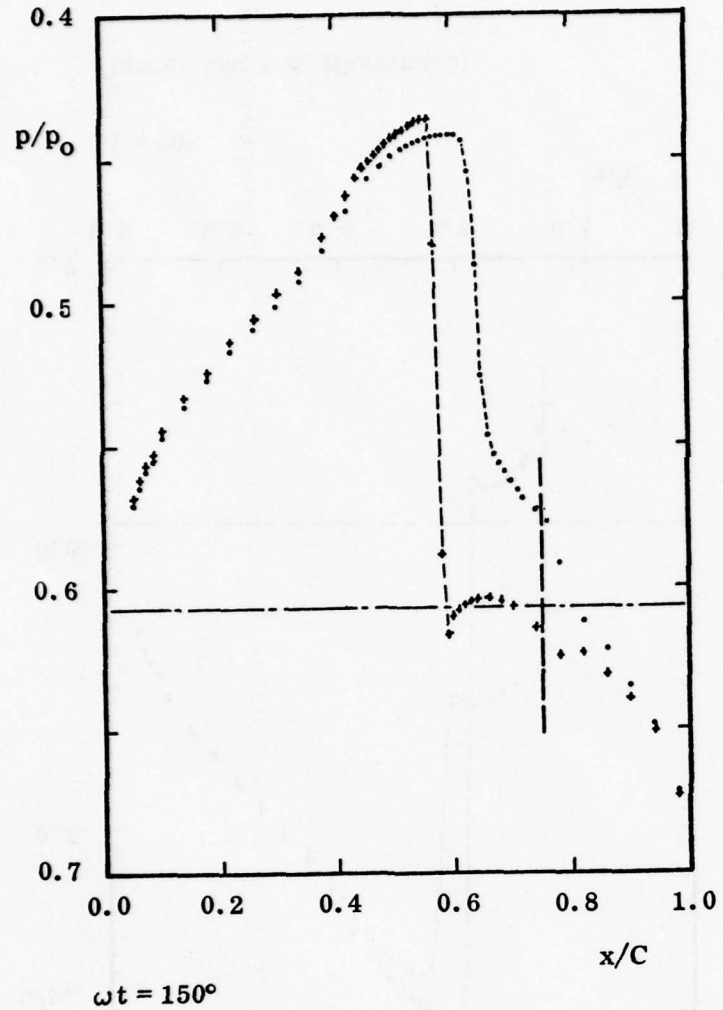

ωt = 150°

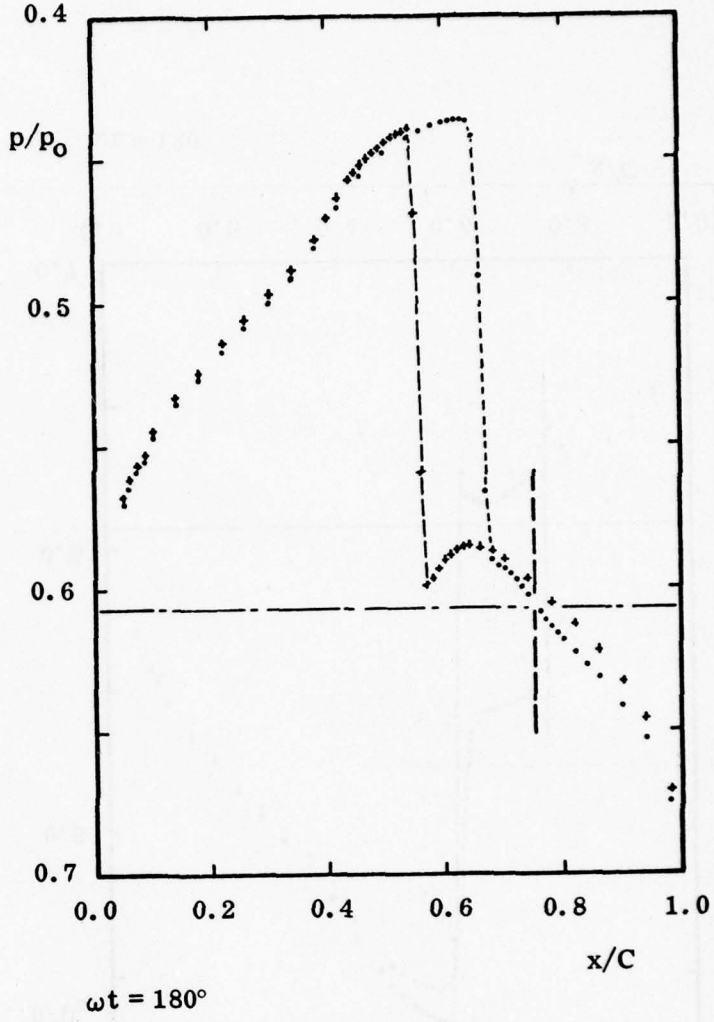

ωt = 180°

Figures 20e & f. Instantaneous Pressure Distributions on NACA 64A006 with Quarter-Chord Oscillating Flap. Zero Angle-Of-Attack in Ventilated Wall Tunnel. Mach 0.875, Flap $\delta = 0 \pm 1.0°$, $k = 0.468$ (Concluded)

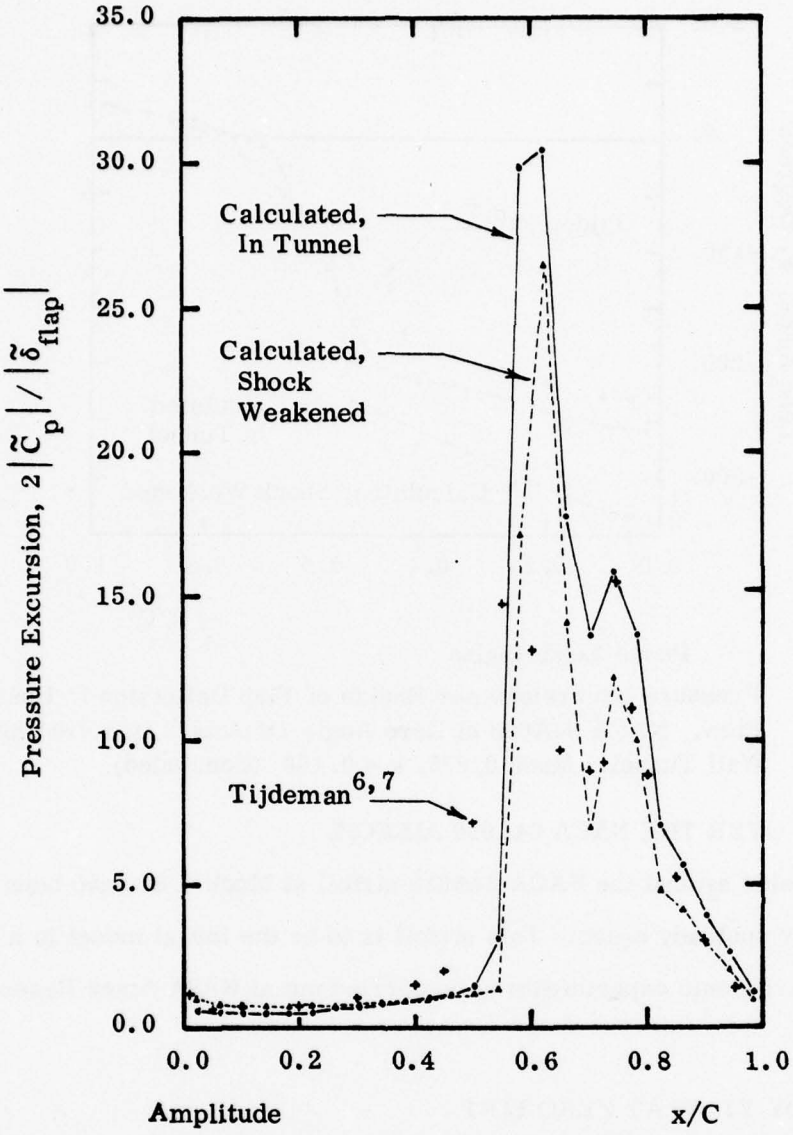

Figure 21a. Pressure Excursions per Radian of Flap Deflection in Unsteady Flow. NACA 64A006 at Zero Angle-Of-Attack in a Ventilated Wall Tunnel. Mach 0.875, k = 0.468 (Continued)

Ballhaus[14] has found by comparing calculations in free air and in a restricted stream with free-jet boundaries, that shock motion pattern could be altered from Type A in free air to Type B in the free-jet.

[14]Ballhaus, W. G. and Goorjian, P. M., "Efficient Solution of Unsteady Transonic Flows About Airfoils" 44th AGARD Structures and Materials Panel Meeting, Lisbon, 18 April 1977

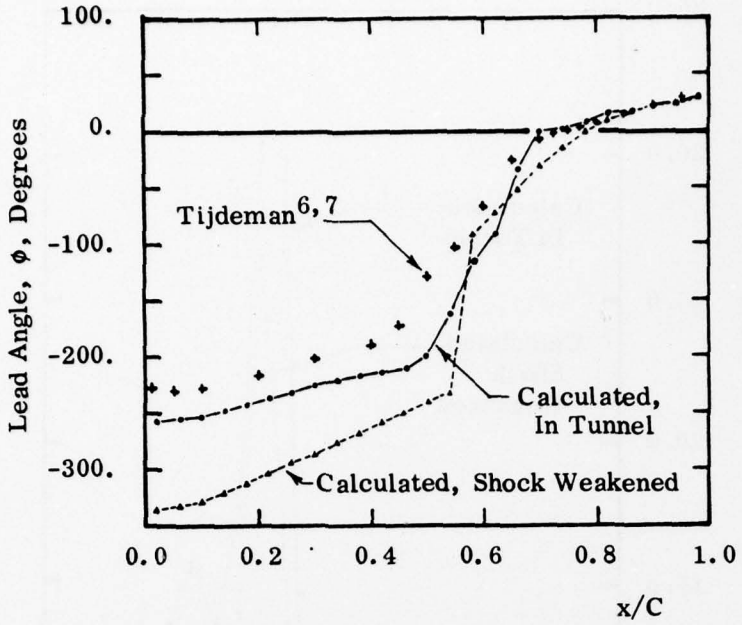

Phase Lead Angles

Figure 21b. Pressure Excursions per Radian of Flap Deflection in Unsteady Flow. NACA 64A006 at Zero Angle-Of-Attack in a Ventilated Wall Tunnel. Mach 0.875, k = 0.468 (Concluded)

2. FLOW OVER THE NACA 64A010 AIRFOIL

Flowfields around the NACA 64A010 airfoil at Mach 0.80 have been calculated for four unsteady cases. This airfoil is to be the initial model in a series of unsteady transonic experiments to be carried out at NASA Ames Research Center.

2.1 STEADY FLOW AT ZERO LIFT

The pressure distribution calculated at zero angle-of-attack for the symmetric airfoil is shown in Figure 22. Similar calculations by Ballhaus and Goorjian using a program based on the transonic perturbation potential equation[12] and by Steger using a program based on the Euler equations[18] are shown. Experimental data from Stivers (unpublished, $Re \doteq 4 \times 10^6$, natural transition) are also presented.

[18]Steger, J. L., "Implicit Finite Difference Simulation of Flow About Arbitrary Geometries With Application to Airfoils" AIAA Paper 77-665, AIAA 10th Fluid and Plasma Dynamics Conference, Albuquerque, New Mexico, June 27-29, 1977

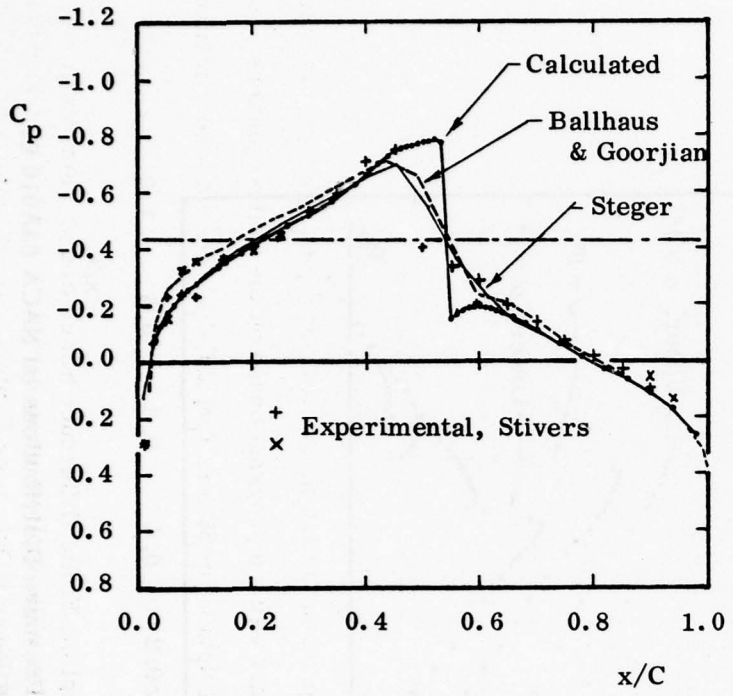

Figure 22. Pressure Distributions on NACA 64A010 at Zero Angle-Of-Attack in Mach 0.80 Flow.

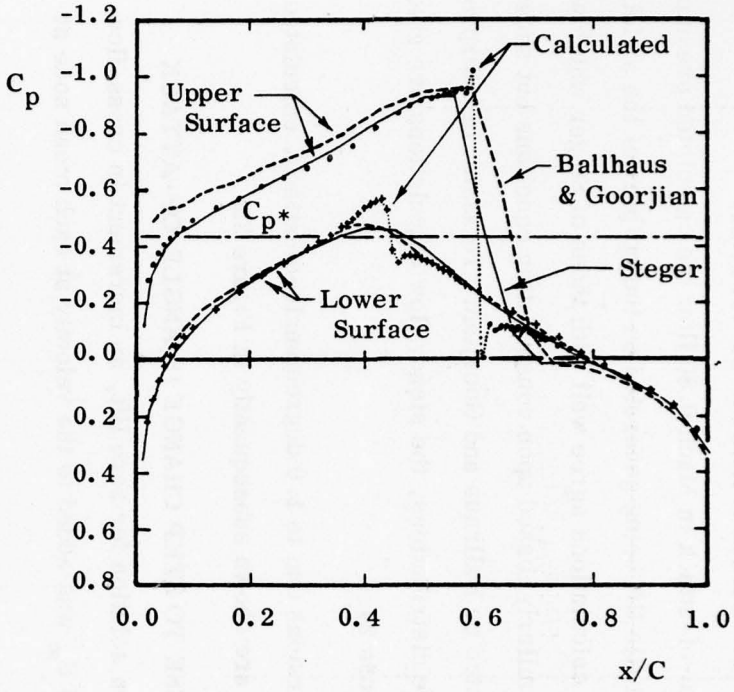

Figure 23. Pressure Distributions on NACA 64A010 at 1.0 Degree Angle-Of-Attack in Mach 0.80 Flow.

2.2 STEADY FLOW AT 1.0 DEGREE ANGLE-OF-ATTACK

At 1.0 degree angle-of-attack in Mach 0.80 flow the calculated pressure distribution shows very little lift being generated on the aft part of the airfoil, Figure 23. The present calculations agree well with those of Steger which were made with a program (similarly) based upon conservation equations but show less lift than that calculated by Ballhaus and Goorjian. To assist in interpreting the unsteady pressure distributions, the steady flow calculations are also presented as p/p_o in Figure 24.

The pressure excursions due to 1.0 degree angle-of-attack, calculated as $(p_{lower} - p_{upper})/2\alpha$ are shown subsequently in Figure 32.

2.3 INDICIAL RESPONSE TO STEP CHANGE IN ANGLE-OF-ATTACK

Starting from a flow solution for zero lift, an increment in cross-flow velocity equal to 0.01745 U_∞ was added to the velocity at each mesh node at zero time.

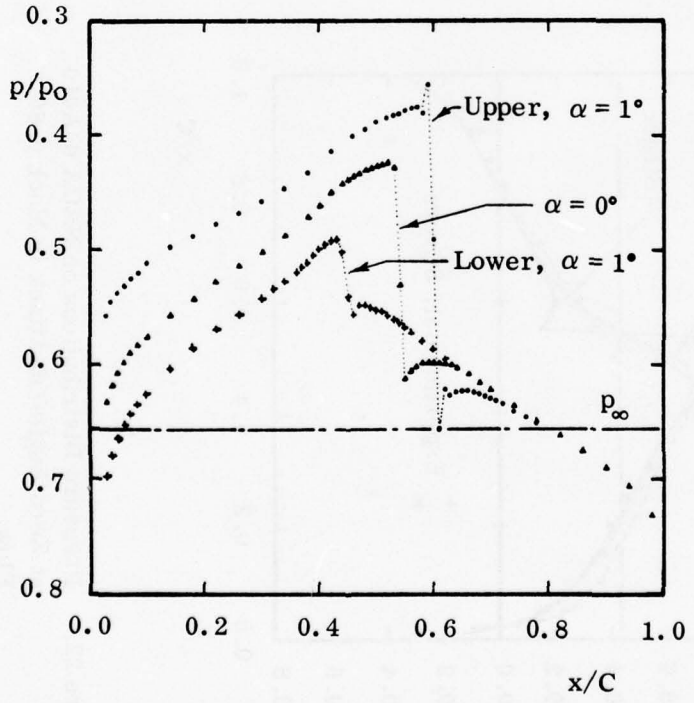

Figure 24. Calculated Pressure Distributions on NACA 64A010 in Mach 0.80 Flow.

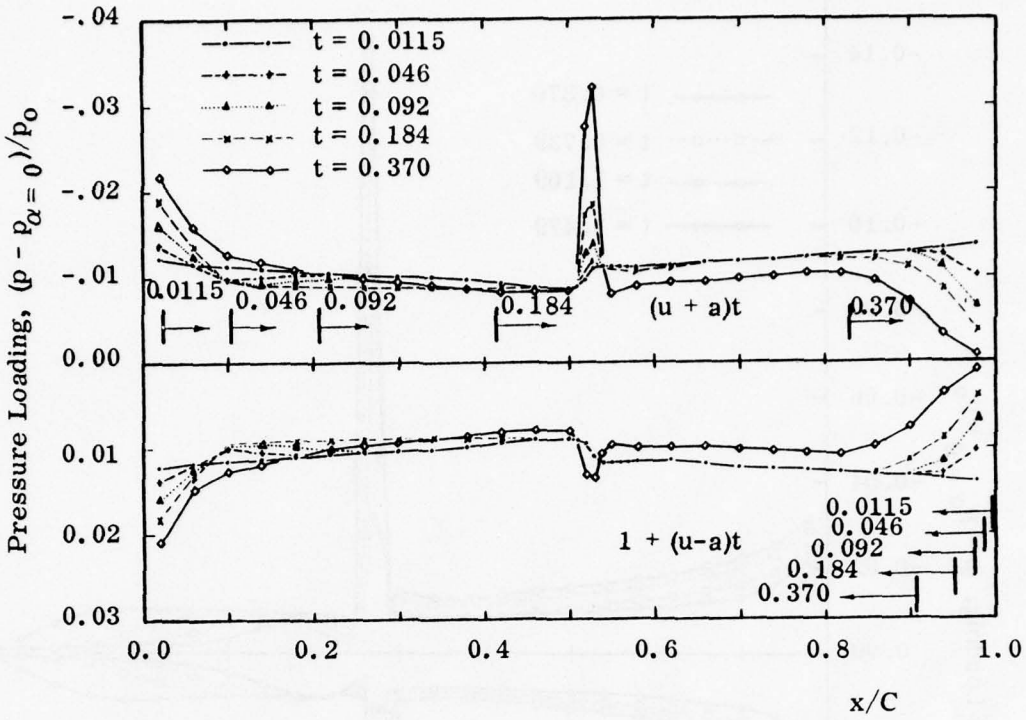

Early Stages

Figure 25a. Pressure Loading on NACA 64A010 Due to Step-Change in Angle-Of-Attack ($\alpha = 0 \longrightarrow 1°$) in Mach 0.80 Flow (Continued)

Chordwise distributions of the increments in pressure loading on the airfoil at several instants in the first chord and a half of travel are shown in Figure 25. During this time period, the rectangular initial loading changes toward a loading pattern peaked at the nose and the loading due to shock movement becomes apparent. Here, a time unit is C/U_∞.

The unsteady lift and pitching moment about the quarter chord are shown as functions of time, Figures 26 and 27, and are compared with the results of similar calculations by Ballhaus and Goorjian and by Steger.

The initial parts of the transients calculated here differ greatly from those calculated by Ballhaus and Goorjian using the perturbation equations.

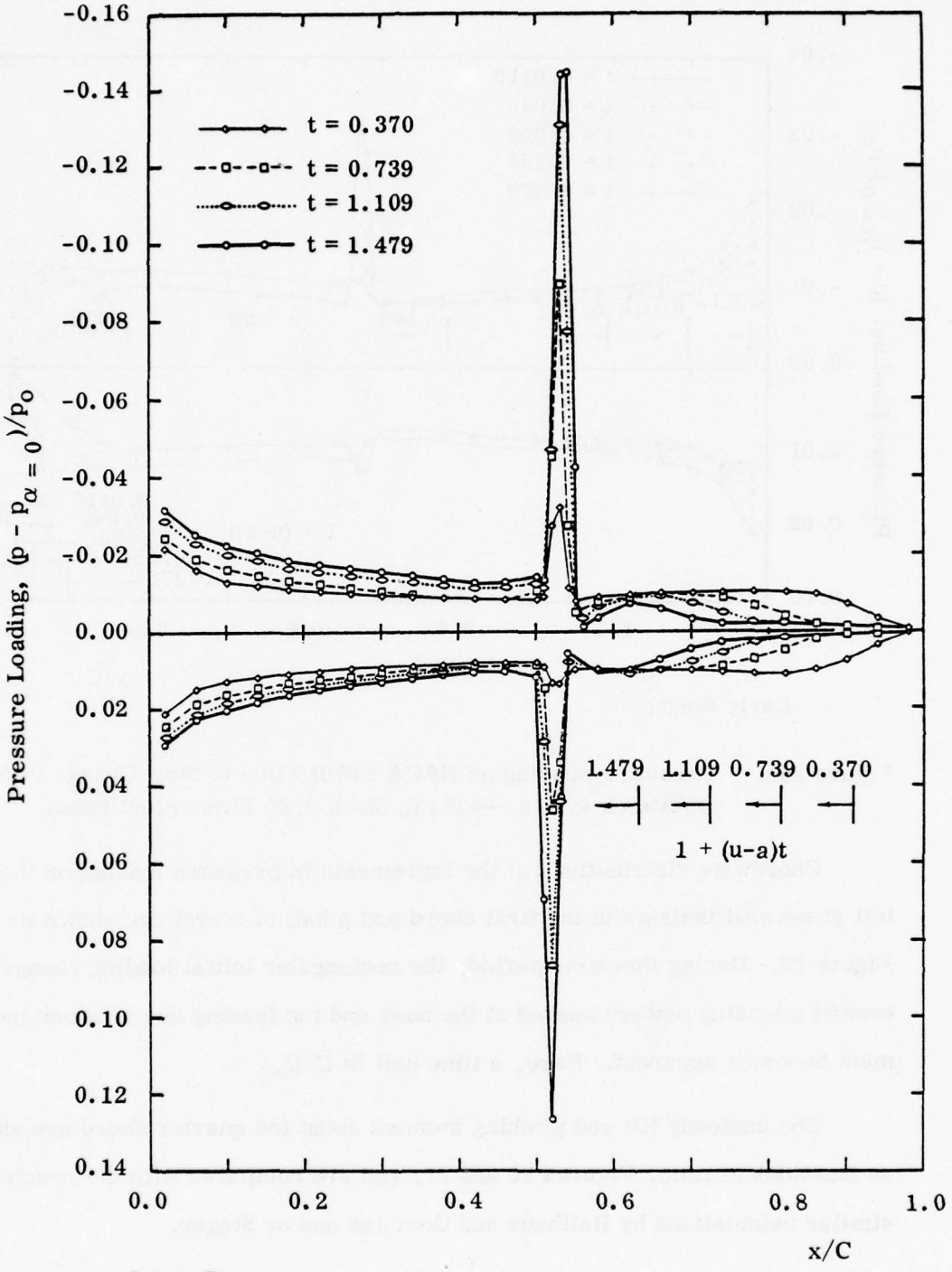

Figure 25b. Pressure Loading on NACA 64A010 Due to Step-Change in Angle-Of-Attack ($\alpha = 0 \longrightarrow 1°$) in Mach 0.80 Flow (Concluded)

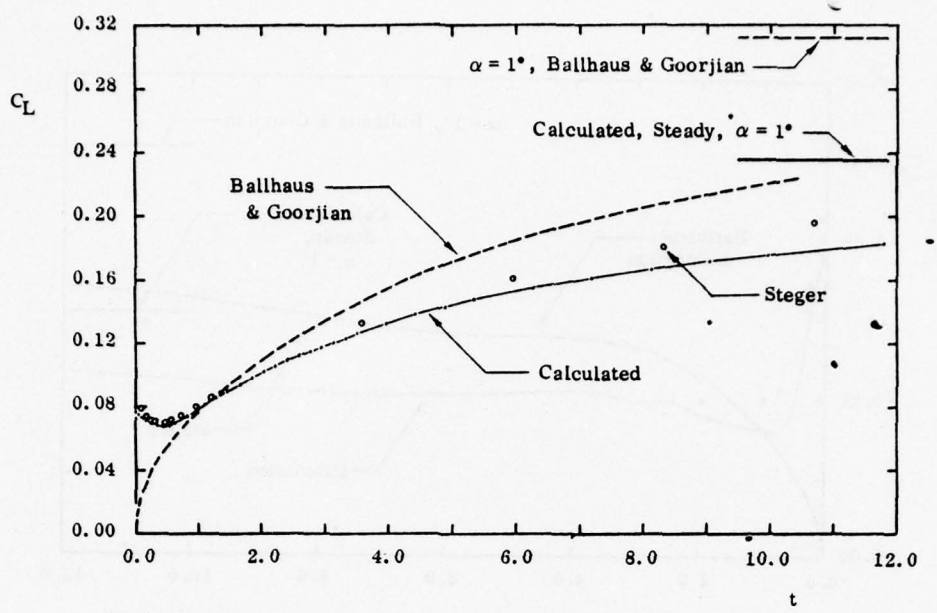

Early Stages

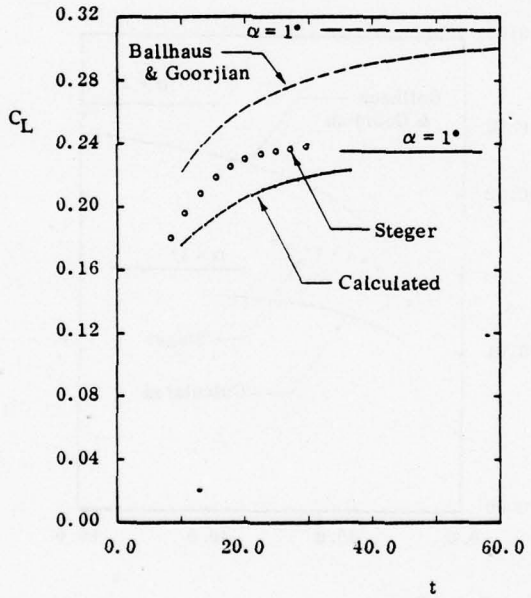

Later Stages

Figures 26a & b. **Transient Lift on NACA 64A010 Due to Step-Change in Angle-Of-Attack ($\alpha = 0 \rightarrow 1°$) in Mach 0.80 Flow**

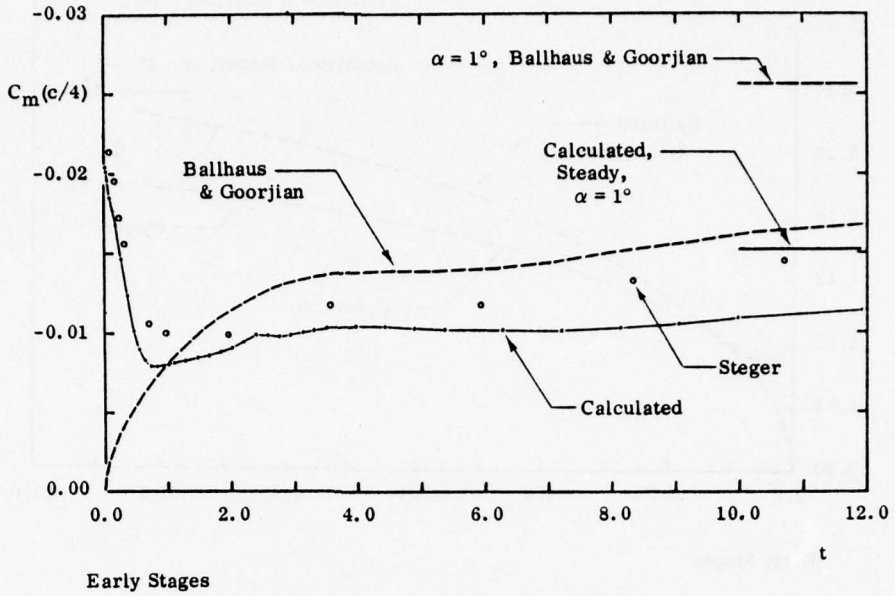

Early Stages

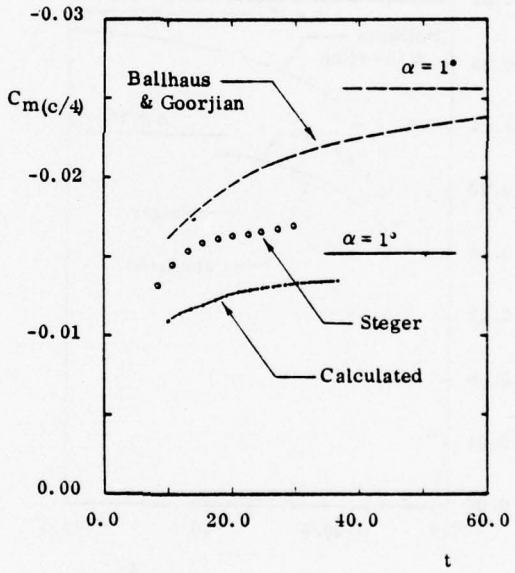

Later Stages

Figures 27a & b. Transient Pitching Moment on NACA 64A010 Due to Step-Change in Angle-Of-Attack ($\alpha = 0 \rightarrow 1°$) in Mach 0.80 Flow. Quarter-Chord Reference Axis, Nose-Up Positive.

The sudden imposition of the cross-flow induces a relatively uniform jump in pressure on the lower airfoil surface and a similar fall in pressure on the upper airfoil surface; see curves labelled t = .0115 in Figure 25a. The lower surface compression and the upper surface rarefaction propagate their influence to the respective opposite surfaces around both the leading and trailing edges.

There is appreciable attenuation of each of the primary disturbances in spreading around the leading edge to the opposite surface. The partial cancellation of the primary waves around the leading edge is swept aft at speed (u + a) causing some drop in lift. These adjustments sweep to the trailing edge in about 0.4 time units. Likewise, the mutual cancellation of the primary disturbances around the trailing edge, which spreads forward at speed (a - u), is well illustrated in Figure 25. During the entire period covered in Figure 25 the loading at the leading edge builds up and spreads aft.

The wave systems mentioned above are all features present in the linearized analysis of Heaslet and Lomax.[19] Because the airfoil is not a flat plate starting with uniform flow as assumed in the linear analysis, the various waves of adjustment interact with the non-uniform flow around the finite-thickness airfoil. Thus, loading spikes develop due to movement of the shocks (Figure 25b) and waves travelling forward from the trailing edge are severly attenuated and delayed by having to detour outboard of the shocks closing the imbedded supersonic regions.

Both the lift and pitching moment decrease in magnitude, Figures 26a and 27a, to minimums at about 0.4 time units after their initial jumps, about

[19] Heaslet, Max. A. and Lomax, Harvard, "The Application of Green's Theorem to the Solution of Boundary-Value Problems in Linearized Supersonic Wing Theory" National Advisory Committee for Aeronautics Technical Note No. 1767, April 1949

the time for information to propagate aft along the airfoil one chord length. The pitching moment holds steady at about 2/3 its "final" value for the period between (roughly) 4 and 7 time units after the step change in incidence; a similar pause is present in the moment buildup calculated by Ballhaus and Goorjian and by Steger, Figure 27a.

2.4 OSCILLATORY UNSTEADY FLOW

The oscillatory unsteady flow over the airfoil at Mach 0.80 was calculated for three oscillation modes:

Mode	Axis	Incidence	Reduced Frequency
Pitching	0.50 chord	0 ±1.0°	0.50
Pitching	0.25 chord	0 ±1.0°	0.40
Plunging		0 ±1.0° (Induced by Motion)	0.40

Instantaneous pressure distributions at six positions in the oscillation cycle for the plunging motion are shown in Figure 28. The pressure distributions for the cases with pitching motion are similar in character but, of course, differ somewhat in their detailed values, Figures 29, 30. Figure 31 shows the upper surface shock location through an oscillation for the three cases calculated.

The amplitudes and phase angles for the pressure excursions for the three cases are shown in Figure 32.

The oscillatory force and pitching moment about the quarter chord (nose-up is positive) are listed in Table 2. In steady flow at 1.0 degree angle-of-attack the present results agree satisfactorily with those of Steger. The lift calculated by Ballhaus and Goorjian is about 1.3 times the average of the other two results. Similarly, the pitching moment calculated by the perturbation method is 1.6 times the average of the other two results.

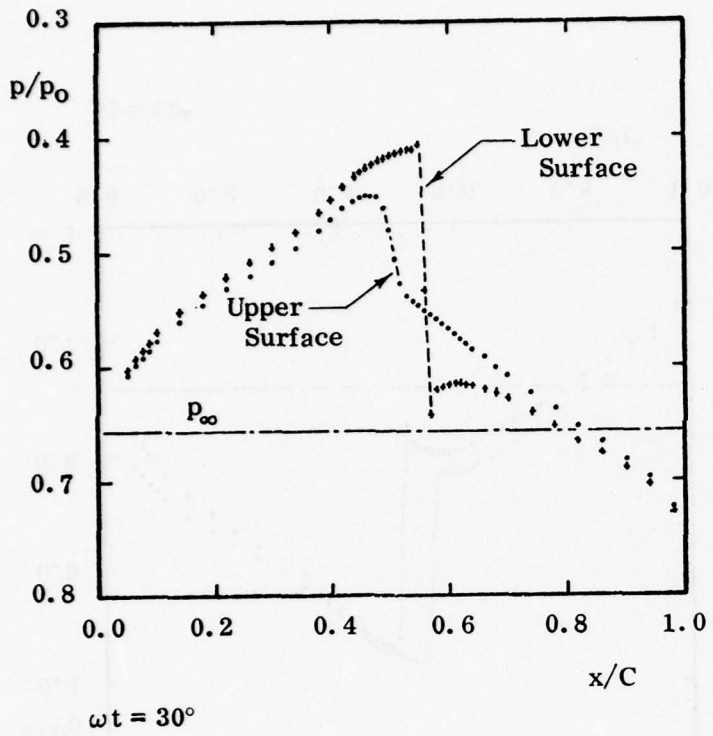

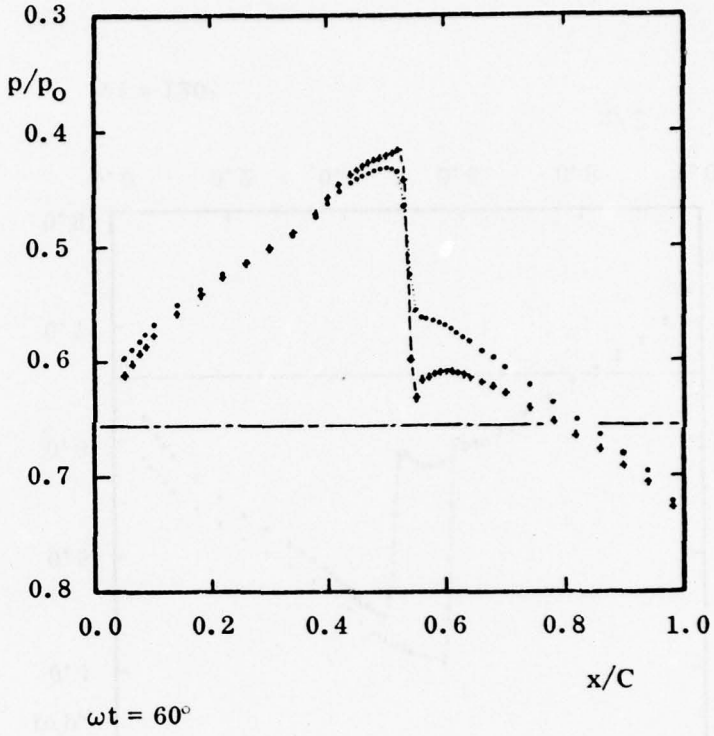

Figures 28a & b. Instantaneous Pressure Distributions on NACA 64A010 in Oscillatory Plunging Motion. Mach 0.80, $\alpha = 0 \pm 1°$, k = 0.40 (Continued)

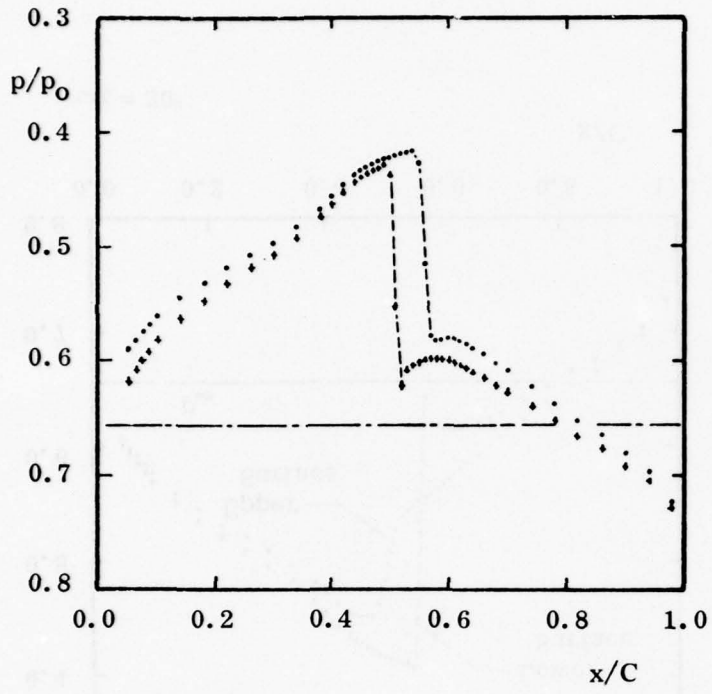

ωt = 90°

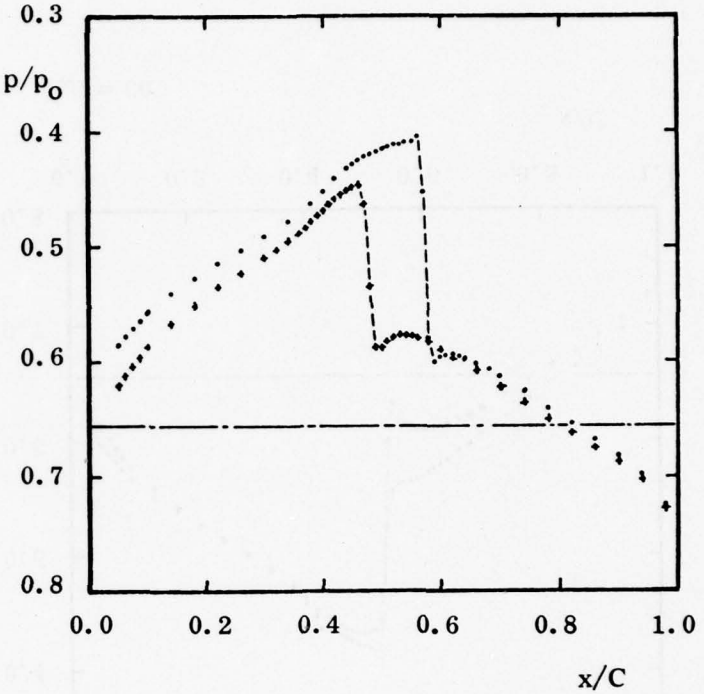

ωt = 120°

Figures 28c & d. (Continued)

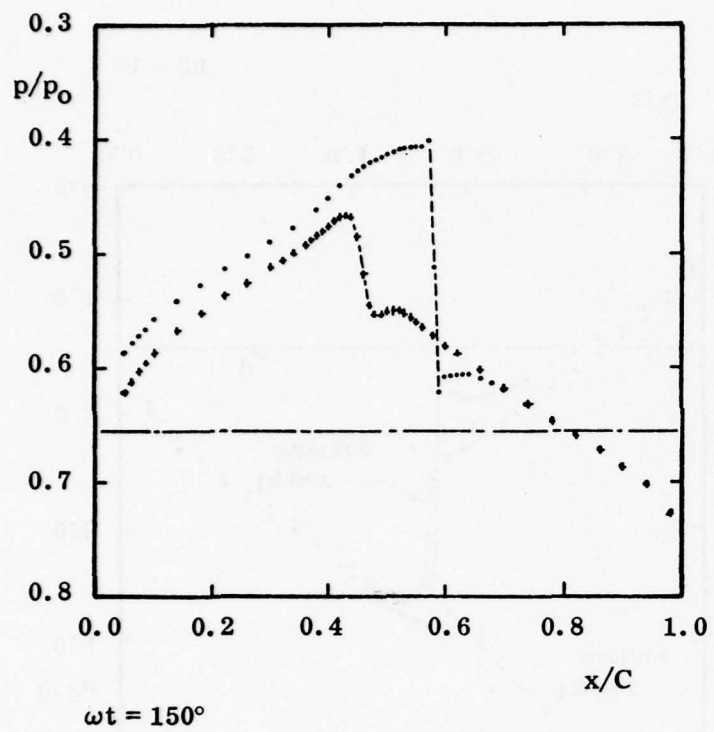

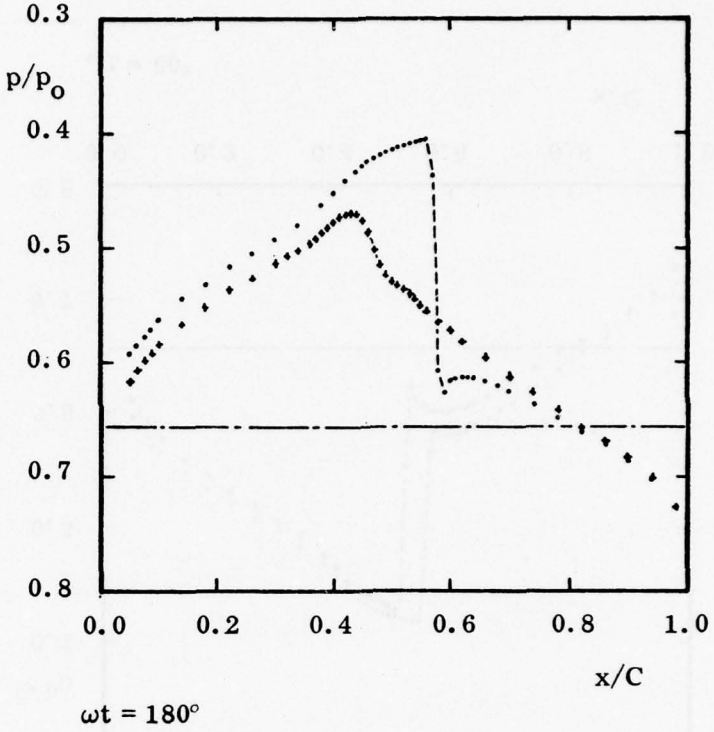

Figures 28e & f. **Instantaneous Pressure Distributions on NACA 64A010 in Oscillatory Plunging Motion. Mach 0.80, $\alpha = 0 \pm 1°$, k = 0.40 (Concluded)**

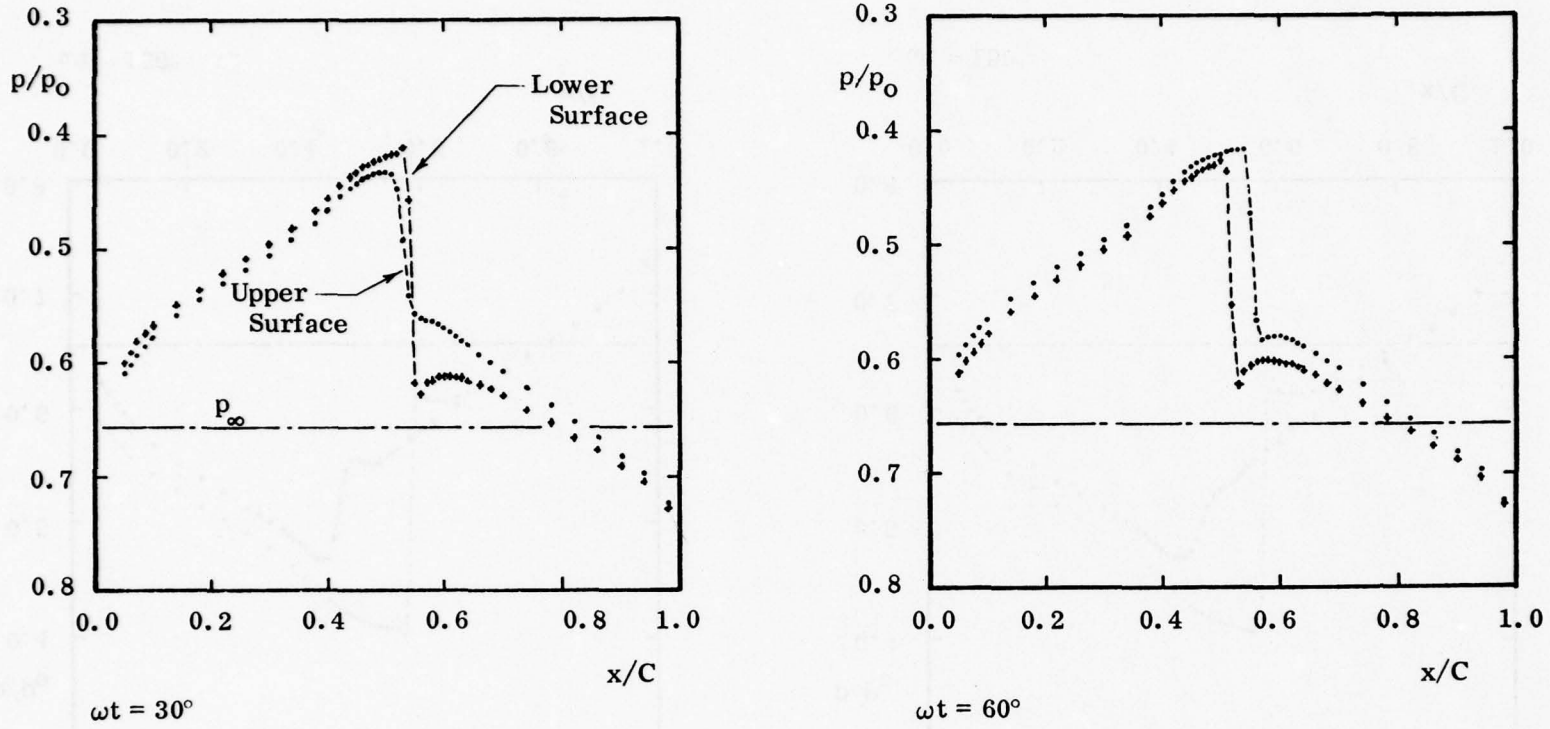

Figures 29a & b. Instantaneous Pressure Distributions on NACA 64A010 in Oscillatory Pitching Motion About a Quarter-Chord Axis. Mach 0.80, $\alpha = 0 \pm 1°$, k = 0.40 (Continued)

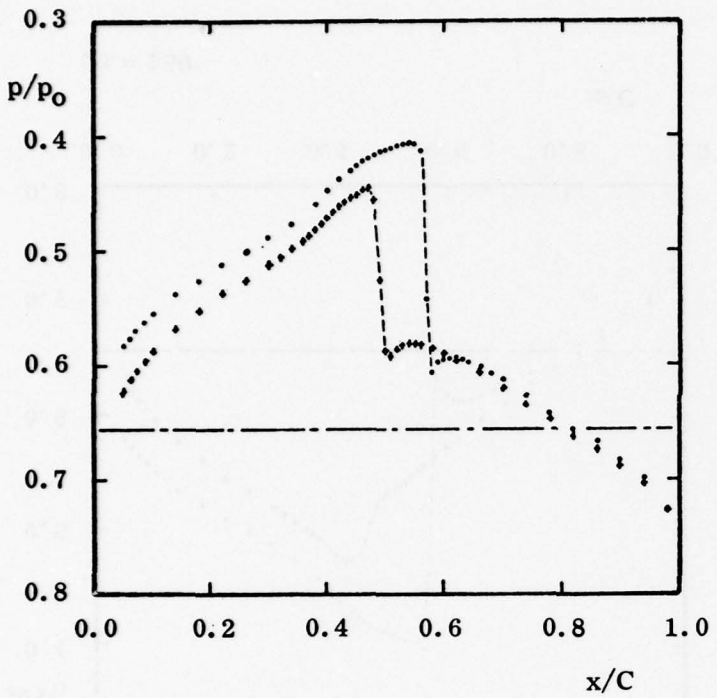

ωt = 90°

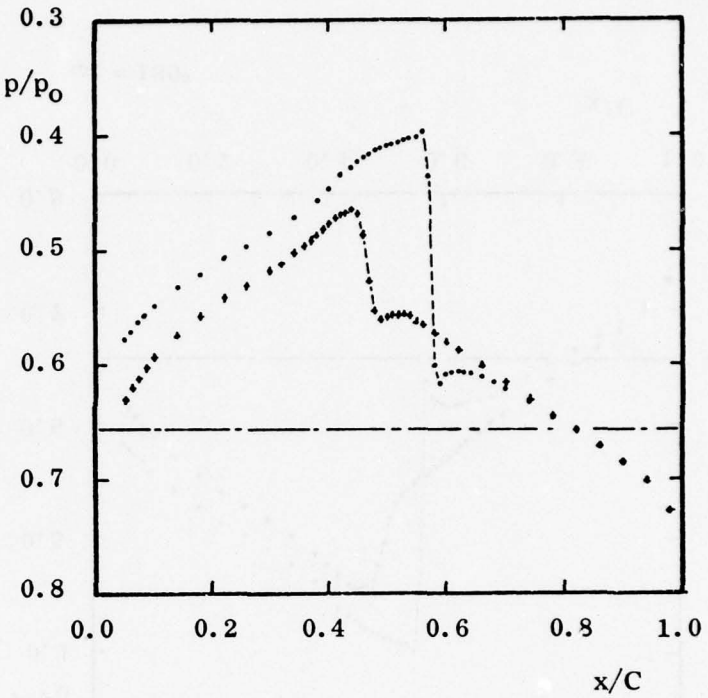

ωt = 120°

Figures 29c & d. (Continued)

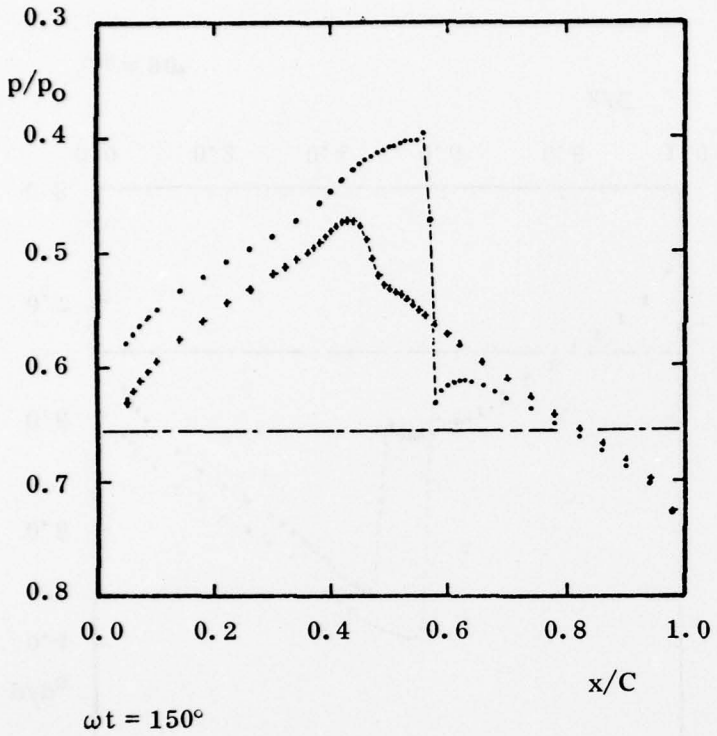

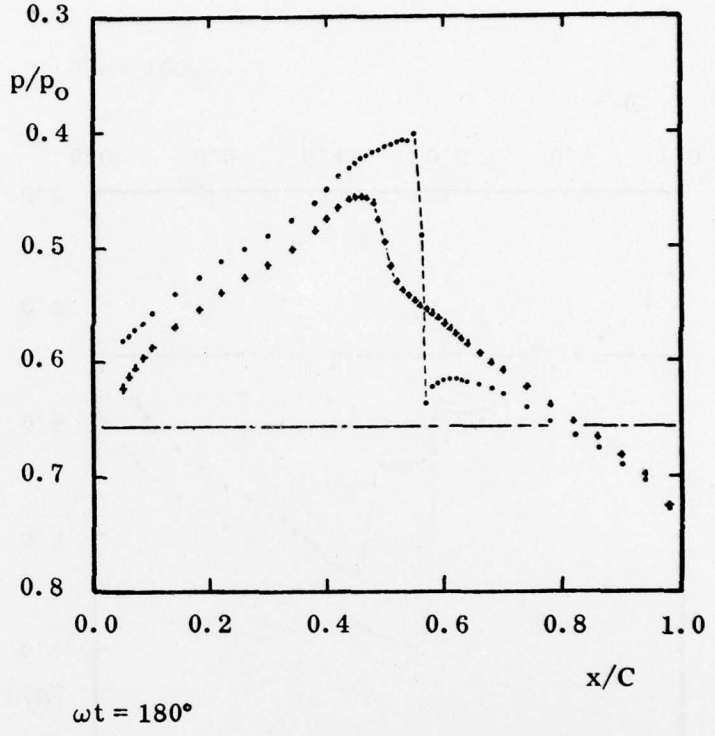

Figures 29e & f. Instantaneous Pressure Distributions on NACA 64A010 in Oscillatory Pitching Motion About a Quarter-Chord Axis. Mach 0.80, $\alpha = 0 \pm 1°$, k = 0.40 (Concluded)

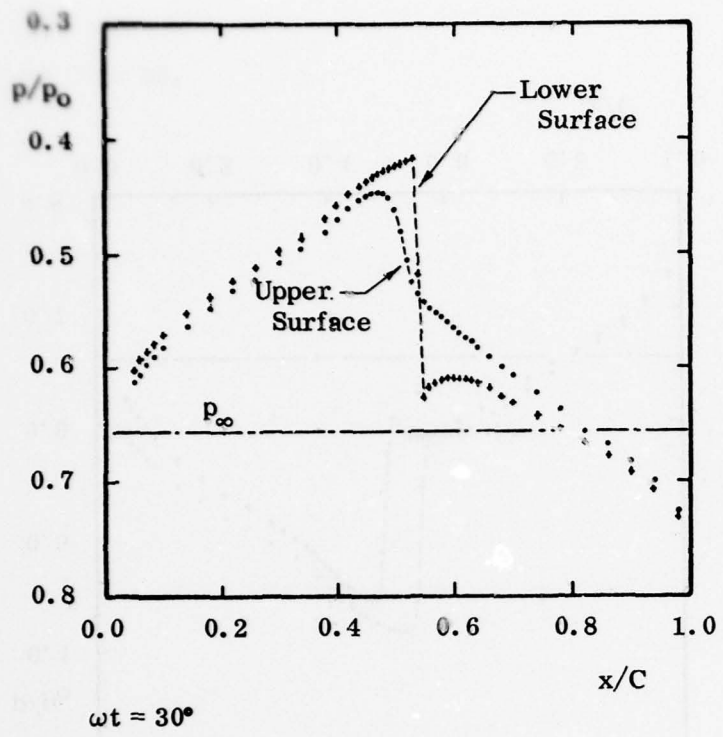

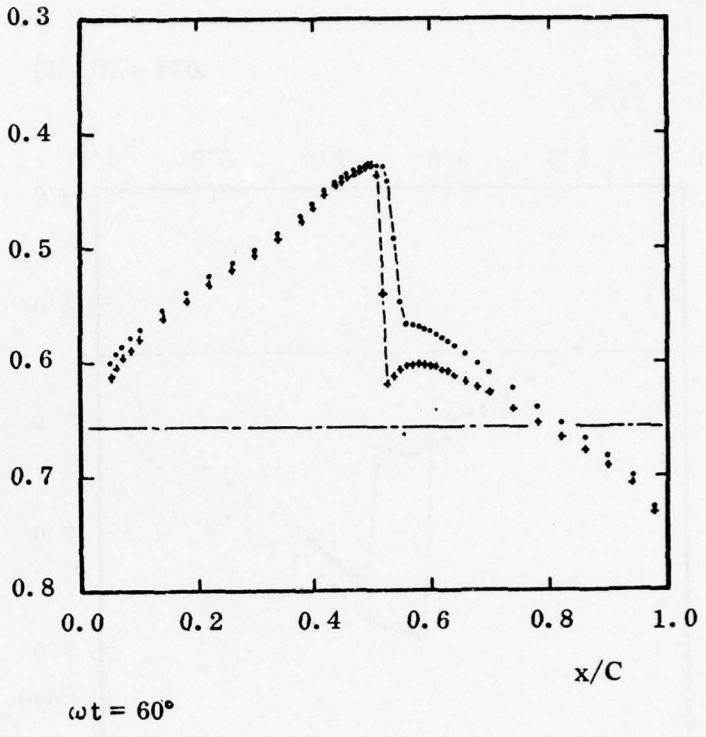

Figures 30a & b. Instantaneous Pressure Distributions on NACA 64A010 in Oscillatory Pitching Motion About a Mid-Chord Axis. Mach 0.80, $\alpha = 0 \pm 1°$, k = 0.50 (Continued)

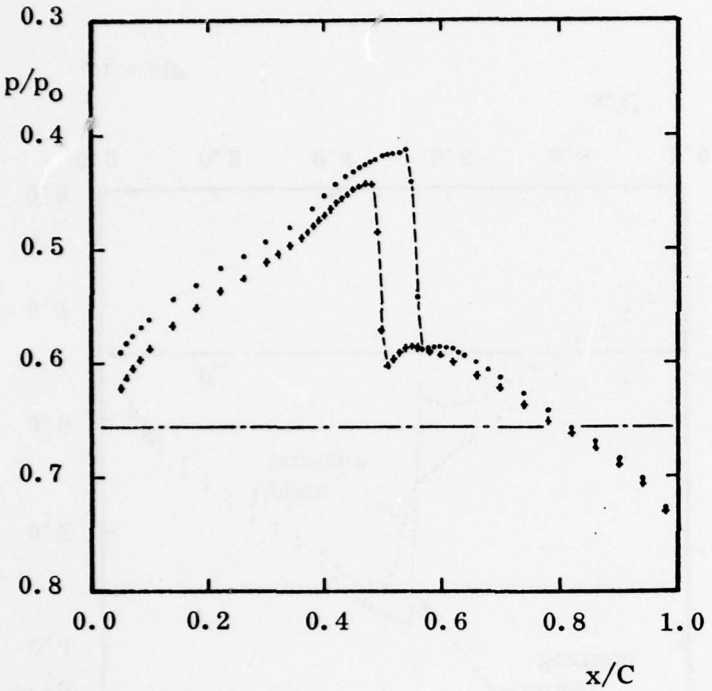

(c) $\omega t = 90°$

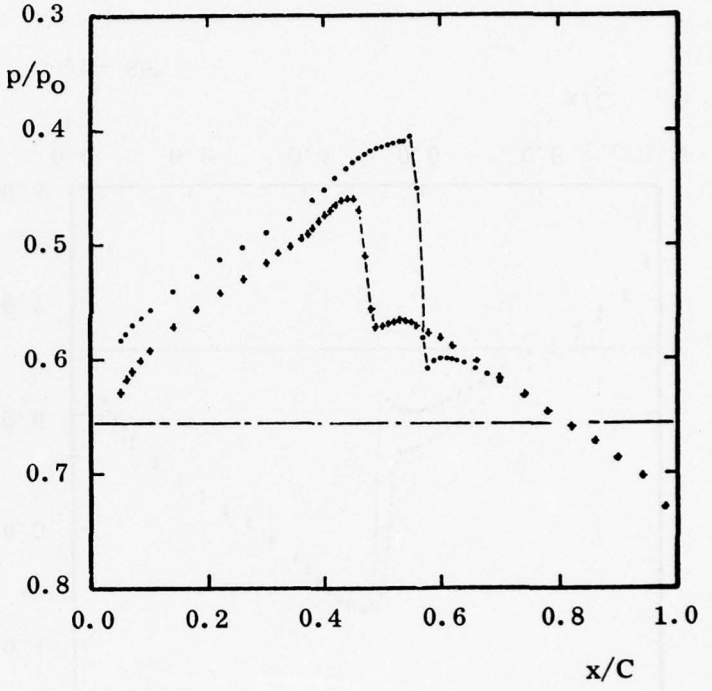

(d) $\omega t = 120°$

Figures 30c & d. (Continued)

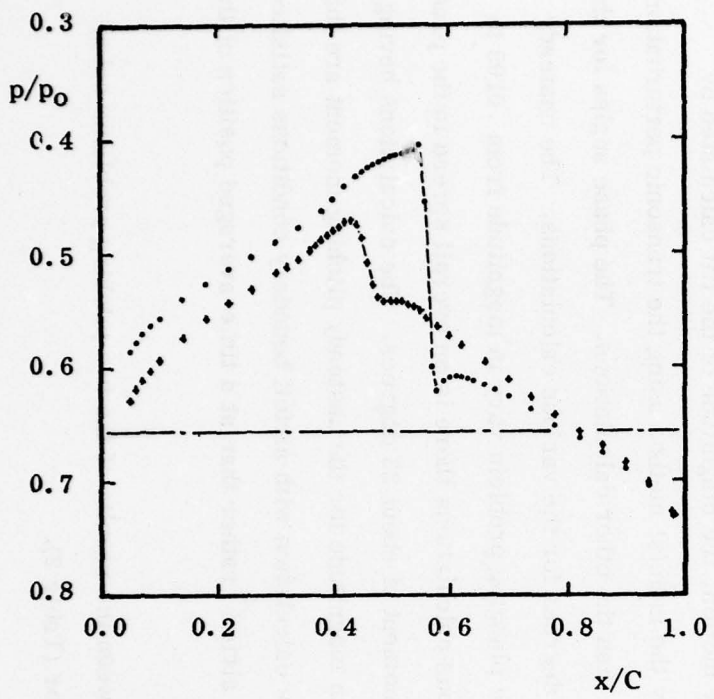

(e) $\omega t = 150°$

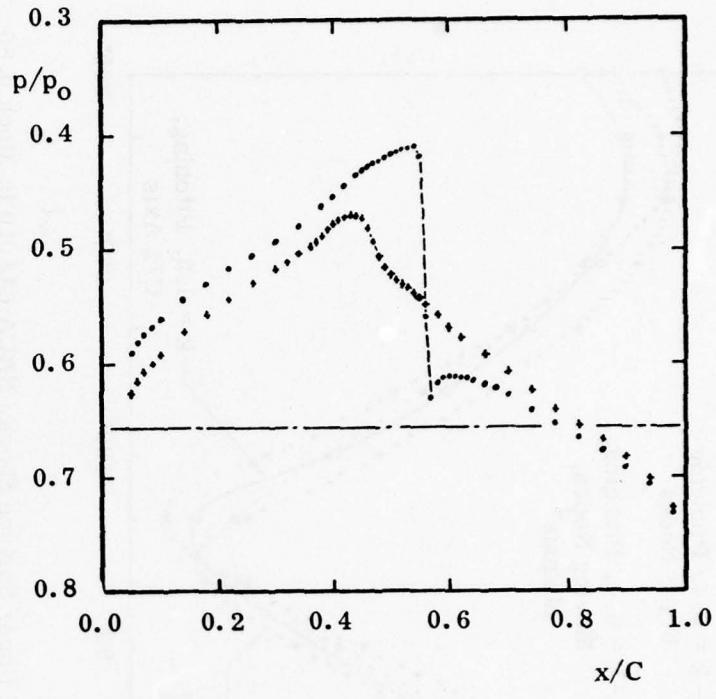

(f) $\omega t = 180°$

Figures 30e & f. Instantaneous Pressure Distributions on NACA 64A010 in Oscillatory Pitching Motion About a Mid-Chord Axis. Mach 0.80, $\alpha = 0 \pm 1°$, k = 0.50 (Concluded)

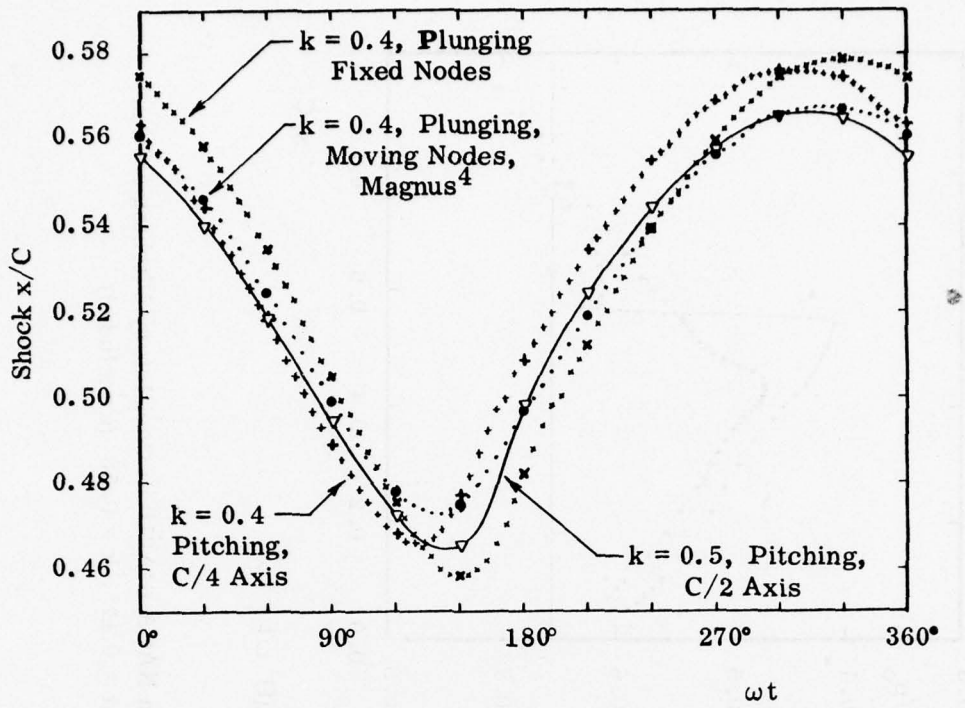

Figure 31. Position of Upper Surface Shock, NACA 64A010 in Mach 0.80 Unsteady Flow

In plunging unsteady motion, the magnitude of the lift calculated by Ballhaus and Goorjian by the indicial method using the transonic perturbation equations is also higher than the other calculations. The phase angles for the lift show a spread of 11 degrees for the various calculations. The unsteady pitching moments for the plunging problem vary in magnitude from .0105 to .0186. Among the various calculations there is an overall spread in the phase angles for the pitching moment of about 23 degrees. The calculations having the greatest difference in magnitude for the unsteady pitching moment are the present and an analogous calculation with airfoil boundary conditions satisfied at nodes on the plunging airfoil[4] rather than at a time-averaged position of the airfoil.

The differences between the results of the two pitching problems calculated are relatively minor (Table 2).

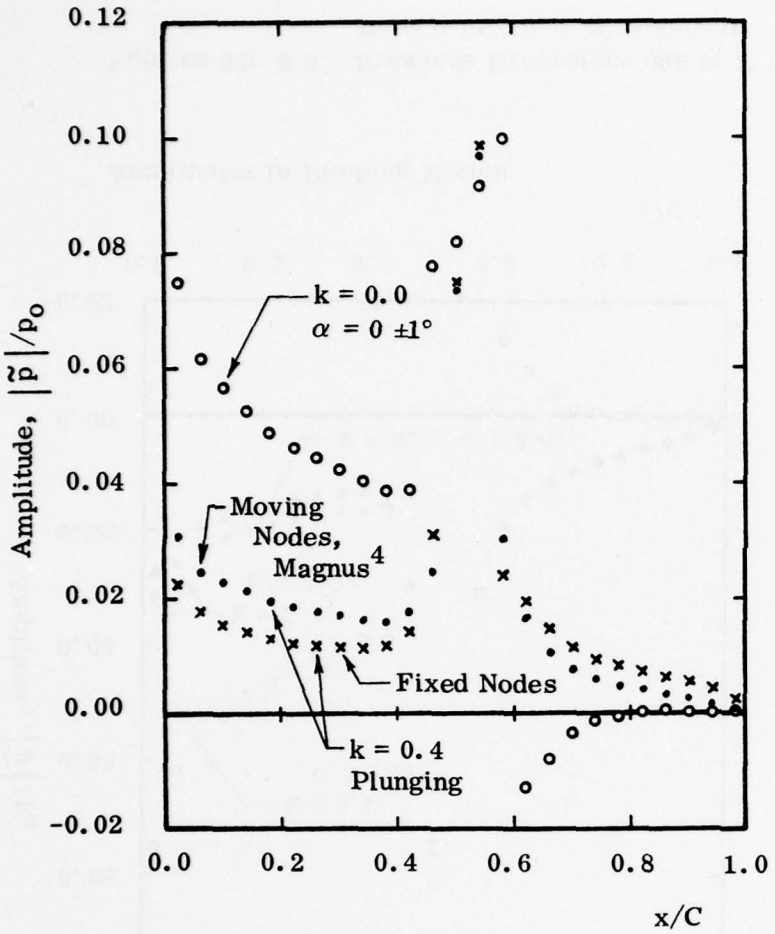

Amplitudes in Plunging Motion

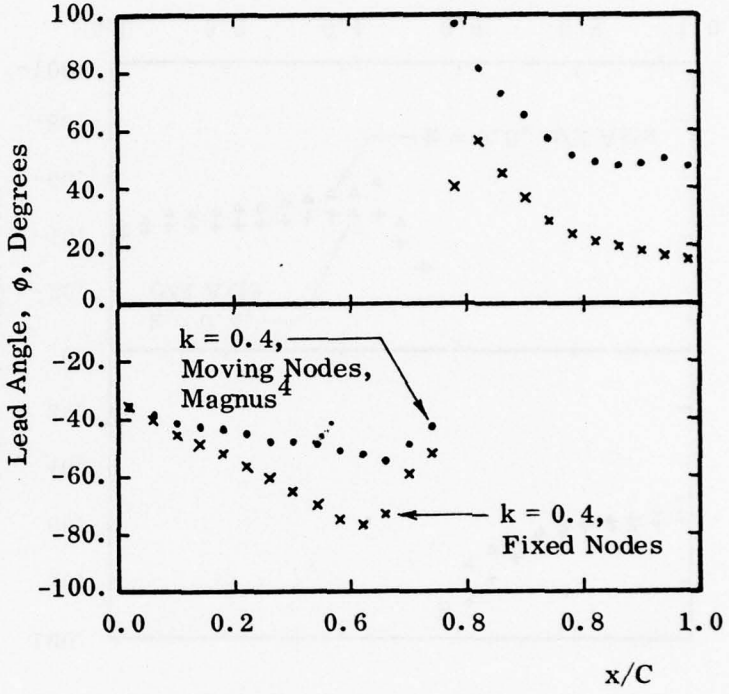

Phase Lead Angles in Plunging Motion

Figures 32a & b. Pressure Excursions due to 1° Angle-Of-Attack Oscillations, NACA 64A010 in Mach 0.80 Flow (Continued)

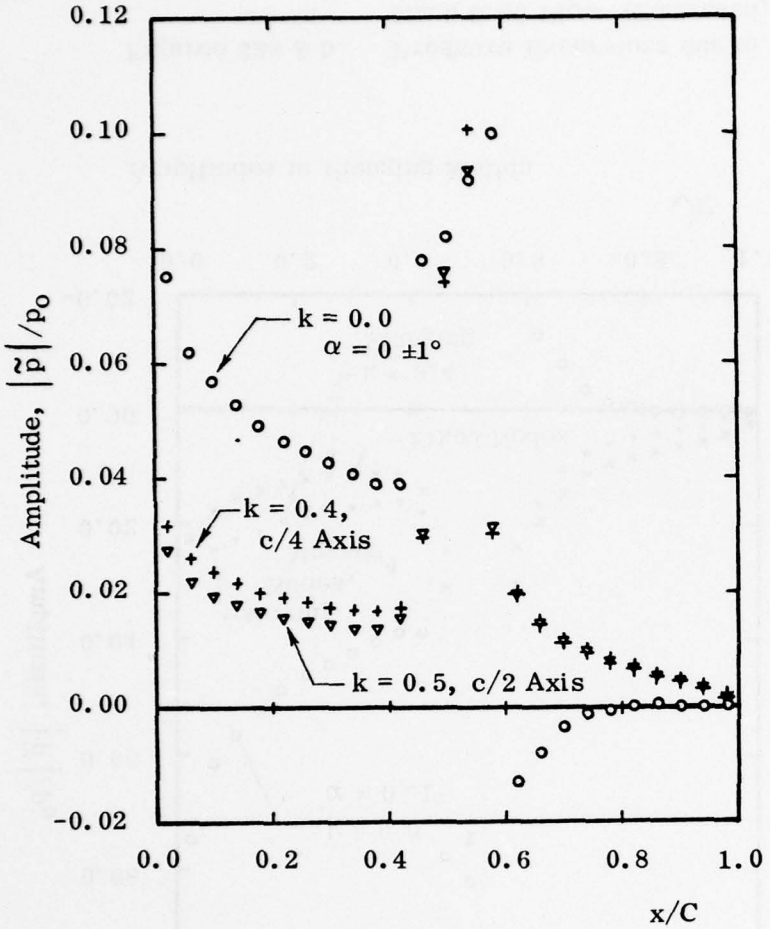

Amplitudes in Pitching Motion

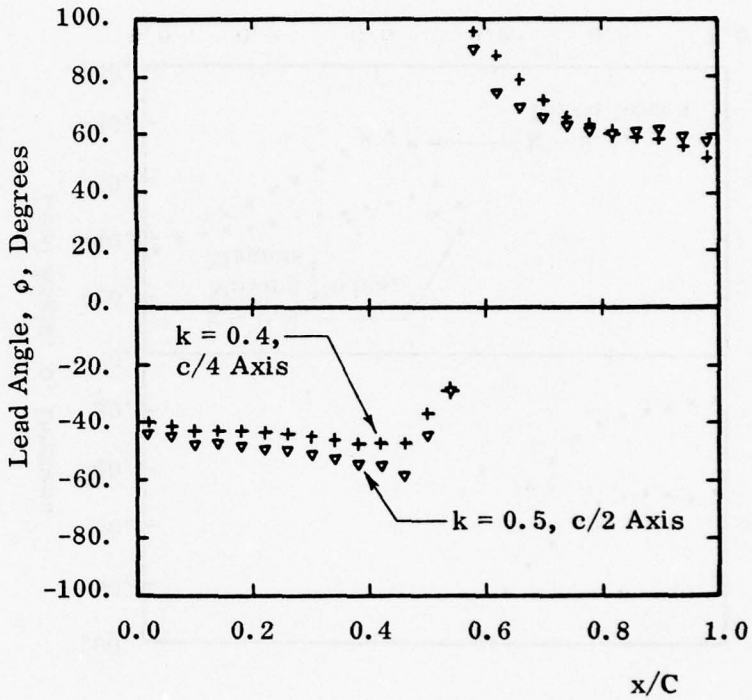

Phase Lead Angles in Pitching Motion

Figures 32c & d. Pressure Excursions due to 1° Angle-Of-Attack Oscillations, NACA 64A010 in Mach 0.80 Flow (Concluded)

Table 2. FORCES AND MOMENTS IN 1.0 DEGREE OSCILLATIONS ABOUT ZERO ANGLE-OF-ATTACK, NACA 64A010, MACH NUMBER 0.80

Angle of Attack:

$\alpha(t) = 1.0^{\circ} \sin(\omega t)$

ω = oscillation rate, radian/time unit

Reduced Frequency:

$k = \frac{\omega C}{U_\infty}$

C = chord

U_∞ = Free stream velocity

Coefficients:

C_L = Airfoil Lift/qC

C_m = Airfoil nose-up moment about quarter chord/qC^2

q = Free stream dynamic pressure

Typical Response Function:

$C_L(t) = \left|\tilde{C}_L\right| \sin(\omega t + \phi)$

If ϕ is positive, the peak C_L occurs before maximum angle-of-attack; *tabulated ϕ in degrees.*

Motion Description, Researcher	$\left\|\tilde{C}_L\right\|$	ϕ	$\left\|\tilde{C}_m\right\|$	ϕ
Quasi-Steady, k = 0.00				
Inviscid Calculation, Magnus	0.235	-	-0.0152	-
Inviscid Calculation, Steger[18]	0.239	-	-0.0170	-
Perturbation Calculation, Ballhaus & Goorjian	0.312	-	-0.0256	-

Table 2 (continued)

Motion Description, Researcher	$\lvert\tilde{C}_L\rvert$	ϕ	$\lvert\tilde{C}_m\rvert$	ϕ
Plunging Motion, k = 0.40, First Harmonics				
Inviscid Calculation, Magnus	0.106	-40.	0.0186	164.
Inviscid Calculation, Magnus,[4] boundary conditions satisfied at moving nodes	0.106	-35.	0.0105	180.
Inviscid Calculation, Steger[16]	0.104	-33.	0.0116	-173.
Perturbation Calculation, Ballhaus & Goorjian,[13] Indicial Method	0.123	-44.	0.0137	166.
Pitching Motion, k = 0.40, First Harmonics Axis at quarter-chord				
Inviscid Calculation, Magnus	0.113	-25.	0.0156	-159.
Pitching Motion, k = 0.50, First Harmonics, Axis at mid-chord				
Inviscid Calculation, Magnus	0.0962	-28.	0.0149	-157.

SECTION IV

DISCUSSION

The calculations completed ought to have two uses; first, as examples of what might be expected from a straightforward numerical solution of the inviscid unsteady Euler equations as compared to other solutions and, second, as an aid in interpreting what has been found in experiments.

1. CORRESPONDENCES BETWEEN VARIOUS CALCULATIONS

When checking for agreement between results of various unsteady calculations one should expect differences to occur because of the diversity in formulations of the problem and in the mechanizations for approximate numerical solution.

Most investigators have calculated steady flows around the airfoil being studied to establish a limit of zero reduced frequency or as a basic step in the solution sequence. It can be seen, Figure 33, that there is considerable spread in the results of solving what might be expected to be a simple flow problem, namely flow past a thin airfoil at zero lift. There is only fair agreement on obvious features which ought to be important, namely the size and placement of the supersonic region.

When the unsteady problem under study is the oscillating flap, widely different results could be expected in the responses if the basic flows had different-sized supersonic regions because of the different delays and attenuations of the signals from the moving flap reaching the front of the airfoil via paths which (certainly) extend outboard of the imbedded supersonic regions. When the problem being studied is pitching or plunging, the interplay of signals originating from changes and attitude or velocity of the elements on the airfoil surface as a whole is more complicated than for the oscillating flap problem. Still, the delays in propagation of information forward from the trailing edge are important in determining the load on the complete airfoil.

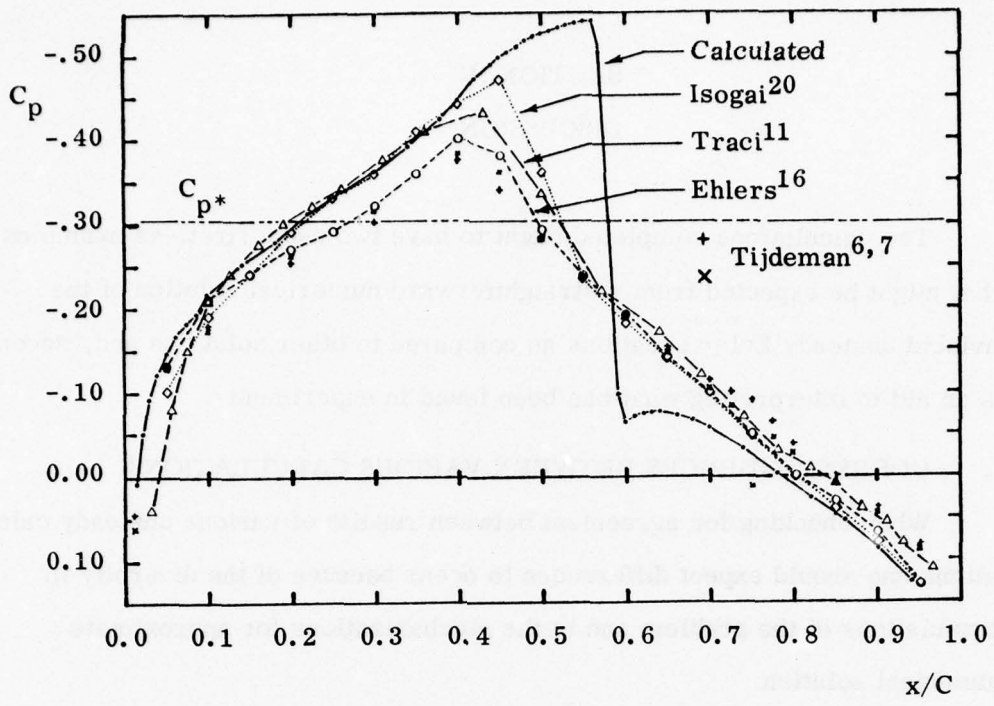

Figure 33. Pressure Distributions for NACA 64A006 at Zero-Lift in Mach 0.85 Flow

Even if there is little prospect of absolute agreement between methods it would be of value to determine whether the methods predict the same trends as parameters (such as Mach number, reduced frequency and amplitude of oscillation) are varied. There might be agreements with some bias-like shifts. That is, increasing the Mach number slightly for method "A" might make it agree better with method "B" because the two then would show flows with roughly the same basic supercriticality. Likewise, method "C" might consistently show less pitching moment than method "D" because in "C" a coarser mesh was employed and the shock capturing scheme places the shock consistently further forward on the airfoil than for method "D".

Unfortunately, of the literature examined, there have been only two research teams, namely Ballhaus and Goorjian[12,13] and Traci, et al,[11] who

[20] Isogai, Koji, "Calculation of Unsteady Transonic Flow Over Oscillating Airfoils Using the Full Potential Equation" AIAA Paper 77-448, AIAA Dynamics Specialist Conference, San Diego, California March 24-25, 1977

have calculated systematic sequences of cases. The number of cases calculated in the present research is too small and the parameters have not been varied systematically enough to demonstrate an orderly dependence of response characteristics on the problem parameters.

Where the parameters for the calculations were deliberately picked so that direct comparisons could be made between the present method and that of Ballhaus and Goorjian,[12,13] the relative values predicted by the two methods have been puzzling. Referring to Table 1, at Mach 0.822 the present method predicts a lower oscillating lift than the method of Ballhaus and Goorjian; at Mach 0.875, the opposite is true. Also, the disagreement between the two styles of calculation seems greatest at the lowest Mach number examined.

On the problem of Mach 0.80 flow over the 64A010 in plunging oscillations or in a step change in angle-of-attack, the disagreement between the present results and those of Ballhaus and Goorjian[13] seems to stem from the non-agreement as to the steady flows.

Where a direct comparison has been made between the present method (modified to satisfy boundary conditions at nodes which move with the plunging airfoil)[4] and that of Steger,[18] see Table 2, the agreement has been relatively good. The two methods are similar in solving a coupled system of four unsteady conservation equations with shock capturing schemes. The programs differ in that Steger[18] uses a single automatically generated mesh and an implicit scheme and is coded to solve viscous flows using the Navier Stokes equations with a turbulence model; the program used here has used patches of different sized mesh to provide the resolution, an explicit scheme, and is coded

for the inviscid Euler equations. The effects of two approximations made in the immediate antecedent to the present program, handling of boundary conditions at the airfoil surface and the assignment of flow properties at the perimeter of the computation field were studied recently.[4] The study demonstrated that modest changes in the magnitudes and phase angles for lift and pitching moment response could be expected if the calculation were to be performed in a truly unbounded computation field rather than the 9.6 chord square which had been used in that study. The present calculations have used a stretched y-mesh in an attempt to lessen the effect of imperfection in applying the outer boundary condition but the errors occasioned by this practice have not been evaluated. Applying the airfoil boundary conditions at fixed nodes located at the time-averaged position of the oscillating airfoil (which is what was done in all calculations in the present study) increased the magnitude and increased the lag angle for the pitching moment by about 16 degrees on the one example studied see Table 2, Section III 2. of the present report. Ostensibly these particular errors should be proportional to the linear velocities at airfoil surface elements and are, therefore, dependent on oscillation amplitude. Thus, it would be best to regard the results of the calculations in the present report as being applicable to problems with vanishingly small amplitude. The only program, of those examined here, incorporating a combination of equations and boundary conditions which seems suitable for problems involving thick airfoils in finite amplitude oscillations is that of Steger.[18]

In seeking data for comparisons of the present results with those of other investigators it was apparent that there is not much standardization on presentation of data. Thus, we can find reduced frequency defined more than one way, oscillatory data presented as real and imaginary components and as magnitudes and phase angles, diverse non-dimensionalizations to obtain coefficients, pitching moments about the nose, the quarter-chord and mid-chord. This is not a suggestion that all investigators should solve the same

problems and present the results in the same fashion. Certainly programs which are based on particular abridged equations will be useful on problems which do not violate the basic assumptions and new programs will be needed to work on problems which, because of their peculiar features or severity, cannot be handled by present methods.

2. CORRESPONDENCES BETWEEN CALCULATIONS AND EXPERIMENTS

The ultimate purpose of calculations should be the prediction of the behavior of oscillating wings at flight Reynolds numbers. Considering cost and other feasibility factors, it is unlikely that experimental data under flight conditions will be available soon. Thus, the programs ought to be capable of duplicating findings in wind tunnel tests and then extendable by logical changes to predict behavior under flight conditions. The changes should account for Reynolds number differences between flight and wind tunnel conditions and for variations in external influences, that is three-dimensional geometry in free-air rather than two-dimensional or other idealized geometry in a channel with ventilated walls.

According to Kacprzynski,[21] the combined uncertainties as to the precise effects of wind-tunnel wall interference and the effects of viscosity may result in 20% error between theory and experiment on studies of steady transonic flows over modern supercritical airfoils. It is probably unreasonable to believe that much better agreement will be achieved in studies of unsteady flows at present.

The oscillatory forces and moments found by Tijdeman,[6,7] see Table 1, Section III, generally show less lag behind the flap motion than the calculations. The calculated magnitudes for the forces and moments are well scattered about the experimental values.

[21] Kacprzynski, J. J., "Viscous Effects in Transonic Flow Past Airfoils" ICAS Paper No. 74-19, The Ninth Congress of the International Council of the Aeronautical Sciences, Haifa, Israel, August 25-30, 1974

Not much effort has been expended on calculating flows where the shocks have been weakened deliberately and, in controlled fashion, shifted to positions on the airfoil which agree with those seen experimentally. In steady transonic airfoil calculations, palatable pressure distributions might be obtainable by use of non-conservative differencing at "shocks" or by using coarse mesh so that artificial viscosity in the scheme distorts and smears the shock pressure rise out over an appreciable fraction of the airfoil chord. These artifices might not be useable for unsteady flow because they might not properly model the complex interplay between the boundary layer, the shock pressure rise, the shock obliquity near the surface, and the shock propagation along the airfoil surface under dynamic conditions.

Imprecision in modelling the shock-boundary-layer effects might have a large effect on the airfoil pitching moments because the shock is in the wrong location, the motion of the shock (amplitude and wave form) during the oscillation is incorrect, and the pressure jump when the shock crosses a given airfoil station is incorrect. Unrealistic shock motion is a feature of the results mentioned in Section III 1.4 of the present report. Definitive measurements of the pressure jump which occurs when a shock crosses a given pressure tap in an experiment on an oscillating airfoil would be valuable.

Exploratory calculations by Traci[11] and by Ballhaus[14] and those made in the present investigation indicate a possibility of strong influence of the wind tunnel walls on results of the quasi steady and unsteady experiments of Tijdeman.[6,7]

The method used here and the others mentioned no doubt would be inadequate if the problem were to analyze transonic unsteady flow over an airfoil with partial or massive separation and reattachment occurring during the oscillation.

REFERENCES

1. Magnus, R. and Yoshihara, H., "Inviscid Transonic Flow over Airfoils" AIAA Journal, Vol. 8, No. 12, pp. 2157-2162, December 1970

2. Magnus, R. and Yoshihara, H., "Unsteady Transonic Flows over an Airfoil" AIAA Journal, Vol. 13, No. 12, pp. 1622-1628, December 1975

3. Thommen, Hans U., "Numerical Integration of the Navier-Stokes Equations" Journal of Applied Mathematics and Physics, (ZAMP) Vol. 17, Fasc. 3, pp. 369-384, May 1966

4. Magnus, R. J., "Computational Research on Inviscid, Unsteady, Transonic Flow Over Airfoils" Convair Rpt. CASD/LVP 77-010, January 1977

5. Tijdeman, H. and Bergh, H., "Analysis of Pressure Distributions Measured on a Wing With Oscillating Control Surface in Two-Dimensional High Subsonic and Transonic Flow" Rpt. NLR-TR F.253, March 1967

6. Tijdeman, H. and Schippers, P., "Results of Pressure Measurements on an Airfoil with Oscillating Flap in Two-Dimensional High Subsonic and Transonic Flow (Zero Incidence and Zero Mean Flap Position)" Rpt. NLR TR 73078U, July 1973

7. Tijdeman, H. and Schippers, P., "Results of Pressure Measurements On a Lifting Airfoil with Oscillating Flap in Two-Dimensional High Subsonic and Transonic Flow" Rpt. NLR TR 73018L, November 1974

8. Tijdeman, H., "On the Motion of Shock Waves on an Airfoil With Oscillating Flap in Two-Dimensional Transonic Flow" Rpt. NLR TR 75038U, March 1975

9. Tijdeman, H., "High Subsonic and Transonic Effects in Unsteady Aerodynamics" Rpt. NLR TR 75079U, May 1975

10. Tijdeman, H., "On the Unsteady Aerodynamic Characteristics of Oscillating Airfoils in Two-Dimensional Transonic Flow" Rpt. NLR MP 76003U, March 1976

11. Traci, R. M., Albano, E. D. and Farr, J. L., Jr., "Small Disturbance Transonic Flows About Oscillating Airfoils and Planar Wings" Rpt. AFFDL-TR-75-100, August 1975

12. Ballhaus, W. F. and Goorjian, P. M., "Implicit Finite-Difference Computations of Unsteady Transonic Flows About Airfoils, Including the Treatment of Irregular Shock-Wave Motions" AIAA Paper 77-205, Los Angeles, California, January 1977

13. Ballhaus, W. F. and Goorjian, P. M., "Computation of Unsteady Transonic Flows by the Indicial Method" AIAA Paper 77-447, Dynamics Specialist Conference, San Diego, California, March 24-25, 1977

14. Ballhaus, W. F. and Goorjian, P. M., "Efficient Solution of Unsteady Transonic Flows About Airfoils" 44th AGARD Structures and Materials Panel Meeting, Lisbon, 18 April 1977

15. Yu, N. J., Seebass, A. R., and Ballhaus, W. F., "An Implicit Shock-Fitting Scheme for Unsteady Transonic Flow Computations" AIAA Paper 77-633, AIAA 3rd Computational Fluid Dynamics Conference, Albuquerque, New Mexico, June 27-28, 1977

16. Ehlers, F. Edward, "A Finite Difference Method for the Solution of the Transonic Flow Around Harmonically Oscillating Wings" Rpt. NASA CR-2257, July 1974

17. Magnus, R., Yoshihara, H., Lee, D., and Rogers, L., "Wall Interference in 2D Ventilated Wind Tunnels at High Subsonic Mach Numbers" Rpt. AFFDL-TR-74-63, June, 1974

18. Steger, J. L., "Implicit Finite Difference Simulation of Flow About Arbitrary Geometries With Application to Airfoils" AIAA Paper 77-665, AIAA 10th Fluid and Plasma Dynamics Conference, Albuquerque, New Mexico, June 27-29, 1977

19. Heaslet, Max. A. and Lomax, Harvard, "The Application of Green's Theorem to the Solution of Boundary-Value Problems in Linearized Supersonic Wing Theory" National Advisory Committee for Aeronautics Technical Note No. 1767, April 1949

20. Isogai, Koji, "Calculation of Unsteady Transonic Flow Over Oscillating Airfoils Using the Full Potential Equation" AIAA Paper 77-448, AIAA Dynamics Specialist Conference, San Diego, California, March 24-25, 1977

21. Kacprzynski, J. J., "Viscous Effects in Transonic Flow Past Airfoils" ICAS Paper No. 74-19, The Ninth Congress of the International Council of the Aeronautical Sciences, Haifa, Israel, August 25-30, 1974

*U.S.Government Printing Office: 1977 — 757-001/106